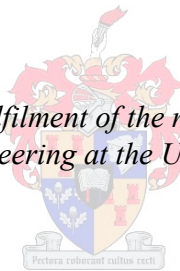


An experimental cost model for composite parts using vacuum assisted resin transfer moulding (VARTM)

by

Christian Vogt

*Thesis presented in partial fulfilment of the requirements for the degree
Master of Science in Engineering at the University of Stellenbosch*



Supervisor: Prof. Kristiaan Schreve
Faculty of Engineering
Department of Mechanical and Mechatronic Engineering

March 2011

Declaration

By submitting this thesis electronically, I declare that the entirety of the work contained therein is my own, original work, that I am the sole author thereof, that reproduction and publication thereof by Stellenbosch University will not infringe any third party rights and that I have not previously in its entirety or in part submitted it for obtaining any qualification.

March 2011

Copyright © 2011 University of Stellenbosch

All rights reserved

Abstract

Vacuum assisted resin transfer moulding (VARTM) belongs to the category of resin infusion techniques that use lower than atmospheric pressure to infiltrate a reinforced cavity. This technique has various advantages; however, manufacturing costs can be relatively high due to more difficult shapes fabricated and a lack of knowledge regarding cost driving factors.

The objective of this study was to develop a cost model for composite parts. Such a model allows the estimation of manufacturing costs of shapes of different geometries. Therefore, it provides a comparison to alternative manufacturing techniques, such as metal forming or composite spray lay-up and helps to avoid unnecessarily expensive design features. The proposal was made to split complex shaped composite parts into individual basic shapes, which are further investigated here.

For the basic shapes, an experimental approach was used where the manufacturing times of each process step are measured and then statistically analysed. Infusion simulation software was used to obtain additional filling times to complete the design of experiments. This method allows the estimation of manufacturing times of composite parts with different geometries. The manufacturing times were validated to that of a complex shaped industrial part, with reasonable results. Finally, a flexible cost model was developed to compare different manufacturing techniques and to estimate the manufacturing costs.

Opsomming

Vakuumgesteunde harsinspuitingsgietwerk (VARTM) behoort tot die kategorie harsinspuitingstegnieke wat laer-as-atmosferiese druk gebruik om'n versterkte holte binne te dring. Hierdie tegniek hou verskeie voordele in. Tog kan vervaardigingskoste betreklik hoog wees wanneer dit by ingewikkelder vorms en 'n gebrek aan kennis met betrekking tot kostesnellers kom.

Die doelwit van hierdie studie was om 'n kostemodel vir saamgestelde onderdele te ontwikkel. Die model maak voorsiening vir die raming van die vervaardigingskoste vir verskillende afmetings. Sodoende bied dit 'n vergelyking met alternatiewe tegnieke, en help voorkom onnodig duur ontwerpkenmerke. Daar is voorgestel dat dele met ingewikkelde vorms in individuele basiese vorms verdeel word, wat dan hier verder ondersoek word.

Vir die basiese vorms word'n eksperimentele benadering gebruik waar die vervaardigingstye in elke prosesstap gemeet en statisties ontleed word. Voorts word inspuitingssimulasiesagteware gebruik om komplementêre inspuitingstye te bepaal ten einde die eksperimentele ontwerp te voltooi. Hierdie metode maak dit ook moontlik om die vervaardigingstye vir saamgestelde materiaal onderdele van verskillende afmetings te raam. Die vervaardigingstye word dan bevestig aan die hand van dié van 'n kompleks gevormde industriële onderdeel, met redelike resultate. Uiteindelik word 'n buigsame kostemodel ontwikkel om verskillende vervaardigingstegnieke te vergelyk en die vervaardigingskoste te raam.

Dedication

To my parents, my brother and my girlfriend, Liana Meyer, as well as my friends, for their inspiration, patience and love during my master's studies – their encouragement enabled me to reach another important milestone in my life.

Acknowledgements

I would like to convey a special thank you to my supervisor Prof. Kristiaan Schreve for his valuable help and encouragement, and the time he spent on this subject.

I thank the students who supported me in my work.

Furthermore, I would like to thank Formo Fibreglass for their unconfined input and time raised.

I would also like to thank the advanced manufacturing technology strategy (AMTS) for funding my research.

Table of contents

Abstract	ii
Opsomming	iii
Dedication	iv
Acknowledgements	v
Table of contents	vi
List of figures	xi
List of tables	xiii
List of abbreviations.....	xiv
List of symbols	xv
1. Introduction.....	1
1.1. Background.....	1
1.2. Motivation	2
1.3. Research objective	3
1.4. Outline	3
2. Literature review	4
2.1. Composite manufacturing techniques	4
2.1.1. Classical techniques	4
2.1.1.1. Hand lay-up and spray lay-up	4
2.1.1.2. Pultrusion	5
2.1.1.3. Filament winding	5
2.1.1.4. Prepreg and tape placement	5
2.1.1.5. Vacuum bag moulding and autoclave moulding	6
2.1.1.6. Pressure bag moulding.....	6
2.1.1.7. Compression moulding.....	6
2.1.2. Infusion techniques	6
2.1.2.1. Categorisation of infusion techniques.....	6
2.1.2.2. Categorisation of mould types	7
2.1.2.3. Resin transfer moulding.....	8
2.2. Vacuum assisted resin transfer moulding.....	8
2.2.1. Design considerations	9

2.2.1.1.	Port and vent positioning	9
2.2.1.2.	Mould sealing.....	9
2.2.2.	Material properties	10
2.2.2.1.	Fibre permeability	10
2.2.2.2.	Matrix material.....	11
2.2.3.	Effect of mould temperature on infusion	12
2.3.	Design of experiments	13
2.3.1.	Taguchi method.....	13
2.3.2.	D-optimal method	13
2.4.	Infusion simulation software	14
2.4.1.	Available software.....	14
2.4.2.	Software method	15
2.4.3.	Validation methods	16
3.	Materials and methods	17
3.1.	Methods and limitations	17
3.2.	Materials	18
4.	Experimental set-up and mould manufacturing.....	19
4.1.	Experimental set-up.....	19
4.2.	Composite part dimensions	20
4.3.	Mould design and manufacture	21
5.	Analytical procedure and statistical methods	22
5.1.	Analytical procedure.....	22
5.1.1.	Steps in the analytical procedure.....	23
5.1.2.	Predictors and responses	23
5.2.	Statistical methods and evaluation	24
5.2.1.	Design of experiments.....	24
5.2.2.	Measurement of the central tendency.....	25
5.2.3.	Measures of spread.....	25
5.2.4.	Regression analysis	26
5.2.4.1.	Types.....	26
5.2.4.2.	Quality.....	26
5.2.5.	Correlation analysis.....	27
5.3.	Methods of displaying the data.....	28

6.	Simulation.....	29
6.1.	Why use infusion software?	29
6.2.	Procedure involved in using the software.....	29
6.2.1.	Procedure of considering draping effects.....	30
6.2.2.	Procedure of neglecting draping effects.....	30
6.2.3.	Conclusion.....	31
6.3.	Material properties and process parameter settings.....	31
6.3.1.	Material properties	31
6.3.2.	Simulation settings	33
6.4.	Experimental verification of simulation.....	34
6.4.1.	Verification method.....	34
6.4.2.	Verification and result.....	35
6.5.	Conclusion.....	38
7.	Process analysis of basic shapes	39
7.1.	Set-up.....	39
7.1.1.	Laminate cutting.....	39
7.1.1.1.	Measurement methods	39
7.1.1.2.	Results.....	40
7.1.2.	Application of mould release agent.....	42
7.1.2.1.	Measurement methods	43
7.1.2.2.	Results.....	43
7.1.3.	Laminate lay-up.....	48
7.1.3.1.	Measurement methods	48
7.1.3.2.	Results.....	49
7.1.4.	Mould clamping, positioning, pipe mounting and resin mixing	54
7.1.4.1.	Measurement method.....	55
7.1.4.2.	Results.....	55
7.2.	Infusion.....	57
7.2.1.	Measurement method	58
7.2.2.	Results	58
7.2.3.	Application graphs	59
7.3.	Curing.....	63
7.4.	Demoulding	64

7.4.1.	Measurement method	64
7.4.2.	Results	64
7.5.	Mould cleaning	67
7.5.1.	Measurement method	67
7.5.2.	Results	67
8.	Transformation to complex shaped parts	69
8.1.	Mould release agent application, laminate lay-up and demoulding	69
8.2.	Infusion	69
9.	Cost method and model	72
9.1.	Cost method	72
9.1.1.	Modification of the full costing method	72
9.1.2.	Direct material costs	73
9.1.3.	Manufacturing cost	73
9.1.4.	Special once-off expenses	75
9.2.	Summary and cost model	75
9.2.1.	Summary of working time equations	75
9.2.2.	Cost model	77
10.	Case study: Refrigerator panel	79
11.	Summary and conclusion	80
	References	81
	Appendices	86
	Appendix A: Analytical procedure and analysis	86
	A.1 Examples of data types	86
	Appendix B: Process analysis of basic shapes	87
	B.1 Application graphs for mould releasing agent	87
	B.2 Infusion	88
	B.3 Demoulding	88
	B.4 Mould cleaning	88
	B.5 Transformation error	89
	Appendix C: Simulation	90
	C.1 Equivalent permeability for "runners", and inlet and outlet zones	90
	C.2 Runners, and inlet and outlet zones: properties	90
	C.3 Further simulation verification figures	90

Appendix D: Cost model	93
D.1 Full costing method modifications.....	93
D.2 Direct material costs.....	94
D.3 Hourly cost rate.....	95
D.4 Special once-off expenses.....	96
D.5 Company related assumptions.....	96
D.6 Calculation of total manufacturing cost.....	97
Appendix E: Case study: Refrigerator panel	98
E.1 Laminate cutting.....	99
E.2 Application of gelcoat	99
E.3 Laminate lay-up.....	100
E.4 Infusion.....	100
E.5 Mould clamping, positioning, pipe mounting and resin mixing	102
E.6 Demoulding	102
E.7 Mould cleaning.....	102
Appendix F: Mould dimensions	104
F.1 Flat shaped mould drawings	104
F.2 L-shaped mould drawings.....	105

List of figures

Figure 1: Categorisation of composite manufacturing techniques.....	8
Figure 2: Examples of splitting a complex shape.....	17
Figure 3: Experimental set-up of the VARTM process using two rigid mould halves.....	19
Figure 4a: L-shaped mould	
Figure 4b: Flat shaped mould.....	20
Figure 5: Composite part dimensions.....	20
Figure 6: Manufactured moulds used for testing	21
Figure 7: Milling of L-shaped mould	21
Figure 8: Procedure followed in processing the measurements	22
Figure 9: Infusion simulation procedure considering draping effects.....	30
Figure 10: Infusion simulation procedure	31
Figure 11: Resin viscosity data points of Prime 20 ULV	33
Figure 12: Data flow diagram of experimental verification of simulation	35
Figure 13: Comparison of experimental to simulation results at 70 kPa	37
Figure 14: Variables that possibly influence the laminate cutting process	40
Figure 15: Dependence of cutting velocity on the number of plies in a batch.....	41
Figure 16: Logarithmic regression of cutting velocity based on the median	41
Figure 17: Variables that possibly influence the mould release agent application process	43
Figure 18: Linear estimation of handling time for flat shaped parts	44
Figure 19: Linear estimation of handling time for L-shaped parts	45
Figure 20: Handling factor based on the flat shape.....	45
Figure 21: Mould release agent application process, case 1	46
Figure 22: Mould release agent application process, case 2	46
Figure 23: Box-plot of handling time for flat- and L-shape.....	47
Figure 24: Pareto diagram of predictors on the total mould release agent application time....	47
Figure 25: Variables that possibly influence the laminate lay-up process	48
Figure 26a: Simplified test flat shape	
Figure 26b: Simplified test L-shape	49
Figure 27: Residual working time for one fibre ply lay-up by flat shaped cavity	50
Figure 28: Pareto diagram for the variables of the flat shape lay-up time	51
Figure 29: Working time for laminate lay-up for flat shaped parts.....	51
Figure 30: Residuals working time for one fibre ply lay-up for L-shaped cavity.....	52
Figure 31: Pareto diagram for the variables of the L-shape lay-up time.....	52
Figure 32: Working time for laminate lay-up for non-flat shaped parts	52
Figure 33: Lay-up complexity factor on base of flat shaped lay-up	53
Figure 34: Variables that possibly influence the CPFM process	54
Figure 35: Sequence of mould and resin preparation.....	55
Figure 36: Clamping time comparison for both shapes	56
Figure 37: Variables that possibly influence the infusion process.....	57
Figure 38: Influence of angle and part area on infusion time	60
Figure 39: Influence of radius and part area on infusion time	61
Figure 40: Influence of part thickness and part area on infusion time	61
Figure 41: Influence of fibre volume fraction and part area on infusion time	62
Figure 42: Influence of infusion pressure and part area on infusion time.....	62
Figure 43: Influence of resin temperature and part area on infusion time	62

Figure 44: Possible predictors of the curing time	63
Figure 45: Temperature measurement of Prime 20 ULV	64
Figure 46: Demoulding times for flat and L-shaped parts	65
Figure 47: Chronological measurements for the part removal sequence	66
Figure 48: Measurements for the working time spend for cleaning the tools.....	67
Figure 49: Schematic of flow path and resistance.....	70

List of tables

Table 1: Fibreglass properties of 195 PW Tight	32
Table 2: Mixed resin system properties Prime 20 ULV	33
Table 3: Physical properties of the validation part.....	36
Table 4: Specifications for infusion simulation	36
Table 5: Comparison of total filling times for flat shapes.....	38
Table 6: Median of the mould and resin preparation process times.....	55
Table 7: Median of mould and resin preparation process times combined.....	56
Table 8: Range of resin infusion variables tested.....	59
Table 9: Common values used for the VARTM infusion	59
Table 10: Proposed components of direct material costs	73
Table 11: General production process plan	74
Table 12: Determination of hourly cost rate	74
Table 13: Distinction between standard machine cost and special once-off expenses	75

List of abbreviations

ACCEM	Advanced composite cost estimation manual
AMTS	Advanced manufacturing technology strategy
CAD	Computer aided design
CPFM	mould clamping, mould positioning, pipe mounting and resin mixing
DF	Degrees of freedom
DFM	Design for manufacture
DOD	Department of defence
DOE	Design of experiments
FAW	Fibre area weight (per ply)
HF	Handling factor
LCM	Liquid composite moulding
LRTM	Light resin transfer moulding
NASA	National aeronautics and space administration
RARTM	Rubber assisted resin transfer moulding
RIFT	Resin infusion under flexible tooling
RMS	Root mean square
RTM	Resin transfer moulding
SCRIMP	Seemann composites resin infusion moulding process
SRIM	Structural reaction injection moulding
TERTM	Thermal expansion resin transfer moulding
VARI	Vacuum assisted resin infusion
VARTM	Vacuum assisted resin transfer moulding
VIP	Vacuum infusion process
VRTM	Vacuum resin transfer moulding

List of symbols

Symbol	Description
A_1	Experimentally determined constant for fibre permeability
A_2	Experimentally determined constant for fibre compressibility
A_p	Part area
A_s	Part surface area
b_1	Experimentally determined constant for fibre permeability
b_2	Experimentally determined constant for fibre compressibility
C_{Ap}	Circumference of part area
C_{As}	Circumference of part surface area
C_D	Direct material costs
c_f	Specific heat fibre
c_M	Material consumption
C_M	Manufacturing costs
c_r	Specific heat resin system
c_R	Resistance coefficient
C_S	Special once-off expenses
C_{Total}	Total estimated cost for manufacturing
D	Thickness of the cavity, composite part thickness, diameter of the "runner", diameter of in and outlet
ϵ_{RMS}	Root mean square error
i	Index variable
k_1, k_2, k_3	Carman-Kozeny constant in x-, y-, z-direction
$\mathbf{K} = \langle \mathbf{K}_1, \mathbf{K}_2, \mathbf{K}_3 \rangle$	Permeability tensor in the x-, y-, z-direction
\mathbf{K}_{eff}	Permeability of "flexible mould"
$k_{eff,f}$	Effective conductivity fibre
k_p	Number of polynomial regressions
$k_{th,f}$	Thermal conductivity
$k_{th,r}$	Thermal conductivity
L_o, L_i	Shape length (outside, inside)
n	Number of tests, number of values
n_l	Number of applied layers
n_p	Number of plies in a batch, -in a laminate

p	Gauge pressure, differential pressure
\vec{p}	Pressure vector
p_0	Ambient pressure
p_{VAC}	Vacuum pressure
p_R	Degree of regression
R	Outer radius
R^2	Coefficient of determination
R_a	Range
R_{adj}^2	Coefficient of determination
r_f	Fibre radius
R_H	Hourly cost rate
r_i	Residual
R_M	Coste rate per unit of material
RV	Repurchase value
r_{xy}	Correlation coefficient
s	Standard deviation
T	Temperature
t_{app}	Total time for mould release agent application
t_{CFPM}	Total time for mould clamping, mould positioning, pipe mounting and resin mixing
t_{clamp}	Clamping time
t_{clean}	Total time for mould cleaning
$t_{clean \ A_s=4}$	Cleaning time for $A_s = 4 \text{ dm}^2$
t_{curing}	Total time for curing
t_{cut}	Total time for laminate cutting
$t_{demould}$	Total demoulding time
t_{dry}	Evaporation time of mould release agent
t_{handle}	Handling time of mould release agent
t_i	Time for each working step
t_{inf}	Total time for infusion process
t_{lay-up}	Total time for lay-up
T_M	Mould temperature
t_{open}	Time for opening the mould
t_{prep}	Preparation time
T_R	Room temperature

$t_{removal}$	Time for removing the part from the mould
T_{RS}	Resin temperature at infusion
t_S	Start of infusion time
t_{work}	Laminate lay-up working time
v	Fluid velocity
V	Volume (incl. fitting)
\vec{v}	Fluid velocity vector
v_{ar}	Variance
v_{cut}	Cutting velocity (manual or automatic)
\vec{v}_f	Interstitial Darcy velocity of the fluid
V_f	Fibre volume fraction
w	Porosity of cavity
W	Shape dimension, width
x	Value (x-axis)
\bar{x}	Mean value (x-axis)
Δx	Specimen thickness
x_{min}	Smallest value in range
x_{max}	Largest value in range
x_{Q1}	Quantile 1
x_{Q2}	Quantile 2
x_{Q3}	Quantile 3
y	Measured value (y-axis)
\bar{y}	Mean value (y-axis)
\hat{y}	Predicted value (y-axis)
μ	Dynamic viscosity of fluid
$\bar{\mu}_{arithm}$	Arithmetic mean
Ψ	Angle
ρ_f	Fibre density
σ	Standard deviation

1. Introduction

Designs that include polymer composites have the advantages of better performance and lower weight compared to conventional metal designs. Polymer composites are used in many different applications, from aircraft and space structures to automotive, marine and sports applications. Their greatest advantages are that the composites can be designed to meet the specific needs of a particular structure and there is a wide variety of manufacturing processes available. Each of the manufacturing processes has its characteristics that define the product type to be produced. However, the high cost of manufacturing composites remains an economic barrier to their increased usage.

In this study, the manufacture of complex shaped composite parts using the vacuum-assisted resin transfer moulding (VARTM) technique with two rigid mould halves is investigated. Various design features and the total manufacturing costs are investigated. Complexity in this context is used to characterise composite parts with difficult geometries and is related to the difficulties encountered in producing the required shape, and with the expected characteristics.

The sections that follow include the following: background to the topic, motivation for the study, the research objectives, and a brief description of the outline of the document.

1.1. Background

Today's high performance companies in the aerospace and aircraft industry make use of advanced composite structures. Polymer composites belong to the category of advanced composites, and are considered high performance lightweight materials. Despite the excellent properties of composites, their acceptance in other industrial fields is low. A composite is typically utilised if there are no suitable alternative manufacturing processes or if the characteristics of a composite are significantly better than other materials.

There is a perception that polymer composites are expensive products. This is the case if the wrong design or manufacturing technique are chosen. One of the major problems however is that composite structures do not follow the same design rules as conventional structures do. Today's steel structures are often replaced by a composite part in the same design. This often leads to unsuitable and unnecessarily expensive designs, and sometimes it is impossible to directly replace the part by using a composite. Each composite manufacturing technique has its specific advantages, and some techniques are not suitable for a required part or a desired production volume. By selecting the incorrect technique, one increases the costs of manufacture unnecessarily. A cost model can facilitate solving some of these problems; however, only a few researchers have considered this. The reason might be that composites are not homogenous materials, such as steel and plastic are, and it is more difficult to determine production costs when complex geometries are involved.

Zaloom & Miller (1982) have reviewed cost estimation techniques. They commented that Northrop and the US Air Force carried out one of the first attempts at cost estimation. This model is called the advanced composite cost estimation manual (ACCEM). It is a knowledge-based engineering tool to estimate cost and weight of composite aerospace structures at the conceptual stage of the design process, and allows trade-off comparisons of materials and cost effective design decisions. The model consists of parametric equations with a high level of detail, however, it is based on old manufacturing concepts and the database is outdated. Another disadvantage is that the model is only available to US governmental contractors, and complex shaped parts are not mentioned. Zaloom & Miller (1982) also mention the department of defence (DOD)/ national aeronautics and space administration (NASA) Structural Composite Manufacturing Guide. This guide presents the manufacturing cost per hour on an A-9 aircraft. A learning curve with the number of parts and the cost per hour gives an indication of the final manufacturing cost. According to Zaloom & Miller (1982) this model is also outdated, and only available to US governmental contractors. The models described are all rather old and the estimation approach seems to be very rough.

Gutowski et al. (1994) developed a simple theoretical cost model for the manufacturing of advance composites. Their estimation focused on human time and machining activities, divided in three steps: the development of simple dynamic steps, the summation and simplification of these steps, and the development of a complexity theory. They first investigated flat shapes and then they used the "information theory" developed for the communication field to account for parts that are more complicated, such as stiffeners. Their model gave good results compared to hand lay-up experiments and the ACCEM model. However, their paper still leaves many unanswered questions; more complex parts, such as double curved ones, were not investigated. This model also does not look at infusion techniques. Most of the other available articles about cost models for composites are based on the ACCEM cost model and implement them in computer aided design (CAD) software. There is therefore a clear need for a cost model that is based on experiments, has a higher level of detail, is flexible for adaption to newer materials, and allows the comparison of manufacturing concepts.

1.2. Motivation

The advanced manufacturing technology strategy (AMTS) of the South African Government wants to improve the competitiveness of the South African composite industry to position itself well for the future and to increase the manufacturing of composites. The use of resin infusion techniques is seen as one of the solutions to achieve this goal. However, these techniques require research, and expertise has to be created.

As indicated earlier, there is a need to reduce the resistance to the use of resin infusion techniques. This can be achieved by establishing expertise in this field. An infusion cost estimation model will provide a base to compare different manufacturing techniques and to select the most cost effective manufacturing method. This should contribute to increased

acceptance of infusion composite manufacturing techniques and composites in general, and result in a higher competitiveness on the global market. Based on results of experimental tests, a cost model should give a preliminary cost estimation with the materials and geometry as well as the process parameters. Further, a cost model will highlight cost drivers, thus generating knowledge required for the design for manufacture (DFM), which supports designers during the development stage to manufacture a part at the lowest possible cost.

1.3. Research objective

The objective of this research study is the development of a preliminary cost estimation model for the VARTM technique based on the use of two rigid mould halves. This cost model, based on initial design and process data, generates a baseline to compare manufacturing costs of different techniques and enables further developments and optimisations in this production process. Shapes with various complexities were taken into account and their influence on the manufacturing process and costs are displayed. The cost model can be used as a DFM tool and to select the most cost effective manufacturing technique.

The focus here is on small to medium sized components for prototypes, and low production volumes. The structure has to be modular, open for adaptation to other infusion techniques, as well as flexible for use in industry. Some composite companies do not make use of CAD software; therefore, the estimation must be simple and able to be performed manually.

1.4. Outline

The study commences with a literature review in Chapter 2, which gives the necessary insight into several relevant topics, and presents evidence for decisions that were made during this study. Chapter 3 presents the principal approach to making complexity measurable, and points out the limitations of this study. Chapter 4 describes the experimental set-up, the mould design, and the manufacturing process. The analytical procedures and the necessary statistics are described in Chapter 5. An introduction to and validation of the simulation software is described in Chapter 6. Chapter 7 presents a detailed analysis of basic shapes and Chapter 8 explains how the basic shapes are applied to complex shapes. The final cost model is presented in Chapter 9. Chapter 10 includes a case study, where the model is compared to an industry part. Conclusions and recommendations are contained in the final chapter, Chapter 11.

2. Literature review

The literature review briefly covers aspects that are essential to overcome the challenges that are taken on in this study. The purpose is to provide more insight into selected aspects and to provide reasons for certain decisions that were made. The following main topics are addressed: composite manufacturing techniques, the VARTM technique, the design of experiments (DOE) methods, and infusion simulation software.

2.1. Composite manufacturing techniques

It is not only the resulting light weight of composites that makes them widely applicable for different technologies; several other interesting features contribute to their amazing properties, for example, chemical resistance, high tensile strength, high dynamic strength, high elastic modulus, good shock absorption, a low thermal expansion coefficient and crack toughness. There is also a broad range of available manufacturing techniques. However, their greatest advantage lies in the combination of these properties. The advantage of low weight in combination with high stability is the most important factor for the aerospace industry. Surgery and measuring instruments make use of composites because of the body's acceptance of certain composites and the low thermal expansion coefficient, respectively. The principal composite manufacturing techniques are described here. The purpose is to provide an overview and to show the applicability of each process type. First the classical techniques are addressed – here classical techniques mean all major alternatives to infusion – and then the infusion techniques are addressed.

2.1.1. Classical techniques

In order to understand the application of the VARTM technique it is necessary to first understand the nature of competing techniques. This sub-section will provide a brief overview of these classical techniques. The following are explained: the hand and spray lay-up, the pultrusion, filament winding, prepreg, tape placement, vacuum bag moulding and autoclave moulding, pressure bag and compression moulding.

2.1.1.1. Hand lay-up and spray lay-up

The hand lay-up is one of the oldest techniques and belongs to the open mould category. The operator places the reinforcement and the resin mix manually on a one-sided mould and thereafter the resin-reinforcement mixture is compressed with a hand roller.

The spray lay-up is also an open mould technique. Here the operator sprays the reinforcement and the resin on one mould half. The fibre is usually already chopped and mixed with the resin stream before the spraying process.

The advantages of the two processes are high design flexibility and low tooling costs due to the simplicity of the process. The repeatability and the quality of the parts depend mainly on operator expertise. (Peters, 1997)

2.1.1.2. Pultrusion

The pultrusion technique is one of the best-automated composite manufacturing techniques. It stands for the manufacturing of a continuous profile with a constant cross-section. There are two pultrusion techniques: the open and the closed techniques. In the open technique the fibres are wet in a resin bath, and then formed through a heated die, where the heat catalyses the resin cure. In the closed technique, the resin is applied when the reinforcement is already in the desired cross-section dimensions. (Peters, 1997)

2.1.1.3. Filament winding

Filament winding is the coiling of wetted reinforcements on a rotating core. The core represents the inner dimension of the manufactured product. There are two methods of filament winding: the "wet method" and the "dry method". The wet method uses dry fibres that are wetted with resin and wound in several layers on the core. The dry method utilises pre-impregnated fibres. The tension of the reinforcement string determines the characteristics of the composite part. Higher tension during winding leads to stiffer parts with higher strength, whereas lower tension leads to part with more flexibility. Larger angles ("hoop") increase the crush strength and smaller angles increase the tensile strength. The process is fully automated, but limited to round and rectangular parts. Advantages include good repeatability and high fibre content. (Peters, 1997)

2.1.1.4. Prepreg and tape placement

Manufacturing with "prepregs" is a widely used technique in the composite industry, due to high reproducibility and good product quality. A prepreg is pre-impregnated fibre with a pre-cured resin. The fibre is usually in the form of woven mats. The end manufacturer places the prepreg plies on one mould half and completes the cure with heat. The fibre content is easily controlled and the product quality is very stable. However, the costs of production and storage are relatively high. Tape placement is the automated variant of the prepreg placement, carried out using an automated prepreg roller. (Peters, 1997)

2.1.1.5. Vacuum bag moulding and autoclave moulding

Vacuum bag moulding and autoclave moulding make use of a flexible membrane such as a plastic bag and a rigid mould half. The hand lay-up or prepreg placement can be used in combination with the vacuum bag moulding or the autoclave moulding. The process commences with the lay-up, followed by the sealing of the membrane on the rigid mould half. Then a vacuum, of up to 100 kPa gauge pressure, is applied on the cavity between the mould and the membrane, and thus the laminate is compacted. Finally, the set-up is placed in an oven or autoclave to complete the curing process.

The option that includes the autoclave is called autoclave moulding. Here a higher than atmospheric gauge pressure, in the range 200 kPa to 700 kPa, is applied to provide additional pressure to the vacuum from the outside on the membrane. This further removes volatile matter and enables control of the laminate thickness. The composite parts manufactured by this method are known for their high quality, and are therefore suited for high performance parts. However, the production costs are high, which limits the applications. (Peters, 1997)

2.1.1.6. Pressure bag moulding

Pressure bag moulding uses a similar set-up to vacuum bag moulding but, in the case of the former, the compressing pressure results from a pressure bag mounted on top of the rigid mould half. The bag is inflated to a gauge pressure of 200 kPa to 350 kPa. (Peters, 1997)

2.1.1.7. Compression moulding

Compression moulding commences with the placement of the reinforcement on one mould half, followed by the addition of resin. Then the other rigid mould half is lowered to compress the laminate. The resin is pressed into the laminate and the excess resin can exit the mould during compression. Optional heat can be applied to reduce the cycle times. (Peters, 1997)

2.1.2. Infusion techniques

This sub-section explains the different resin infusion manufacturing techniques. The following topics are addressed: categorisation of the composite infusion techniques, categorisation of mould types, and the resin transfer moulding (RTM) technique.

2.1.2.1. Categorisation of infusion techniques

One polymer composite manufacturing category is liquid composite moulding (LCM). Here the reinforcement and matrix material are combined during the manufacturing process. The resin infusion techniques are part of LCM where pressure is used to infiltrate the

reinforcement. VARTM is part of the resin infusion techniques. Beckwith (2007) describes the resin infusion as "an alphabet soup" of acronyms pertaining to well over 40–50 processes that are often considered part of this technology. He categorised the resin technology into two distinct categories, RTM and the vacuum infusion process (VIP). RTM uses pressure higher than atmospheric pressure and VIP uses pressure lower than atmospheric pressure to infuse a resin mix into the mould cavity. Beckwith (2007) also states that VIP is often called VARTM as a generic term in the industry. Other terms like vacuum-assisted resin infusion (VARI) and vacuum resin transfer moulding (VRTM) exist for the same production method. The reasons for there being so many terms are related process innovations and marketing.

Beckwith (2007) further mentions a third hybrid category, which makes use of both the first and the second category. Examples of the hybrid category are thermal expansion resin transfer moulding (TERTM) and rubber-assisted resin transfer moulding (RARTM). It should be noted that some infusion processes, such as the Seemann composites resin infusion moulding process (SCRIMP), are patented (U.S. Pat. No. 5316468). Williams et al. (1996) reviewed the development of resin infusion under flexible tooling (RIFT) and the patented SCRIMP, which belongs to this category, and stated that the technique is clean and economical, and should be considered for future research. Advantages are reduced styrene emissions and relatively inexpensive tooling for small to medium applications, compared to that of other methods such as RTM.

2.1.2.2. Categorisation of mould types

Modern applications have ever-higher requirements for dimensional accuracy and surface quality. It is mainly the mould type that defines these characteristics. A distinction is made between open mould type processes and closed mould type processes (Owen et al., 2000). The open mould types can be further split into the "one-sided rigid moulds", where one side is solid and the other side is open (Rudd et al., 2007), the rotating mandrel, the heated die and the heated mould which represent the tool for the process.

The closed mould types have the advantage of reducing the exposure of the operator to poisonous volatile matter. These processes can be further split into the one-sided rigid mould and the "two-sided rigid mould". The one-sided rigid mould uses a flexible membrane such as a plastic bag to close the mould cavity. The two-sided rigid mould consists of two rigid mould halves or one rigid and one semi-rigid mould half (Rudd et al., 2007). Here semi-rigid stands for a slightly flexible mould half, to allow compression due to the vacuum pressure. This mould half can be made from material such as fibreglass.

The author identified the need for a categorisation of manufacturing techniques. Categorisation of composite manufacturing techniques, including the selected VARTM technique, with two rigid mould halves, is presented in Figure 1.

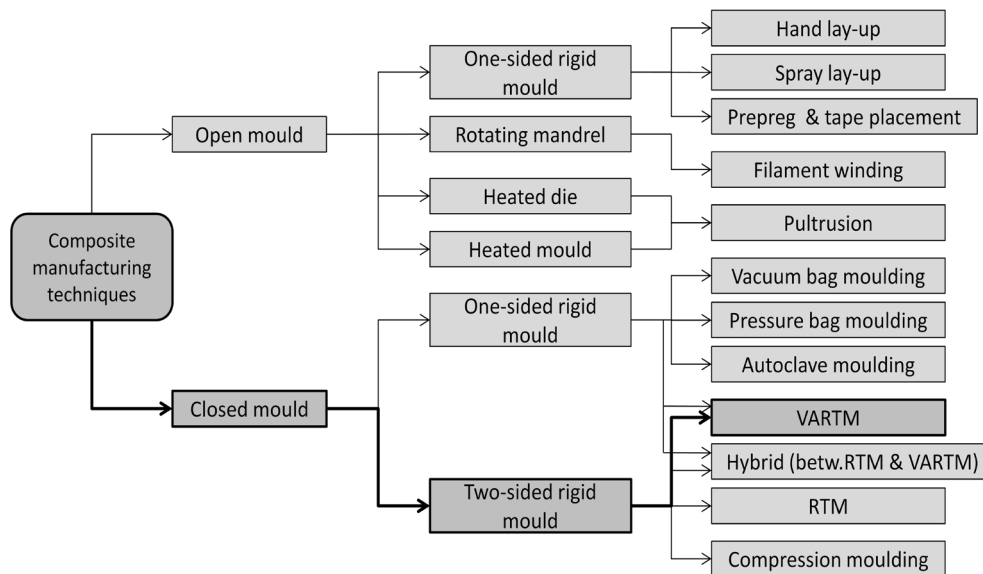


Figure 1: Categorisation of composite manufacturing techniques

Characteristics

The one-sided rigid mould has only one high quality surface finish, has less expensive tooling costs and a higher flexibility for demoulding in comparison to a two-sided rigid mould (Williams et al., 1996). Two rigid mould halves are characterised by higher tooling costs, especially for larger moulds (Chin & Wong, 1996). Therefore, they are preferred for small to medium sized moulds. Advantages of the two-sided rigid moulds are relatively high automation possibilities, faster set-up times for closing the mould, higher repeatability (Moore & Bland, 1999), and a high dimensional stability up to near net shape quality. However, the design rules for mould making (Veldsman, 1995) have to be followed to allow demoulding without damaging the parts.

2.1.2.3. Resin transfer moulding

The RTM process makes use of the closed mould type (Beckwith, 2007) with the two rigid mould halves. Pressure higher than atmospheric pressure (100 kPa to 700 kPa) is applied to inject the resin into the cavity. The tooling costs are usually higher than in the case of VARTM because of the higher pressures that the mould has to withstand. (Peters, 1997)

2.2. Vacuum assisted resin transfer moulding

The VARTM technique, with the configuration of two rigid mould halves, is used in this study. This technique infiltrates the reinforcement at pressures lower than atmospheric pressure. This section reports information gathered from a literature research on composite manufacturing, manufacturing of the moulds, and the simulation settings. The following

specific topics are addressed: design considerations, material properties, and the effect of the mould temperature.

2.2.1. Design considerations

Rudd et al. (2007) have presented a detailed description of mould design, including different mould materials, mould design procedures and the use of shell moulds. The most important considerations in this study are safe part release, tight sealing at all times, and the port and vent placement. The port and vent positioning, and the mould sealing are now addressed.

2.2.1.1. Port and vent positioning

The success of infiltrating the laminate depends heavily on the positioning of the appropriate inlet and outlet ports. Veldsman (1995) has presented a basic guide for the port positioning and other design considerations. According to him, the infusion port should be at the lowest point of the cavity and the vents should be on top of the cavity to facilitate complete air removal. Furthermore, the infusion should be done from the thicker to the thinner areas to avoid dry spots. Hsiao et al. (2001) developed an analytical model for RTM and VARTM to predict the pressure distribution in a cavity with two air vents. This model can be further used to change the pressure gradients on the flow front, and therefore control the mould filling. The analytical model is derived from a "sink and source" model and it compares well to verified simulation software. However, the model accuracy decreases with higher preform permeabilities and when the distance to the vents decreases. These results are similar to earlier findings, which reveal the sensitivity of the flow front controlling techniques to higher permeability.

2.2.1.2. Mould sealing

A stable manufacturing process requires, besides suitable manufacturing parameters, reliable sealing of the mould. There are two principal mould-sealing methods, the first involves the use of an O-ring and the second involves vacuum sealing. The first method requires a conventional O-ring, which is tightened with bolts to compress it. This method is time consuming and more complex shaped moulds are difficult to seal. The second option is vacuum sealing, which requires a double sealing around the mould and stronger vacuum as used in the cavity. In the case of a leak, the resin flows in the sealing cavity instead of air entering the mould. Advanced mould design can drastically reduce the clamping time (Veldsman, 1995) as well as the number of defective parts due to a leaking seal.

2.2.2. Material properties

Important material properties of the composite constituents that are required to ensure repeatable composite manufacturing and to allow an accurate infusion simulation are now discussed. These include the fibre permeability and the matrix properties.

2.2.2.1. Fibre permeability

The reinforcing material can be fibreglass, carbon fibre or aramid fibre, and optional cores such as a honeycomb core. Only fibreglass was used in this study. Fibre permeability describes the resistance of a fibre to infiltration. A brief review of how other researchers determined the value of fibre permeability value follows.

Gutowski et al. (1987) investigated the dependence of the permeability on the fibre volume fraction. They found a strong influence of the fibre volume fraction and showed that the Carman-Kozeny equation gives good agreement with the permeability measurement in the axial fibre direction when using silicon oil to infiltrate the fibre. They also observed an over-prediction when using a bleeder ply. Joubaud & Trochu (2002) studied the permeability behaviour in the RTM and VARTM methods. According to them, the most commonly used equation for the description of the permeability (K) depends on the fibre volume fraction (V_f) and two characteristic constants. Equation 2.1 presents this relationship. The constants A_1 and b_1 must be determined for each fibre.

$$K = A_1 V_f^{b_1} \quad (2.1)$$

They further state that this formula is reasonably acceptable for rigid mould halves, but not for a mould with a flexible membrane. They therefore presented a modified "flexible mould" permeability (K_{eff}), shown in equation 2.2. Here A_2 and b_2 are compressibility parameters of the laminate, p_0 is the ambient air pressure, and p_{VAC} is the applied vacuum pressure.

$$K_{eff} = A_1 A_2^{b_1} (p_0 - p_{VAC})^{b_2 b_1} \quad (2.2)$$

The exponential equations of Joubaud & Trochu (2002) were applied on the "Multimat" (Syncoglass, Belgium) and the results are compared to exponential interpolated radial permeability measurements obtained by Luo (2001). The flexible mould permeability measurements showed reasonable agreement, which then led to the implementation of the equations into the LCMFlot software. The LCMFlot software simulation was finally to an experimental ambulance roof filling compared and showed good agreement. Van de Ven et al. (2006) designed a device to measure the out-of plane, or so-called transversal, permeability and compression. They described the fundamentals of the device and stated that the measurements agreed well with those reported by other researchers. However, their device is better than other devices because the fibres can be rapidly changed.

Scholz et al. (2007) presented their device for measuring gaseous and fluid transversal permeability. They measured the influence of fibre thickness and vacuum debulking on different fibre preforms. The permeability difference between the fluid and the gaseous medium was found to be relatively small. They also found the following: the permeability variation of one plain-woven fibre in the same batch is 8% and vacuum debulking reduces this to 5%, and vacuum debulking by 15 fibreglass layers reduces the transversal permeability by more than 15 times.

Visconti et al. (2003) also investigated the in-plane permeability, but on different types of fibreglass, and validated the well-known Carman-Kozeny equation. The Carman-Kozeny relationship for the x-direction is presented in equation 2.3 and is determined by measuring the permeability in a device. If the characteristic Carman-Kozeny constant (k_1) and the fibre radius (r_f) are known, then the permeability can be calculated for other conditions such as higher fibre volume fractions.

$$K_1 = \frac{r_f^2}{4k_1} \frac{(1 - V_f)^3}{V_f^2} \quad (2.3)$$

Visconti et al. (2003) further presented an analytical model, based on the electrical resistance, to calculate the permeability of a stack consisting of two different fibres. They claim that this model correlates with experimental results.

Golestanian (2008) investigated preform permeability and porosity. He tested three different fibre configurations with three different porosities, respectively, for constant pressure, resin system and different materials. His experiments showed that the woven preform permeability for carbon and fibreglass was orthotropic and that the permeability increased drastically in the case of a "certain" increase in porosity (0.49–0.56). He therefore recommends a decrease in permeability and an increase in fibre volume fraction to achieve faster manufacturing cycle times and cost savings. He further found that the carbon fibre mats had about three times lower permeability values compared to fibreglass mats with the same configuration; thus the carbon mat infusion will take much longer.

Gokce et al. (2005) generated a numerical model for the permeability estimation of the distribution media. This model enables the prediction of in-plane and out-of-plane permeability, despite race tracking and the use of mixed composite materials. The results were validated in a virtual environment and using a 1D flow experiment. Large deviations were recorded.

2.2.2.2. Matrix material

The matrix material that surrounds the reinforcing fibre holds it together and protects it from damages and environmental influences. There are typically three types of matrix materials, polyester resin, vinyl ester resin and epoxy resin. Optional fillers, accelerators and pigments

can be used to modify the properties of the resin mixture. The following two sub-sections explain the resin system degassing and the resin viscosity.

Degassing

Degassing is performed after the resin mixing. After the resin system and the optional components are mixed in a calm way, the mixture is placed in a pressure chamber at close to high vacuum. This degassing removes dissolved volatile matter from the mixture and prevents degassing in the mould cavity during infusion. (Rudd et al., 2007)

Viscosity

The viscosity of the resin system is a fundamental property of the VARTM process. The general rule is that the lower the viscosity the better is the wetting out of fibre plies. An increase in temperature will result in thermal thinning and a decrease in viscosity (Grujicica et al., 2005). The resin will subsequently begin to decrease the gel time and the viscosity will increase as the degree of polymerisation increases (Rudd et al., 2007).

2.2.3. Effect of mould temperature on infusion

Kaynak et al. (2008) conducted tests on the effects of mould preheating and resin temperature, and on using optional vacuum for the RTM process. They tested the strength, Charpy impact toughness and flexural strength. They also measured the void content with the percentage of decibel loss to determine the number of defects in the part. They found that mould preheating to 60 °C resulted in the best mechanical properties. They also found that an optional applied vacuum of 0.03 bar resulted in the lowest void content, and that the resin temperature had a similar effect to the mould preheating. However, lower temperatures of around 15 °C led to reduced mechanical properties.

Lebrun et al. (1996) studied the influence of mould preheating and its effects on the pressure distribution in the cavity. Temperature profiles were measured at different locations and different temperature measurement methods were evaluated. It was found that steel-sheathed thermocouples are more practical than thermocouple wires in the reinforcement. The steel-sheathed J-type thermocouples placed 2 mm away from the mould wall conditions gave best results. It was also shown that temperature control is important for the success of the infusion process, because a thermal boundary layer is developed during infusion process. This layer and other aspects such as different part thicknesses lead to temperature gradients in the cavity, which causes material defects.

Grujicica et al. (2005) implemented non-isothermal filling equations into a non-commercial VARTM simulation software for isothermal filling. Further, they use optimization to minimise the infusion process time with changing mould temperature, using tool plate heating

and an epoxy resin. It was found that tool heating is especially beneficial for smaller parts. A simple rectangular geometry was found to have the shortest infusion process time by 80% ambient temperature filling and 20% tool plate heated filling with 3.2 K/s. In this case, the optimisation algorithm reduced the filling time by about 5%.

2.3. Design of experiments

The experimental test planning depends mainly on the number of predictors, the experience with the subject as well as the cost and time. The experimental design should cover the range that has to be investigated. A rising number of predictors increase the number of tests which can be time and cost expensive, especially with traditional methods that changes only one factor at a time. DOE is a more efficient method for the planning of tests and for the processing of data. The aim is to describe the relationship between predictor and response with a systematic analysis by keeping the number of tests by a minimum. There are various types of DOE methods. The conventional method is the full factorial DOE. Others are fractional factorial, central composite, (optimal) Latin hypercube, Plackett-Burman, Box-Behnken, Taguchi and D-optimal (Wember, 2008). Each of these models has its applications and strengths. The Taguchi and the D-optimal methods are reviewed here.

2.3.1. Taguchi method

The Taguchi Method is named after the inventor, Genichi Taguchi. This well-known method is mainly targeted at making processes more robust against deviations from the desired values. Therefore, it can be used to improve a product or process quality by achieving the performance targets and, furthermore, it is possible to minimise the performance variation (Antony & Antony, 2001). The strength of the process is the clear systematic and high speed of the procedure compared to others methods. Many parameters can be reviewed simultaneously. Use of this process is most suitable in cases where the researcher knows that there are no interactions between predictors. The disadvantage is the obscuring of interactions of the different predictors. If it is not possible to distinguish which of the mixed predictors influences the process, one can reach wrong conclusion. In order to implement this method correctly, much training and expertise is required (Nedeß & Holst, 1992).

2.3.2. D-optimal method

The D-optimal method aims to achieve a DOE with the minimum number of tests, and still show distinct effects and interactions. Important characteristics are maximisation of the determinant and minimisation of the correlation and confidence intervals. The advantage is that the user is free to change the experimental test points and steps in the n-dimensional space for each variable. The characteristic of the D-optimal method is that the interaction between the correlation factors and the responses can be extracted from the correlation matrix.

Higher interactions (such as between the parameters A-B-C, A-D-E) are not considered because they usually have a relatively low impact compared to the simple ones (such as between the parameters A-B, A-C). Additional tests can be included (so called "inclusions") and tests that do not match at all (so called "outliners") can be excluded. Optionally, a minimisation of the confidence level for the regression coefficients is possible. The DOE is not fully orthogonal because of the characteristic that only a relative low number of tests are necessary, however the deviation is usually low. One difficulty is that the DOE has to be generated by an algorithm (exchange algorithm or randomised algorithm) (IMech, 2002; Wember, 2008).

2.4. Infusion simulation software

The commercially available state-of-the-art software and recent developments made in this field are now discussed, including different software packages, the software method and software validation methods.

2.4.1. Available software

Although liquid composite modelling is not new, there exist only a few commercial software packages for the simulation of the infusion process. Well-known products are the RTM-Worx (2010) from Polyworx and PAM-RTM (2010) from ESI (previously known LCMFlot). Another product is Autodesk Moldflow (2010), originally developed for plastic injection processes, but which is also applicable for RTM infusion.

Professional infusion software packages are relatively expensive compared to other simulation tools. The reason might be the high development costs and the limited competition. The author tested the software myRTM (2010) from the University of Rapperswil (Switzerland), which is available under the General Public License. The university claims however that the current version still has some restrictions for the import of complex shaped parts and that there is a problem with filling time calculations. During testing, it was found that the current release allows only one infusion port. MyRTM (2010) provides a first impression for the mould filling and is simple to use, but at this stage it is not competitive with commercial programs. Another university's software product is Liquid Injection Moulding Simulation (LIMS), developed at the University of Delaware (USA). Unfortunately, however, it must be purchased (Liu et al., 1996). This software is generated for RTM, but drape and flexible mould plug-ins are available. It allows the use of 3D elements and several ports and vents.

The software packages from ESI and Polyworx have various additional features, particularly the option for non-isothermal filling with 3D elements, mould preheating, mould filling and curing analysis, as well as a VARI option, making them more advantageous over competing packages.

Moldflow (2010) uses optimisation to determine the ideal port locations. This is done via "cavity balancing", where the original geometry is changed to achieve a desired flow pattern. PAM-RTM (2010) minimises the number of micro-and macro-voids enclosures (García et al., 2010), however the curves of the void content must be known. Mathur et al. (1999) used a finite-element volume based infusion simulation and implemented generic optimisation algorithms to minimise the dry sport formation and filling time. They defined a process performance index, which balances the relationship between both, minimum dry spot formation and filling time. Case studies and tests were conducted, and proved the method was successful within 99%.

Lam & Seow (2000) investigated changing the flow front pattern to achieve ideal cavity filling. They also used cavity balancing; in this case they predicted the flow front pattern by the so-called "hill climbing algorithm". The algorithm was implemented in the Moldflow (2010) software and was successfully tested in several 2D models.

García et al. (2009) presented a novel alternative method of computing the RTM infusion. This approach uses the meshless natural element method, and is based on the Galerkin method in combination with α -shapes. The new method has no numerical instabilities and needs no mesh. At the time of publication, they had compared 2D model pictures of the flow front progression to the commercial PAM-RTM software and they measured the resin mass conservation. The resin mass measurements and the pictures had a high level of agreement. Their proposed future work will be the extension of the model to 2.5D and 3D.

2.4.2. Software method

Most of the infusion software packages, including the selected PAM-RTM (2010), are based on the finite-element control volume method. Resin systems have a relatively high dynamic viscosity and hence the flow velocities are relatively low. It follows that the Reynolds number is less than 10 and the resin flow can be considered as laminar. Darcy's Law describes the resin flow at this condition and allows the assumption of an anisotropic porous media infiltrated by a fluid.

Darcy's Law, shown in equation 2.4, describes the relationship between the velocity vector (\vec{v}) and pressure gradient vector ($\nabla\vec{p}$) of the resin flow. Here, μ represents the dynamic viscosity of the fluid and \mathbf{K} stands for the characteristic permeability tensor in each direction.

$$\vec{v} = -\frac{\mathbf{K} \nabla\vec{p}}{\mu} \quad (2.4)$$

The interstitial Darcy velocity \vec{v}_f shown in equation 2.5 describes the flow rate through a cross-section. Here w can be calculated from the fibre volume fraction ($w = 1 - V_f$) and is the porosity as a percentage of the combined reinforcement, the so-called laminate.

$$\vec{v}_f = \frac{\vec{v}}{w} \quad (2.5)$$

The mass conservation in and out of a cavity is satisfied by the resin ($\nabla \cdot \vec{v} = 0$), and therefore equation 2.6 follows. This equation describes the flow through a constant porous medium in a rigid cavity, as is the case in this study.

$$\nabla \cdot \left(\frac{K}{\mu} \nabla \vec{p} \right) = 0 \quad (2.6)$$

Boundary effects and capillary forces between the fibres can increase or decrease the flow front velocity. These are assumed to be relatively low, and are therefore neglected in the PAM-RTM software (Rudd et al., 2007).

2.4.3. Validation methods

Black (2008) has reported various software validation methods. A first validation method is the mass conservation measurement while the mould is "bleeding". Therefore, the resin compound in and out of the lay-up is measured over time, and then compared to the simulation. Sensors can be used to obtain additional information of the local flow front behaviour. Black (2008) measured the mass conservation and compared their software filling simulation to an experimental aerospace part filling. The measurements agreed well and the software comparison showed a slight difference. This could be due to fibre permeability and simplified mould geometry.

Further review of validation methods reveals that Song et al. (2004) validated their isothermal software model by monitoring the characteristic flow pattern on a flat shaped part. They then compared their results with experimental results. Zhou et al. (2008) developed an analytical model to characterise the dual scale porous media flow pattern for the 1D case, at constant pressure. The dual scale flow pattern stands for a different flow pattern in the fibre strings than in the spaces between the fibre strings. Therefore, they used the bulk permeability and the string permeability with different fibres. They compared their analytical model to the experimental data by looking at the flow front pattern over time. According to Zhou et al. (2008) the developed function can be used to predict the permeability of preforms that show dual scale flow.

Lee et al. (1994) described the necessary mould filling equations for the RTM and structural reaction injection moulding (SRIM) processes in detail. They developed infusion software to simulate the mould filling, considering heat transfer and resin curing. When the temperature and curing conversion profiles of simple geometries were compared to the experimental data, they showed good agreement. At that stage, the models were limited to 3D for isothermal filling and to 2-1/2D for non-isothermal filling.

3. Materials and methods

This chapter explains the methods, and their limitations, and the materials used in this study.

3.1. Methods and limitations

Complex shaped composite parts are parts such as brackets with angles and radii, or double curvatures. The different geometries and shapes make cost estimation difficult. This is further compounded because composites are not homogenous materials, and a new approach to estimating the cost of manufacturing these parts is now required.

When considering the competing classical techniques (Section 2.2.1) and at the infusion techniques (Section 2.1.2) it is evident that virtually all techniques are applicable to the manufacture of shapes that have a sheet-like nature. Therefore, this study can be limited to sheet-like shapes. Here the complex shapes were split into simpler basic shapes. A review of competing techniques shows that round and rectangular shapes can be neglected, because these are well manufactured by the fully automated filament winding technique. Further investigation into shapes shows that flat and the L-shaped parts describe almost all complex shaped parts. Based on the above-mentioned information, it was decided to investigate such flat and L-shaped parts and its manufacturing time as well as the influence of more complex shaped parts on the production time. Depending on shape design, a complex shaped part can be split into many basic shapes and ultimately the manufacturing time can be estimated using existing laws described in Chapter 8. This allows a principal cost estimation of the manufacturing costs. Figure 2 illustrates the idea of splitting a complex part into basic shapes, the split is represented as a line inside the part. The infusion time is very sensitive to angles and radii, thus it was in detail investigated.

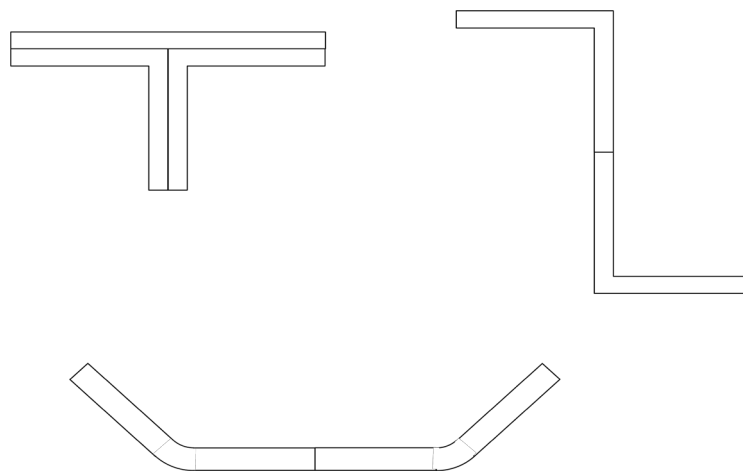


Figure 2: Examples of splitting a complex shape

In order to determine the cost model, the following procedure was followed:

- Design and manufacture simple shaped moulds
- Select a DOE and determine the analytical procedure
- Establish the experimental set-up
- Conduct various experimental tests
- Select infusion simulation software and perform infiltrations
- Analyse the data
- Carry out the transformation from simple to complex shapes
- Develop a flexible cost model
- Compare the findings to the findings of other researchers

There are many methods and material types applicable to the manufacture of polymer composite parts, and hence the scope of the present study had to be limited. Based on the characteristics of infusion and mould techniques reviewed in Section 2.1.2, it was decided to use the VARTM technique because of the relative inexpensive equipment and tooling. The two-sided rigid mould has a high dimensional quality and uniform thickness. Most of the manufactured parts are small- to medium-sized components, hence the study focuses on the maximum composite part dimensions (defined in Section 4.2.), with a length of $L_i = L_o = 500$ mm, a maximum width of $W = 500$ mm and a maximum thickness of $D = 10$ mm. The low pressure that is required leads to reduced tooling costs, which is advantageous for prototypes and low production volumes.

3.2. Materials

This following materials were used in this study. Plain-woven fibreglass (195 PW Tight) with a fibre aerial weight (FAW) of $195 \frac{\text{g}}{\text{m}^2}$ and a thickness of 0.16 mm was used. The reason for this is that the cost of fibreglass is moderate and the associated health and safety precautions are not as strict as for carbon fibre. The resin system used was the epoxy Prime 20 Ultra Low Viscosity (ULV) SP from Gurit (UK). The mould release agent Freecote 770-NC from Henkel was used. The adhesive spray Airtec 2 from 3M was used, as required, to fix the laminate in position. Gelcoat application is optional and was not included in the investigation.

Prices per unit and manufacturer and retailer details are presented in Appendix D.2.

4. Experimental set-up and mould manufacturing

The study is predominantly based on experimental measurements. This chapter describes the experimental set-up and composite part dimensions used in the tests that were conducted. An overview of the mould design and manufacturing phase is also presented.

4.1. Experimental set-up

Figure 3 illustrates the construction of the VARTM process. The process flow commences with the cutting of fibre layers, followed by the specified laminate lay-up in the mould cavity. Then the necessary pipes are connected after the mould is closed and sealed. Vacuum is then applied and the differential pressure between the vacuum pump and the atmosphere pulls the mixed resin through the inlet port and into the mould. The filling process stops when the laminate is infiltrated and the resin passes a certain mark on the vent. A resin trap is positioned behind the mould to avoid resin entering the vacuum pump. Once the curing phase has commenced one must wait until the part reaches dimensional stability before demoulding. Finally, the composite part is demoulded and the mould can be cleaned for the next manufacturing cycle.

The influence of gravity and the suction lift must be considered because of the low differential pressure. The moulds were always positioned such that the inlet port is the lowest point and the air vent is the highest point, as recommended by Veldsman (1995). Figures 4a and Figure 4b indicate the gravity force direction as a red arrow on the two manufactured mould types.

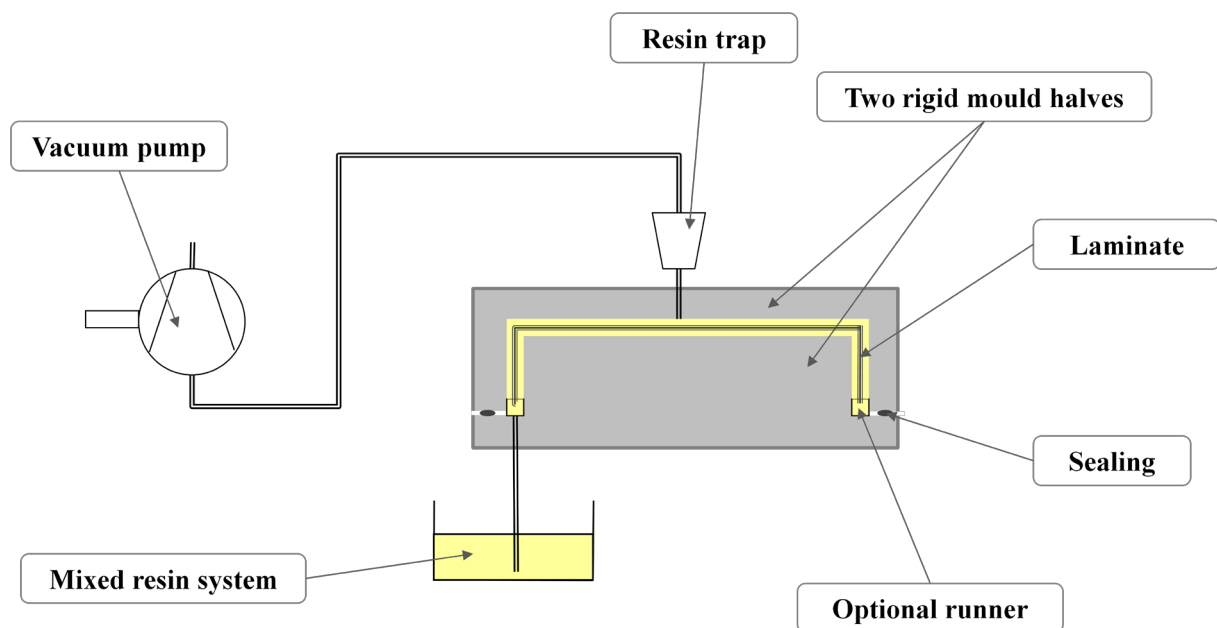


Figure 3: Experimental set-up of the VARTM process using two rigid mould halves

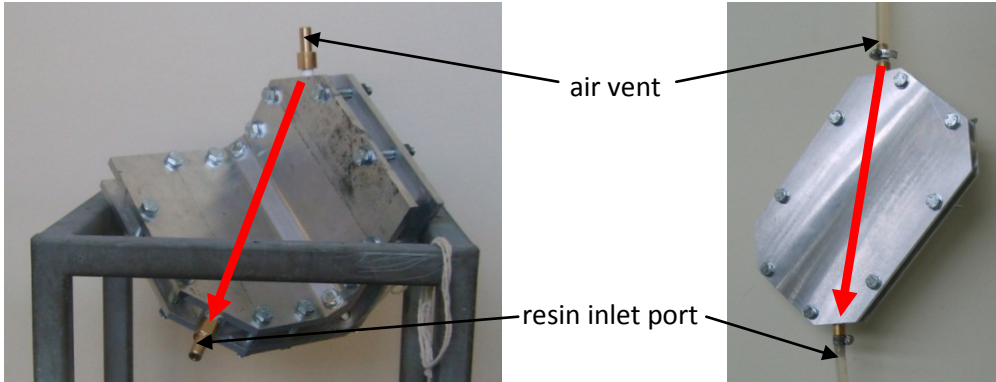


Figure 4a: L-shaped mould with gravity force direction

Figure 4b: Flat shaped mould with gravity force direction

4.2. Composite part dimensions

Figure 5 illustrates the dimensions used for this study. Further parameters are the part area (A_p) in equation 4.1, the part surface area (A_s) in equation 4.2, the circumference of the part area (C_{Ap}) in equation 4.3 and the circumference of the surface area (C_{As}) in equation 4.4.

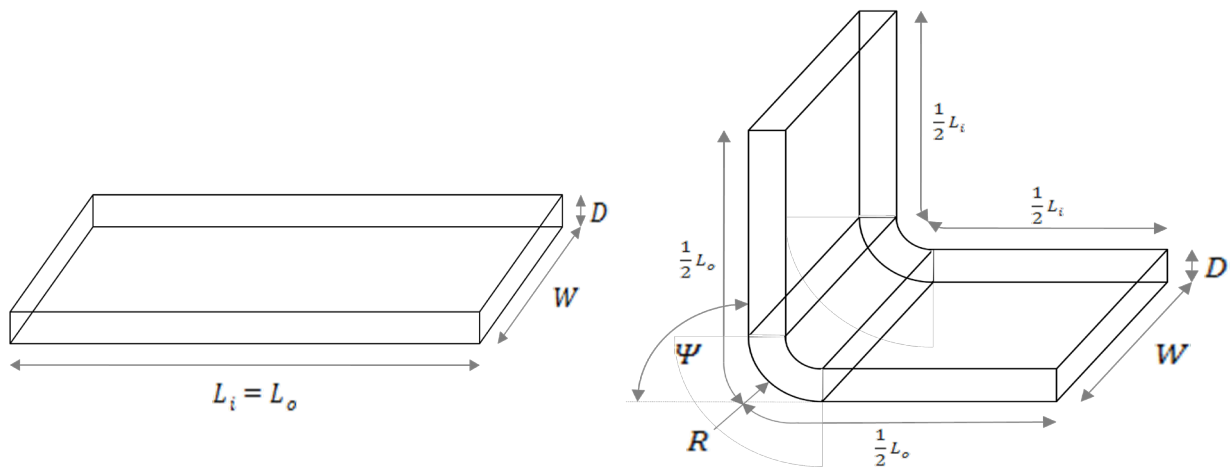


Figure 5: Composite part dimensions

$$A_p = L_i W \quad 4.1$$

$$A_s = W (L_i + L_o) \quad 4.2$$

$$C_{Ap} = 2(W + L_i) \quad 4.3$$

$$C_{As} = 2(2W + L_i + L_o) \quad 4.4$$

4.3. Mould design and manufacture

The moulds used were especially made for this study. The design and manufacturing phase is critical to the success of the composite parts. The most important factors to consider are the part release, port and vent placement, and tight sealing of the mould, as was discussed in Section 2.2.2. For this study, the recommendations of Veldsman (1995) and Rudd et al. (2007) were followed to design the mould. The mould has to withstand extensive testing, and therefore it was decided to manufacture them from a strong aluminium alloy (7075 T6). A CNC program was generated to mill the moulds on a 3-axis CNC-machine, as shown in Figure 7. All moulds are shown in Figure 6. The perspex mould used for the simulation was originally made by Cooper (2010). High production volumes were not a priority in this study, and therefore it was decided to use the well-known O-ring sealing method during the mould design phase. See Appendix F for the mould dimensions.



Figure 6: Manufactured moulds used for testing



Figure 7: Milling of L-shaped mould

5. Analytical procedure and statistical methods

The analytical procedure is the methodology used to obtain an equation for the estimation of the process time for each manufacturing step. The aim is to present a structured procedure for repeatability and to allow an adaption on additional manufacturing steps. The statistical methods refer to the tools used to process the experimental measured times. These methods allow the evaluation of the measured dataset and support the experimental test planning. This section describes the analytical procedure, statistical methods and how the data is displayed.

5.1. Analytical procedure

The general procedure followed to analyse the measured datasets is shown in Figure 8. The given procedure is not binding, and each infusion step was reviewed from different points of view in order to determine a universal characteristic function. All calculations can be manually performed, although this is not recommended for the correlation analysis. An alternative to use mathematical programs (Excel®, Maple®, Mathcad®, Matlab®, Mathematica®) or statistical programs (Minitab®, Statistica®). The author made use of both program types.

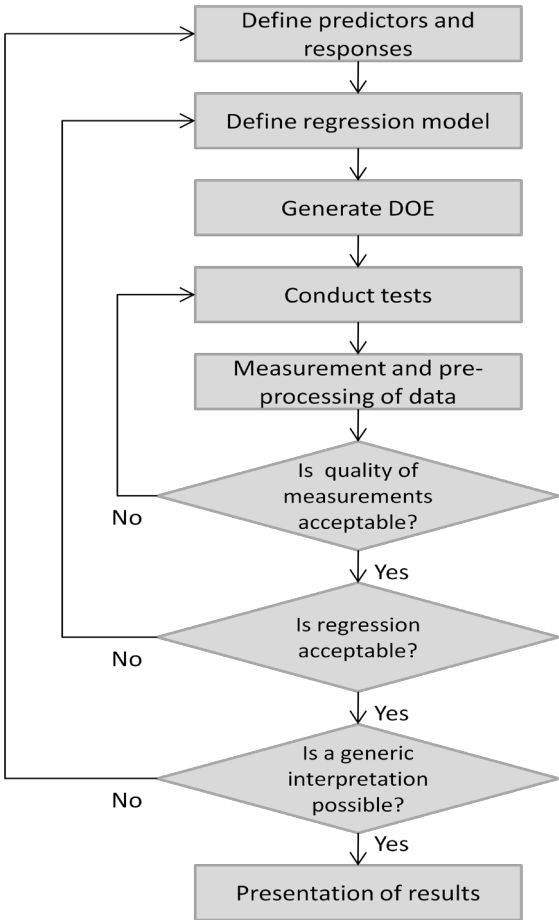


Figure 8: Procedure followed in processing the measurements

5.1.1. Steps in the analytical procedure

The procedure displayed in Figure 8 commences with defining the predictors and responses, and is followed by selecting the aimed regression type (Section 5.2.4.1). The D-optimal method (Section 2.3.2) was selected for use for all analyses. The next step involves conducting the tests according to the generated parameters. If a test cannot be carried out exactly as the DOE proposes, then it is possible to conduct the tests under closely similar conditions and adapt the DOE table. All measurements are collected after the "time study" method (Chase & Aquilano, 1992) and the data are either directly or indirectly used. Indirectly implies that the dataset is pre-processed – when this happens, it will be clearly explained.

First, the dataset is reviewed based on the central tendency, the spread (Sections 5.2.2 and 5.2.3) and possible outliers. A dataset with regression results is now available for processing and can be reviewed. The residual plot shows whether the selected regression adequately describes the dataset or whether another type of regression should be considered. In the latter case, the DOE has to be generated from the beginning. If the dataset in the residual plot is generally higher or lower compared to the estimation positioned, then there is the option of using different transformations (Nisbet et al., 2009) to stabilise the spread.

The result has to be checked in terms of the following:

1. Is a generic interpretation of the function possible?
2. Could a transformation of the responses improve the interpretability?
3. Is it advisable to change any predictors or responses?

5.1.2. Predictors and responses

It is not always known if certain factors have an influence on the prediction and, if so, how strong the influence might be. As many variables as possible have to be taken into consideration in order to test the influence of each variable on the response. However, a negative aspect related to this is that a larger number of variables increases the variance, and therefore the residual, between the measured values and the predicted values. There is then also the need to take more measurements. A trade-off therefore has to be made between both aspects.

There are different methods to determine if a variable has an influence on the system. This subject is only briefly addressed here. For a detailed discussion see the literature (Harrison, 1998; Nisbet et al., 2009; Wember, 2008). One option is to select physical parameters that are obvious. Another option is to use a stepwise regression procedure in combination with the backward elimination. This strategy considers all variables and reduces them systematically according to the significance value of each variable (p-value) (Nisbet et al., 2009). The significance threshold for this study was 3% (commonly 5%). Forward elimination works conversely; one variable is always added to the analysis and the significance values are

reviewed. It should be noted that both procedures do not necessarily arrive at the same result, because the significance considers the whole dataset for the calculation of one value. The preferred procedure is backward elimination, because it starts with all predictors and it gives a good quantification of the standard deviation, except when the number of predictors is so large that a forward elimination would be more efficient (Manson et al., 2003). Backward elimination was selected for use in this study.

5.2. Statistical methods and evaluation

This section covers the statistical methods and an evaluation of the techniques used to process the raw data. Statistical methods are based on the concept of sample tests of a basic population. The data of the underlying measurements are nearly always affected by measuring errors. Therefore, experimental uncertainties that arise can at least be described within certain statistical limits. The statistical test planning is an auxiliary tool to keep the number of tests low and simultaneously achieve acceptable models. One assumes that with the variation of the predictor the response factor will also change. All statements in this thesis are based on the assumptions that the data are normally distributed. The normal distribution results from the sum of many small scattering causes, none of which is dominant and none influence each other too strongly. It is generally recommended for experimental tests and has shown to be reliable (Wember, 2008). The discussion commences with the DOE, followed by the measurements of central tendency, the spread, the regression methods and finally the analysis of correlation.

5.2.1. Design of experiments

Design of Experiments is a tool to achieve an efficient analysis that covers the design space in a systematic way. This tool inspects various variables and their impact on the result. It is also possible to determine interactions between variables. There are two options available when using a DOE. One is to generate an approximation and the other is to use an optimisation algorithm to minimise or maximise a variable (Wember, 2008). The approximation option was used in this study.

Tests are costly to conduct and the ideal is that as few tests as possible be used for accurate predictions. The DOE should capture as much of the experimental space as possible and should be flexible for adaption to new conditions. This is because experiments do not always meet the ideal conditions, for example, the temperature changes. Conventional DOE, like the full factorial methods, is extremely expensive, and does not meet the requirements of this study.

A review of DOE methods is given in Section 2.4. Based on the literature review it was decided to use the D-optimal DOE for all analyses in this study. The main reasons were the

following: the great adaptability, the correlation analysis of parameters, and the requirement for a minimum number of experiments compared to conventional DOE methods.

5.2.2. Measurement of the central tendency

The measurement of the central tendency is given by the mean value. Equation 5.1 gives the arithmetic mean.

$$\bar{\mu}_{arithm} = \frac{1}{n} \sum_{i=1}^n x_i \quad (5.1)$$

The arithmetic mean reflects the focus of the measurements. It presents the average of all values and is strongly influenced by outliers. The median has, on both sides, half of the number of samples. This makes the median generally more robust against outliers.

The median or second quantile (x_{Q2}) is located in the middle of the number series, which is equivalent to the 50% quantile. Further factors are the 25% quantile (x_{Q1}) in equation 5.2 and 75% quantile (x_{Q3}) in equation 5.3.

$$x_{Q1} = round(0.25 (n + 1)) \quad (5.2)$$

$$x_{Q3} = round(0.75 (n + 1)) \quad (5.3)$$

5.2.3. Measures of spread

The spread of a distribution is a good measurement for the variability and therefore the reliability of the data. Common factors used to describe the measures of spread are the range (R_a), the variance (v_{ar}) and the standard deviation (s). The variance characterises the spread of the distribution. It can be used to compare spot tests from different batches. Equation 5.4 presents the variance. The variable \bar{y} is defined in equation 5.10 and σ , the standard deviation, is defined in equation 5.6 .

$$v_{ar} = \sigma^2 = \frac{\sum_{i=1}^n (y_i - \bar{y})^2}{n - 1} \quad (5.4)$$

The range in equation 5.5 is the smallest value subtracted by the largest value. It gives an indication of the statistical spread. It is only a rough indication, but improves as sample size increases.

$$R_a = x_{max} - x_{min} \quad (5.5)$$

The standard deviation of one regression is presented in equation 5.6. It is the most common measurement of the spread of a distribution and gives the width of it. However, the type of distribution must be known.

$$\sigma = \sqrt{var} = \sqrt{\frac{1}{n-1} \sum_{i=1}^n (y_i - \bar{y})^2} \quad (5.6)$$

5.2.4. Regression analysis

Regression analysis describes different statistical analysis methods. It is most often used to describe a quantitative relationship between one or more variables and some responses. This section describes regression types, followed by a qualitative check of whether the selected regression type is appropriate.

5.2.4.1. Types

Regression models are quantitative models for responses depending on some predictors. The simplest form is the linear regression, followed by the quadratic, the cubical, and fourth or higher order polynomials. Alternatives are the exponential or logarithmic approach, which aim to describe a relationship over time, such as the growth of a population. The linear regression will be used as default, because it is the most robust one. A learning effect can take place if a process is being repeated. Is the learning effect not or only infirm represented then a linear regression is suitable. If the learning effect is distinct, then a linear regression might lead by small number of probes to unrealistic values. A more realistic approximation is given with the exponential regression according to Levy (Ezey, 2000). On basis of Levy, a simpler logarithmic function is used.

5.2.4.2. Quality

There are many possible ways to evaluate the quality. In this section the focus will be on the root mean square (RMS) error (ϵ_{RMS}) and the coefficient of determination (R^2). To evaluate the conducted regression, the distance of the measurements to the values of the adjusted function, the so-called residuals (equation 5.7), are compared. Here y_i represents the values observed and \hat{y}_i stands for the predicted values of the associated model. The standard deviation is used to validate the determined values of the vertical distances. The corresponding value is called the RMS error or standard deviation of the regression (equation 5.8). The RMS is an absolute measure in the unit of the scale of the response value. The degrees of freedom (DF) in equation 5.8 is defined as $= n - p_R$, with n the number of values and p_R the degree of the regression. Here p_R will be two for a simple regression and three for a parabola. In the case of an n -dimensional space with many regressions (multiple regression) p_R will be $p_R = k_P + 1$, with k_P the number of polynomial regressions.

$$r_i = y_i - \hat{y}_i \quad (5.7)$$

$$\varepsilon_{RMS} = \sqrt{\frac{1}{DF} \sum_{i=1}^n r_i^2} \quad (5.8)$$

It is sometimes impossible to directly interpret the RMS error if no values are available for comparison. The coefficient of determination presented in equation 5.9 provides a solution. This coefficient can be used for different purposes; for this study it was used to show the proportion of the statistical spread of y caused by the regression. It varies between 0 and 1; the closer the value approaches 1 the better the dataset is described by the regression function. Here \bar{y} is the mean of the data, defined in equation 5.10.

$$R^2 = \frac{\sum_{i=1}^n (\hat{y}_i - \bar{y})^2}{\sum_{i=1}^n (y_i - \bar{y})^2} = \frac{\frac{1}{n-1} \sum_{i=1}^n (\hat{y}_i - \bar{y})^2}{\frac{1}{n-1} \sum_{i=1}^n (y_i - \bar{y})^2} \quad (5.9)$$

$$\bar{y} = \frac{1}{n} \sum_{i=1}^n y_i \quad (5.10)$$

The coefficient of determination tends to over-predict the variance for a small number of tests and a higher number of variables. Therefore there exists another value, the adjusted coefficient of determination, presented in equation 5.11. This value is always smaller or equal to the coefficient of determination and can be similarly interpreted for sample tests with a small degree of freedom.

$$R_{adj}^2 = 1 - \frac{n-1}{DF} (1 - R^2) \quad (5.11)$$

5.2.5. Correlation analysis

The correlation analysis aims to detect a relationship of variables. The correlation coefficient (r_{xy}) in equation 5.12 is a measurement of the linear relation between two measured variables. The coefficient lies between -1 and $+1$, where $r_{xy} = 1$ and $r_{xy} = -1$ states that all points lie on a line. The variables are not significant if r_{xy} is smaller than 0.2 but has a major influence if r_{xy} is larger than 0.8. The sign of this coefficient identifies whether the result increases or decreases with an increasing parameter (Wember, 2008).

$$r_{xy} = \frac{1}{(n-1)\sigma_x\sigma_y} \sum_{i=1}^n (x_i - \bar{x})(y_i - \bar{y}) \quad (5.12)$$

5.3. Methods of displaying the data

Several methods of displaying data are used in this study, three of which are specifically highlighted.

1. For data acquisition, the Ishikawa (or fishbone) diagram is suitable for the process illustration. The purpose is the complete acquisition of the possible predictors and responses, if possible. Bauer (2005) describes how to use the Ishikawa diagram, which is a graphic tool in the Six Sigma toolbox. All critical success factors are drawn on the horizontal backbone and the directly influencing causal factors are drawn as the "bones" of a fish. Ultimately, the factors that possibly could influence the causal factors are identified and drawn as "sub lines" on the "bones". Now each predictor can be analysed without any confusion. This technique is used here to determine the predictors of the reviewed process.
2. The box plot, also known as the box-and-whisker plot, is used to illustrate the spread of the measured data. This graph is well suited for the recognition of outliers and aims to give a quick overview of the dataset. The maximal and minimal values are the top and bottom (dotted lines) and the box is limited in height by the first and third quantile. The line in the box usually stands for the median, and values outside this range are outliers. McGill et al. (1978) investigated different box plots and suggested modified forms thereof to prevent misinterpretations.
3. The Pareto diagram is based on the Pareto principle, which states that most of the impact is caused by a small number of variables. Values with the highest significance are positioned on the left side and go over to the right side. The Pareto diagram shows relative effects in terms of a model. The predictor effects are often based on orthogonally scaled predictor values, so differences in units do not matter here.

6. Simulation

The use of simulation software is introduced in this chapter. The necessity for using infusion software for this study is highlighted, and different procedures used to conduct simulation analysis are explained. Material properties and process parameters, with the necessary simplifications, are described, before reporting on the experimental verification of simulation.

6.1. Why use infusion software?

This section explains the advantages of using infusion simulations and the choice of software used. The infusion process requires expertise. Preliminary simulation can prevent material defects, for example, dry spots, air enclosures, high porosity zones and cracks caused by resin shrinkage. Important factors for stable production quality include ideal port positions, a tightly closed mould during the production process, and a simple and safe release of the part from the mould (Section 2.2.1). Modification of an existing mould is expensive and it takes time.

Veldsman (1995) gives a basic practical guide for the positioning of the ports and vents (Section 2.2.2). The determining of the port and vent positions on complex shaped parts, even when following his guide, is difficult. One of the reasons is that the flow front in the cavity can drastically change due to a change in pressures distribution.

Infusion software allows the determination of port and vents positions as well as a checking simulation if the cavity is fully wetted out. It is possible to achieve an improved mould design, as well as optimisation of the process parameters, which will reduce the risk of part failure. There is a trial by error method and there are software options available that involve the use of optimisation algorithms to determine the ideal positions. A survey of commercially available software and freeware programs is given in the literature (see Section 2.4.1). Based on the reviewed literature on different infusion packages, it was decided to use the PAM-RTM (2010) software from ESI. The various features and the additional support offered were decisive. It would not have been possible to carry out this study in the allotted time period without simulation support. Angled shaped parts at the specified maximum dimensions, particularly, would require months to manufacture and test experimentally.

6.2. Procedure involved in using the software

The steps taken from the initial concept of the part to the simulation results are now reported. The options of considering and of neglecting draping effects are discussed.

6.2.1. Procedure of considering draping effects

This procedure considers different ply lay-ups, overlapping of plies and the exclusion of layers. The fibres are usually placed in the direction in which the strength is needed in order to optimize for a minimum of layers to reduce cost and weight. Strength oriented placement and placement on tools with shapes where the ply will crinkle may lead to gaps and holes in the lay-up. Holes have a similar effect as "runners", and facilitate faster flow of the resin through the micro-channels. This is often the root cause for dry spots. It is possible to simulate this effect, but much effort is required. For this it is necessary to use the software Patran (2010) instead of SimXpert (2010).

After a sheet is drawn in the CAD software it is imported into Patran (2010). The software itself and the included plug-in Laminate Modeller have the possibility to define laminates and the exact lay-up. Another option is to perform the lay-up in FiberSim (2010). The author tested the standard option for laminates in Patran (2010) (not the Laminate Modeller). The lay-up is defined and a so-called draping analysis started, which calculates how the fibre will crinkle. After meshing, the zones can be defined in Patran (2010) and ultimately the draping results, mesh and part are exported and imported into PAM-RTM. PAM-RTM calculates the local permeability from the draping results. The designer now knows the total permeability distribution of the fibres in the whole part. The following infusion simulation will be more accurate. The disadvantage is that if a person does the lay-up, not a machine, the laminate lay-up will always be slightly different and then the fibre might crinkle differently. The entire procedure is time intensive if there is not already a lay-up file available from, for example, a previous finite element calculation. Figure 9 illustrates the full procedure, including considering draping effects. The designer must also be aware that the import of the draping analysis from Patran (2010) into PAM-RTM (2010) is an additional feature that must be purchased. ESI offers PAM-FORM (2010) and the lighter version PAM-Quickform package, as alternative products, to perform a draping analysis.

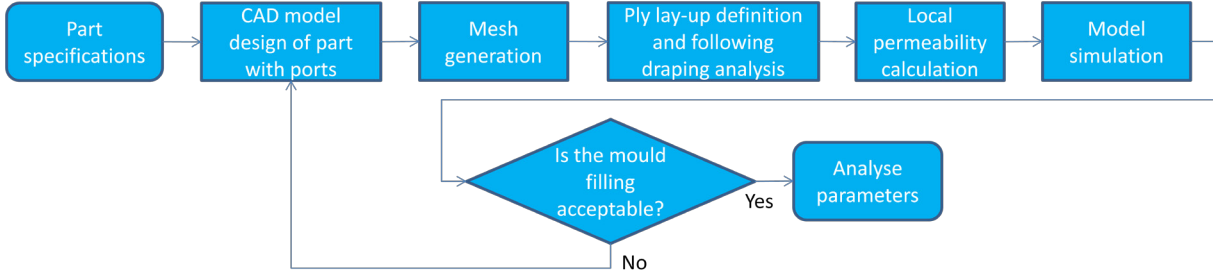


Figure 9: Infusion simulation procedure considering draping effects

6.2.2. Procedure of neglecting draping effects

Figure 10 shows the infusion simulation procedure. All the steps have to be followed for each simulation. The CAD model of the part is drawn in Inventor (2010) according to the

specifications. Then the ports are placed and the model is exported (using *.ipt file). The file is imported into SimXpert (2010) and a mesh is generated. It was found that the mesh must be only be generated with a finite element meshing program. The generated mesh and part is exported (using a *.nas file) and ultimately imported into PAM-RTM (2010). The simulation is started after the zone definition and the necessary parameters are set. A detailed explanation of the infusion software methods is given in Section 2.3.2.

The PAM-RTM (2010) software does not have any automatic port placement, therefore if the port is placed at an incorrect position, and an optimisation is recommended, the procedure has to be repeated from the beginning, as demonstrated in Figure 10.

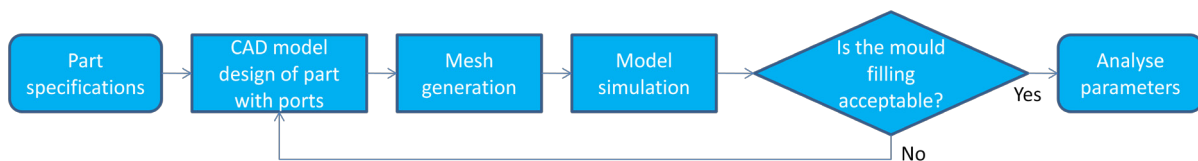


Figure 10: Infusion simulation procedure

6.2.3. Conclusion

After careful consideration, it was decided to neglect the draping effects. The reason was that the repeatability was not good and therefore the analysis would have inaccuracies. The mesh generation program of choice from this point onwards was Patran (2010) (using a *.out file), because it is more stable.

6.3. Material properties and process parameter settings

The section mentions the material properties that must be set for the simulations and the process parameter settings.

6.3.1. Material properties

The fibres are categorised according to the FAW and the specified fibre configuration. Additional parameters are not always readily available. Each fibre configuration and weight differs during infusion and must therefore be tested separately.

The fibre permeability is the most critical parameter to obtain and many researchers have presented different approaches to describe and determine the permeability of the reinforcement (Section 2.2.2.1). Most researchers focus on vacuum infusion using a flexible membrane and a rigid half where the flexible part compresses the reinforcement. In this case the simulation software uses a finite element model to recalculate the initial permeability, depending on the pressure of the flexible part. For this study the procedure of comparing the

flow front progression and time-wise evolution was used, as was done by other researchers such as Black (2008), Lee et al. (1994) and Song et al. (2004) (Section 2.4.3).

The fibre properties of the standard fibre are listed in Table 1. The in-plane permeability values in the table are determined as described in Section 6.4.2. Kim & Daniel (2003) showed that the out-of-plane permeability (K_3) is one order of magnitude lower than the in-plane permeability (K_1, K_2) for the Hexcel 7500 fibre. Others researchers values mostly tended within this region (Bickerton et al., 2000; Lawrence et al., 2002; Lekakou et al., 1996). Therefore, it is assumed that the out-of-plane permeability is one order of magnitude lower than the in-plane permeability.

Table 1: Fibreglass properties of 195 PW Tight

Description	Symbol	Value	Unit
In-plane permeability	K_1, K_2	$2.15 \cdot 10^{-9}$	m^2
Out-of-plane permeability	K_3	$2.15 \cdot 10^{-10}$	m^2
Density	ρ_f	1218.8	$\frac{Kg}{m^3}$
Thermal conductivity (isotropic, const.)	$k_{th,f}$	0.042	$\frac{W}{m \cdot K}$
Effective conductivity (isotropic, const.)	$k_{eff,f}$	0.042	$\frac{W}{m \cdot K}$
Specific heat (const.)	c_f	700	$\frac{J}{Kg \cdot K}$

The inlet and outlet zones need to have an equivalent permeability specification in the software. The properties and the calculations are shown in Appendix C.1.

Resin Properties

In this study, use was made of a low viscosity resin system that cures at room temperature. A resin viscosity measurement was conducted by the manufacturer on request. The results are presented in Figure 11 where the measured data points and the corresponding regression for the specification in the simulation software are shown. A strong temperature dependence is noticed, thus, for a safe estimation, it was decided to stay in the range of ambient temperature (288.15 K to 308.15 K) and therefore in the range of the measured data for all experiments.

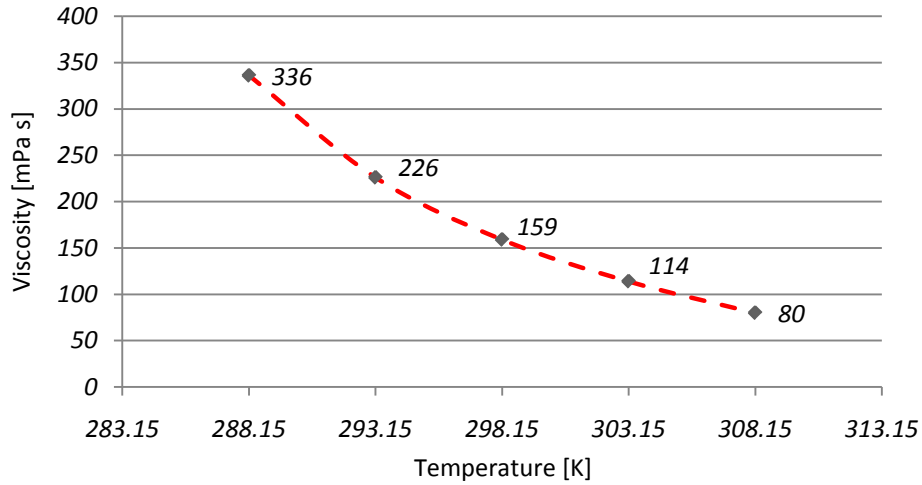


Figure 11: Resin viscosity data points of Prime 20 ULV

Further resin properties are listed in Table 2.

Table 2: Mixed resin system properties Prime 20 ULV

Description	Symbol	Value	Unit
Density	ρ_R	1076	$\frac{\text{kg}}{\text{m}^3}$
Thermal conductivity (const.)	$k_{th,r}$	0.59	$\frac{\text{W}}{\text{m K}}$
Specific heat (const.)	c_r	4185	$\frac{\text{J}}{\text{Kg K}}$

6.3.2. Simulation settings

In this study 3D models and the RTM option were used for all simulations. Based on the literature study, it was decided to neglect the local permeability. The porosity was assumed to be constant throughout one mould cavity thickness. Because the cavity is rigid no change in permeability is expected, and therefore it was taken as being constant. Accordingly, the compressibility was also neglected.

Based on information provided by Kaynak et al. (2008), the resin system was stored under the same temperature conditions as the mould, to eliminate any possible heat flux. A resin temperature difference of 2 °C was neglected which was measured from the time of mixing to the time of infusion, caused by the exothermic chemical reaction.

Temperature has a strong influence on resin kinetics. Literature mentioned in Section 2.2.3 shows that this could have a positive influence on the mechanical properties (Lebrun et al., 1996). On the other hand, temperature can distort the results of the entire filling analysis

significantly. It was therefore decided to conduct the tests under ambient conditions and consider small temperature changes.

For the purpose of simplification, the pressure drop in the plastic hose between the vacuum pump and the mould can be neglected (see Section 4.1 for the experimental set-up). The mass flow of the air and the flow resistance are low. For all experiments the static suction height and the geometry of the hose between the resin pot and mould is almost identical in order to maintain similar starting conditions. The length of the hose is reduced to a minimum (12 cm) to avoid any difference between the experiment and the simulation. The inlet and outlet diameters of the mould fitting were set constant for all experiments and simulations were set to $d_f = 6$ mm to simplify the analysis.

6.4. Experimental verification of simulation

This section discusses the verification method. Software verification and fibre permeability calibration for the software used were performed to show that the experimental results are equivalent to the simulated ones. Comparison criteria are the visual flow front and the total filling time.

6.4.1. Verification method

The PAM-RTM (2010) software is used by many companies that produce high quality parts, including Airbus, Boeing Research & Technology Australia, Chengdu Aircraft Corp., Dassault Aviation, EADS/IW, Eurocopter and Hexcel. Although the software that is being used is reliable, an evaluation of the software and the settings was nonetheless performed. This section describes how the software was validated by comparing its results with the experimental results.

In this study, the software was verified and the fibre permeability calibrated simultaneously. The verification procedure is demonstrated in the data flow diagram in Figure 12, the same procedure of software verification was used by other researchers (Black, 2008; Lee et al., 1994; Song et al., 2004; Zhou et al., 2008).

The first step is the specification of the part. On the left side in Figure 12 is the entire simulation procedure (blue) for all simulations. It starts with the CAD model generation of the part and goes to the mesh generation, followed by the definition of the properties and then infusion simulation. On the right side is an overview of the experimental procedure (green) of designing and manufacturing the part using a perspex mould (Figure 6). The experimental procedure entails the mould specification, mould design and mould manufacturing, through to the final resin infusion. Then the experimental resin infusion and the simulation of the infusion were recorded over time. The flow front progression and the flow front pattern in the received motion picture of both procedures were compared at the same time steps.

Finally, fibre permeability was adjusted until filling patterns compared well, according to the process in the left bottom (orange) in Figure 12.

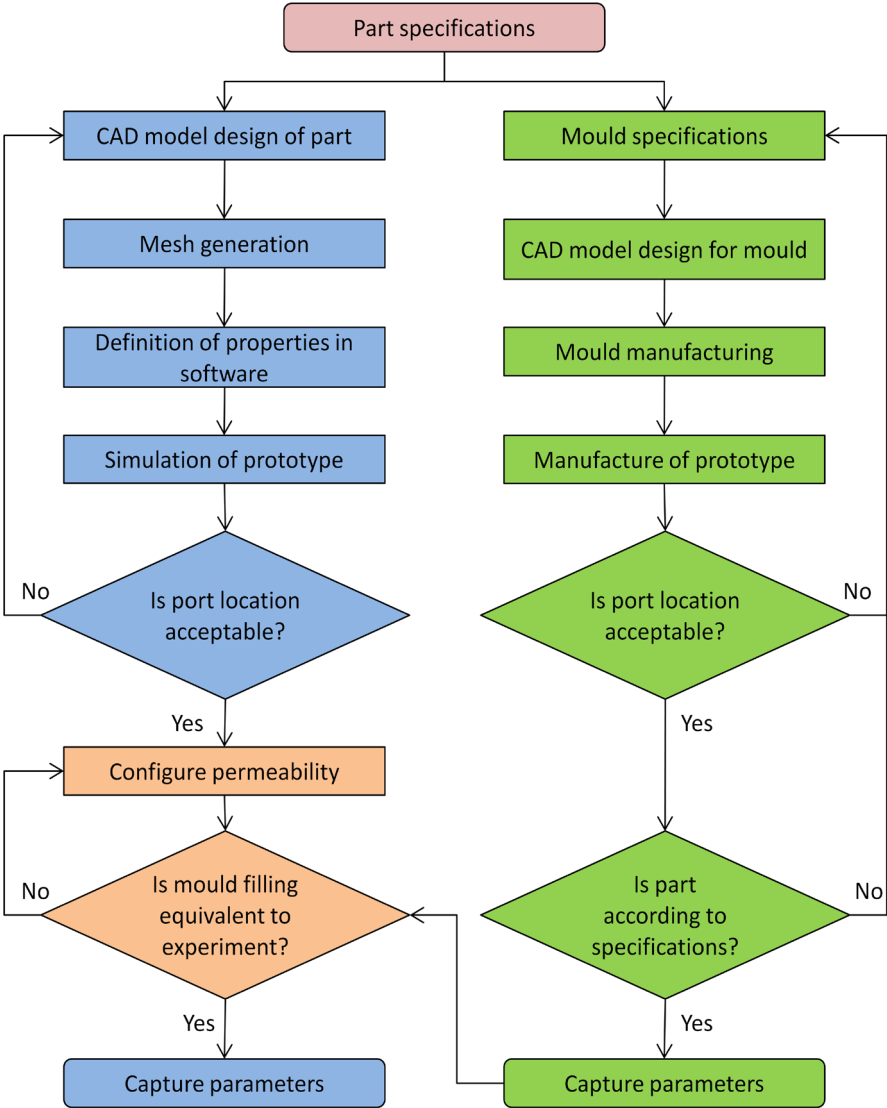


Figure 12: Data flow diagram of experimental verification of simulation

6.4.2. Verification and result

The verification was conducted using a flat shaped part and three different pressure configurations at six time steps. The verification of the 70 kPa gauge pressure is shown in Figure 13 and the (gauge) pressure configurations 35 kPa and 90 kPa are presented in Appendix C.3.

The composite part dimensions for the verification and calibration are listed in Table 3. The large surface area is defined in equation 4.2 (Section 4.2).

Table 3: Physical properties of the validation part

Property	Symbol	Value	Unit
Length	$L_i = L_o$	200.4	mm
Width	W	100.4	mm
Thickness	D	1.4	mm
Volume (incl. fitting)	V	29016	mm ³
Large surface areas	A_s	20120	mm ²

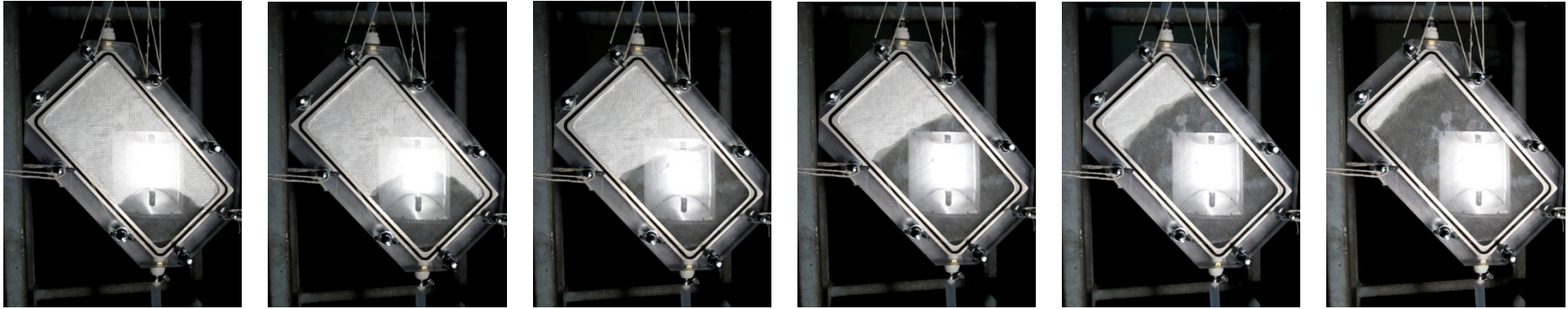
The laminate generally describes the entire ply lay-up in the mould. Table 4 lists the necessary property specifications of the software for all pressure configurations. The measured temperatures of the mixed resin at infusion as well as the measured room and mould temperatures were equivalent. This is because the resin was stored at room temperature and, as mentioned earlier, the mould temperature was assumed to be equal to the resin temperature.

Table 4: Specifications for infusion simulation

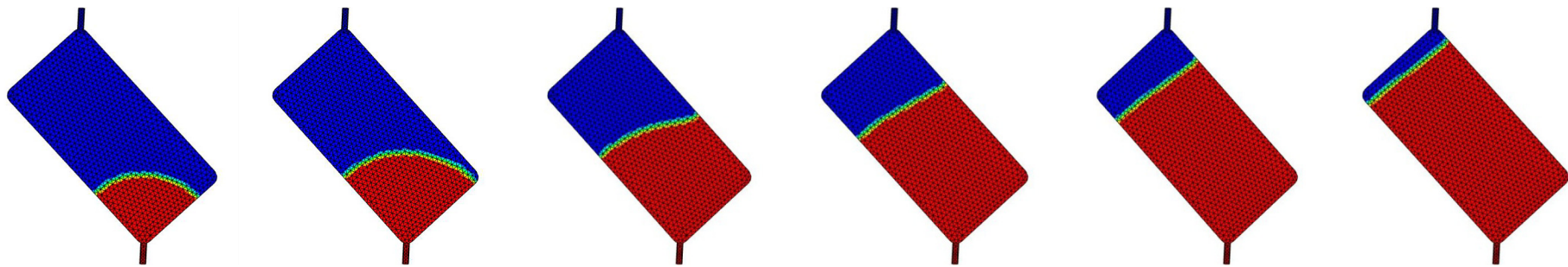
Property	Symbol	Value	Unit
Number of plies	n_p	4	
Room temperature	T_R	291.15/ 291.45/ 292.75	K
Mould temperature	T_M	291.15/ 291.45/ 292.75	K
Resin temperature at infusion	T_{RS}	293.65/ 292.15/ 294.45	K
Differential pressure	p	90/ 70/ 35	kPa

The start time ($t_s = 0$) refers to when the resin enters the mould fitting. The images $a - f$ show the experimental pictures and $g - l$ describe the simulation pictures, for the different time steps. The colour scale indicates the filling factor for the simulation. All three simulations were conducted using gravity. The lowest point is the resin inlet and the highest point is the vent to the vacuum pump, as also used for the experimental set-up in Section 4.1.

a. *b.* *c.* *d.* *e.* *f.*



g. *h.* *i.* *k.* *l.*



$t = 8 \text{ s}$

$t = 16 \text{ s}$

$t = 26 \text{ s}$

$t = 36 \text{ s}$

$t = 45 \text{ s}$

$t = 54 \text{ s}$

Figure 13: Comparison of experimental to simulation results at 70 kPa

With a differential pressure of 70 kPa and 90 kPa the geometrical outline of the flow front and the temporal process are similar. The deviation in the filling times is 1.58% and 0.66%, respectively (see Table 5). With a differential pressure of 35 kPa the geometrical outline of the flow front is similar, however the filling time is less similar and a deviation of 30.13% from the total filling time is observed (see Table 5).

Table 5: Comparison of total filling times for flat shapes

Differential pressure [kPa]	Experimental model [s]	Simulation model [s]	Deviation [s]	Deviation [%]
90	43	43.68	0.68	1.58
70	65	65.43	0.43	0.66
35	79	102.8	23.8	30.13

6.5. Conclusion

Especially at a differential pressure of 70 kPa and 90 kPa the results from the experiment and the simulation correlate well regarding the geometrical outline of the flow front time and the temporal process. The infusion times and flow front progression pictures show a good relation to the simulation to the experiments. Therefore, the simulated filling times were considered suitable for use for time and cost calculations.

7. Process analysis of basic shapes

According to Section 4.1, the manufacturing process is divided into the following stages: set-up, infiltration, curing, demoulding and cleaning. This chapter presents the analysis and the results for the process time of each process stage for basic shapes. The aim is to obtain an equation for the calculation of the manufacturing time.

7.1. Set-up

The set-up is divided into the preparatory sub-processes: the laminate cutting, application of mould release agent, ply lay-up, mould fixing and clamping, final pipe mounting and resin mixing. The discussions of each of these sub-processes cover the following topics: general structure of process definition, measurement methods and results. Where appropriate, application graphs, based on assumptions, are included to illustrate a relationship of variables.

7.1.1. Laminate cutting

Laminate cutting is the cutting-out of fibres to the specified dimensions. Since the focus of this study is on prototype parts and low volume production, it follows that the assumption is manual cutting. Apart from the manual cutting process for prototypes and small quantities, automated machines are commonly used in the composite industry. Cutting is time intensive, and an automated cutting machine is more precise, has a stable cut quality and higher working velocity, and is therefore an option to improve the productivity. Due to these advantages, an automated cutting time is presented here in a simplified form. In the following sub-sections the measurement methods are discussed and the results presented.

7.1.1.1. Measurement methods

The working sequence commences with the preparation; the operator studies the working plan and drawings, then places the reinforcement roll on the workbench, controls the fibre plies, prepares a template, and lays the fibre plies out. The cutting is then carried out with a cardboard cutter. The working time required for each fibre (195 PW Tight) ply in a batch of laminates was timed using a stopwatch. A cardboard cutter and a standard table were used. After cutting, the cut length of the fibre and the fibre weight were noted.

The automatic cutting table (Gerber DSC 2500) is assumed to use a drag blade cutter and only one fibre ply at a time for this study. The cutting table makes movements without cutting between different parts. It cuts after different schemes with varying velocities depending on the length, which has to be cut. The cutting process is complex and the cutting time cannot be allocated to different geometric shapes without tremendous effort. Based on this and the

assumption to cut one fibre ply at a time, it was decided to use the recommended velocity for the drag blade cutter, independent of fibre weight and type.

The assessed variables that can have an influence on the laminate cutting time are shown in Figure 14. The longest line and the corners might have an influence because the worker and machine can accelerate the cutter to a higher velocity when cutting a straight line and, likewise, has to slow down if a radius on a corner is being cut.

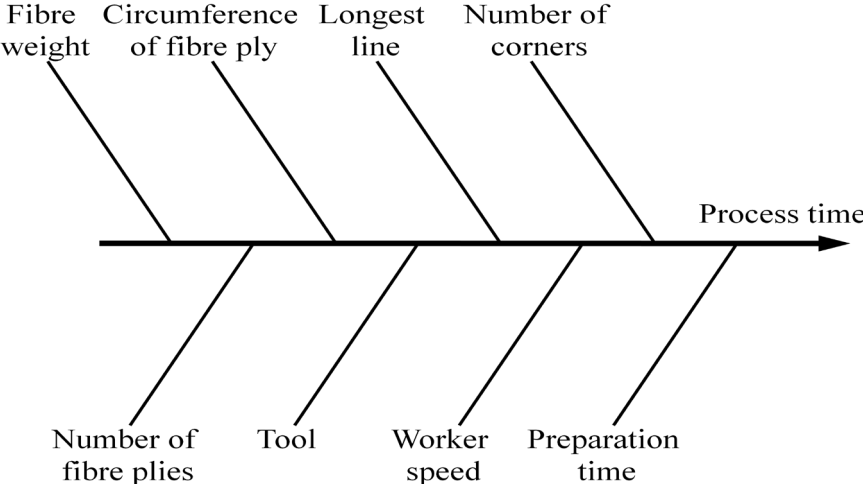


Figure 14: Variables that possibly influence the laminate cutting process

7.1.1.2. Results

The total cutting time is split into the preparation time and the cutting velocity. The velocity can either be represented by manual cutting or by automated cutting. Each cutting velocity is first separately analysed and finally the equation for the total cutting time is given.

Preparation time

The above-mentioned preparation time has to be adapted for local conditions, such as distances in the workshop. A good average value is 5 minutes ($t_{prep, cut}$ [s]); this gives 2 minutes for the acquisition of the necessary parts and tools and 3 minutes for the controlling and the template cutting.

Manual cutting

The average manual cutting velocity ($v_{cut, m}$ [$\frac{cm}{s}$]) was calculated with the circumference (C [cm]) and stopped times for the number of plies in a batch (n_p). After sorting the dataset according to the number of plies in a batch, the expected learning effect in increasing velocity with larger fibre batches was revealed. The investigation was based on 53 measurements, the

spread of which is demonstrated by the box plot in Figure 15. The logarithmic function suits to describe this increasing velocity behaviour for rising batch sizes.

The logarithmic regression in Figure 16 represents the manual cutting velocity, which is based on the median of the investigated number of fibre plies in a batch. The regression function is presented in equation 7.1. The graph shows that the operator becomes more familiar with the cutting process with an increasing number of fibre plies in a batch.

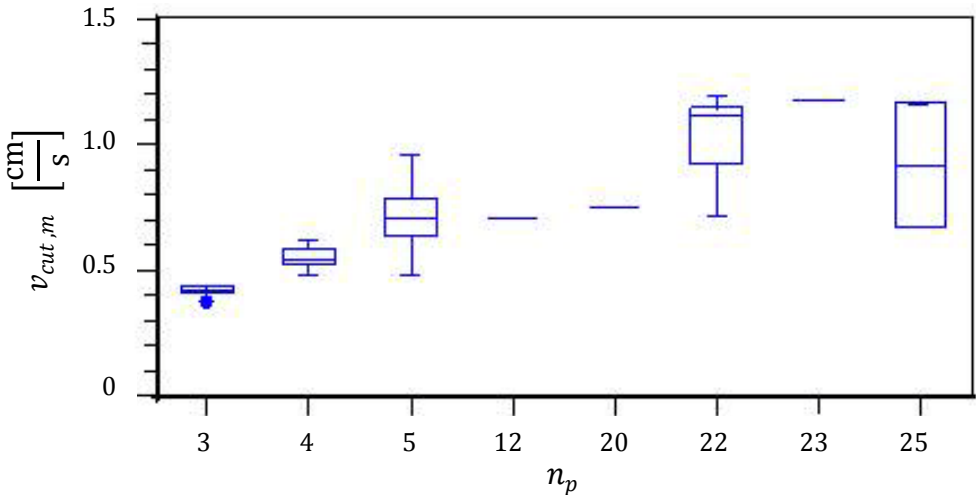


Figure 15: Dependence of cutting velocity on the number of plies in a batch

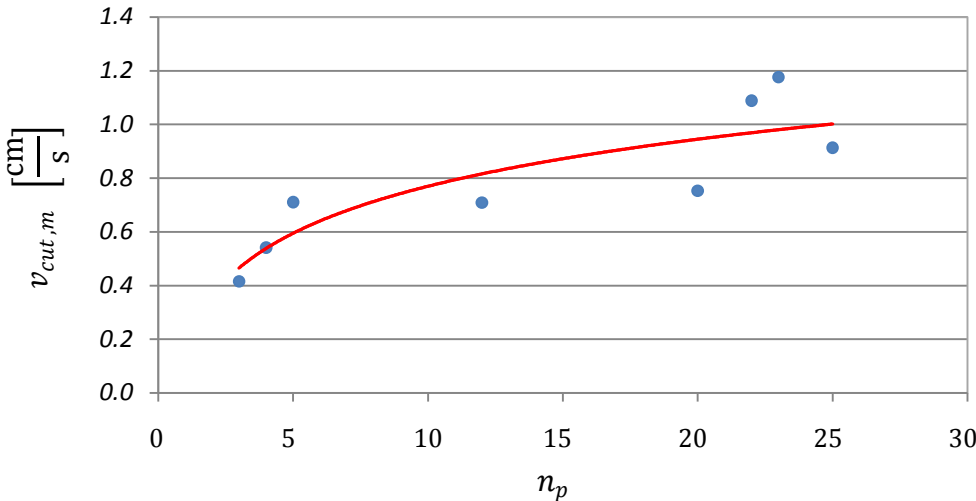


Figure 16: Logarithmic regression of cutting velocity based on the median ($R^2 = 0.735$)

$$v_{cut,m} = 0.253 \ln(n_p) + 0.188 \tag{7.1}$$

Automated cutting

As mentioned earlier, the automated cutting velocity is assumed to be constant for the cutting of one fibre ply at a time. Equation 7.2 shows the recommended speed for a drag blade cutter.

$$v_{cut,a} = 50 \left[\frac{\text{cm}}{\text{s}} \right] \quad (7.2)$$

Total cutting time

The total cutting time presented in equation 7.3, depends on the circumference of the laminate, the number of plies in a batch and the cutting velocity. The cutting velocity is either based on manual or automated cutting, as mentioned above.

$$t_{cut} = t_{prep,cut} + n_p \left(\frac{C}{v_{cut}} \right) \quad (7.3)$$

A universal equation for the total cutting time of the laminate was generated. The designer can choose between manual and automated cutting for the cost estimation. The manual cutting velocity increases up to 120% between 3 fibre plies in a batch and 25 plies in a batch. This effect was already observed during the manufacturing. All measurements in this study were taken for batches of 3 to 25 plies, using a part area of 201 cm².

7.1.2. Application of mould release agent

The mould release agent is a separating material that enables reliable opening of the mould after resin infusion and curing. A mould release agent is required to prevent defects occurring in the composite part surface, like cracking off, due to adhesion of the resin system to the mould, and to avoid high forces during the demoulding process. The process tools are a spray nozzle, a sponge or a paintbrush (depending on whether the release agent is in the form of a wax or liquid). The application can be performed manually, or automatically. In this study, a paintbrush was used to apply the Freecote 770-NC (see Section 3.2) release agent manually. A list of possible predictors of the process is presented in Figure 17. This section will give a universal equation for the application of a mould release agent and insight into the cost driving factors for this process. First, the measurement methods are described, followed by presentation of the results. Then application graphs with assumed values are presented in Appendix B.1, to illustrate the relationships between the variables and to allow visual estimates.

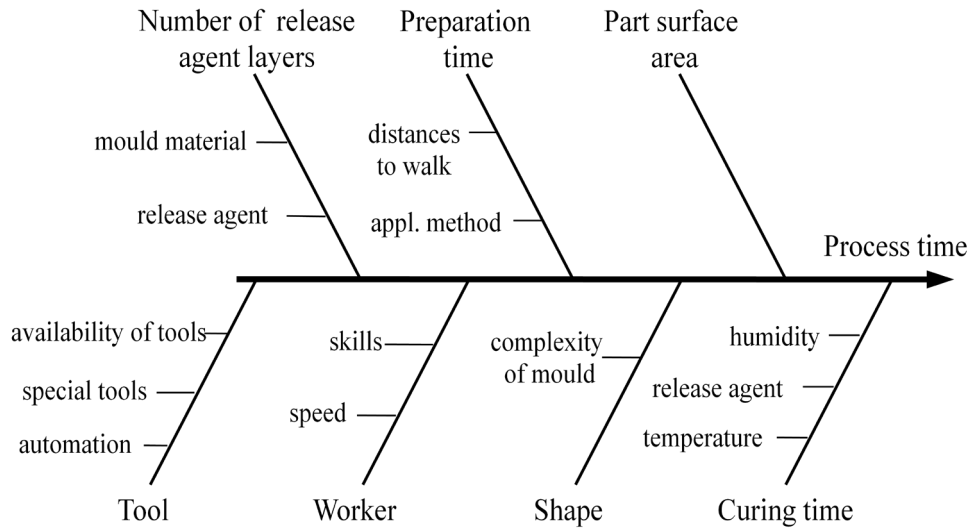


Figure 17: Variables that possibly influence the mould release agent application process

7.1.2.1. Measurement methods

The measurements were recorded with a stopwatch. Many mould release agent layer combinations were applied on different sized shapes. The area of application was the mould cavity, which is defined as the surface area of the part. It should be noted that there is additional area in form of a frame around the mould cavity to the seal. This frame depends on the mould design and has to be added to the surface area in case it is considered for the cost calculation.

The manufactured moulds are relatively small and the experimental tests that were carried out were not able to fill the desired experimental design space. In order to allow a statistical prediction it was decided to also apply the mould release agent on larger flat and L-shaped aluminium sheets. These sheets represent the cavity sizes with their surface areas.

7.1.2.2. Results

The total mould release agent application time (t_{app}) is split into the two different application cases and handling times for different shapes. After the application of one layer of mould release agent there is a waiting period until the mould release agent is touch dry. Two different application cases were generated to account for the drying phase. The handling time ($t_{handle} \left[\frac{s}{dm^2} \right]$) is an operator and tool dependent variable, which represents the relationship of the worker velocity for the tool used. It is based on the absolute measured application time of one layer on different surface areas (without preparation), calculated per dm^2 . Handling times for the flat- and L-shaped parts were determined separately. It was further decided that all non-flat shaped parts are represented by the L-shaped measurements.

Flat shaped parts

The linear regression for the handling time and the corresponding measurements are presented in Figure 18. The regression function based on 22 measurements is given in equation 7.4. Here the second and fourth terms represent a standard deviation of 68 %, which can be seen as the lines around the function in Figure 18. The curves shows a slight decrease of handling time with increasing part surface area (A_s [dm²]). This can be interpreted as an increase in the mould release agent application velocity as the surface area becomes larger. The function is valid in the range of the conducted measurements, $4.01 \leq A_s \leq 30.97$ [dm²], and therefore it is considered safe to use the equation in this interval. Figure 18 shows a decreasing handling time over rising area and therefore the worker velocity increases. Surface areas that exceed the defined dimensions of this study have to be handled with care, because the values higher than the specified range can lead to unrealistic negative values.

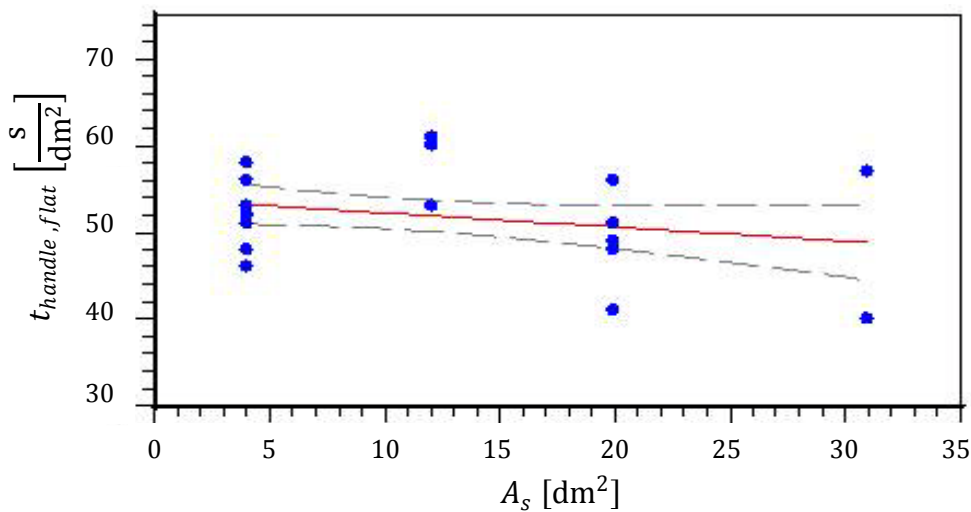


Figure 18: Linear estimation of handling time for flat shaped parts

$$t_{handle,flat} = 53.86 \pm 1.84 - (0.16 \mp 0.13) A_s \quad (7.4)$$

Non-flat shaped parts

The function for the L-shape measurements is illustrated in Figure 19. The resulting approximation in equation 7.5 is based on 14 measurements, in the range $4.01 \leq A_s \leq 19$ [dm²]. The function shows that the handling time is roughly 10% higher than in the case of the flat shape. The L-shape measurements show an increasing handling time over rising surface area which can be interpreted as slightly decreasing velocity with rising part size.

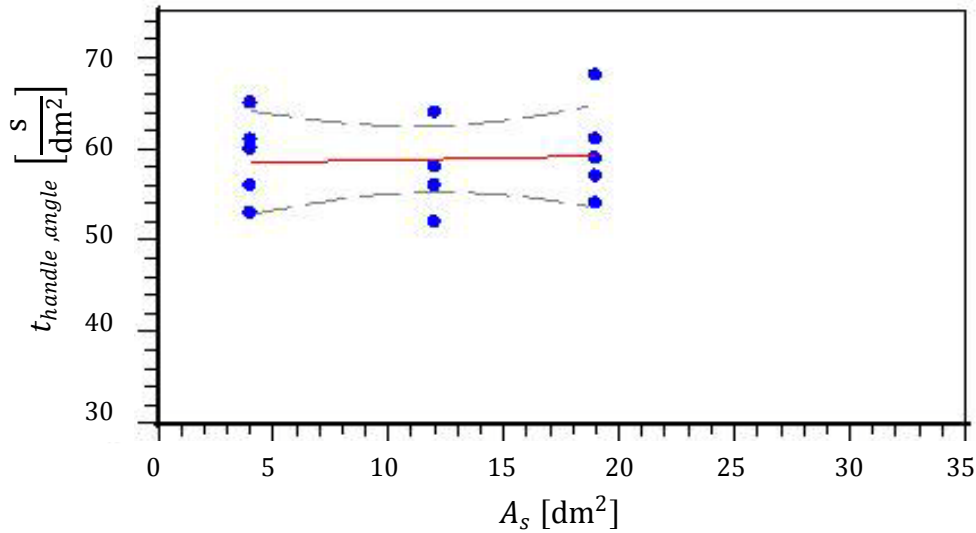


Figure 19: Linear estimation of handling time for L-shaped parts

$$t_{handle,angle} = 58.29 \pm 2.71 + (0.05 \pm 0.20) A_s \quad (7.5)$$

A handling time for the individual speed of the operator with the selected tool is introduced. It was found that the handling time is longer for non-flat shaped moulds. Therefore, the conclusion can be drawn that the L-shape is more complex than the flat shape. Figure 20 introduces the handling factor, which is defined as the elevation of handling time of the L-shape, based on the flat shape. The handling factor is also presented as an exponential function in equation 7.6, and can be multiplied by a handling time of a flat shape to obtain the equivalent handling time for an angled shape.

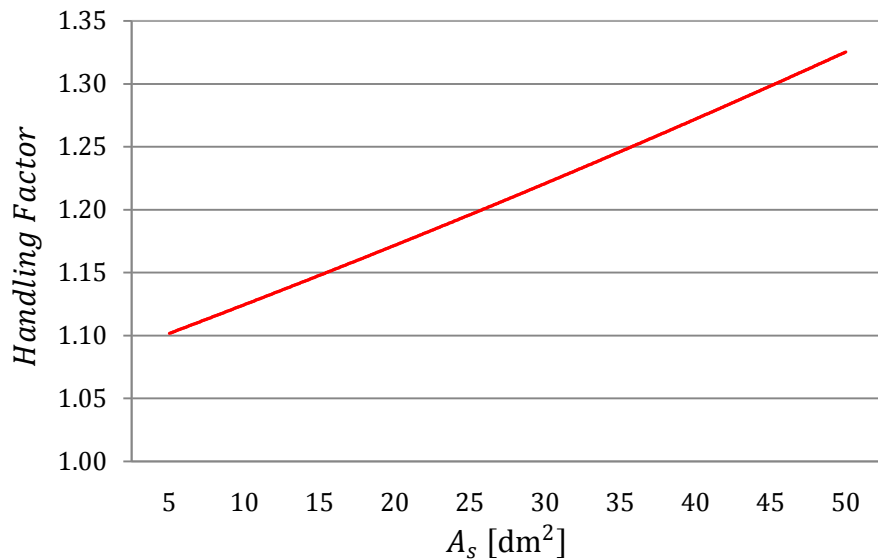


Figure 20: Handling factor based on the flat shape

$$\text{Handling factor} = 1.079 e^{0.021A_s} \quad (7.6)$$

Preparation time

The preparation time ($t_{prep,MRA}$ [min]) has to be adapted for local conditions such as workshop distances. A good average value is here 5 minutes. This allows 3 minutes for the mould and part organisation and 2 minutes for the release and tool organisation.

Drying time

The drying time (t_{dry} [min]) refers to the time until the mould release agent is touch dry. The range of the drying times is large and depends on the mould release agent, humidity and temperature conditions. If no data are available then the value of 5 minutes is recommended. The Freecote 770-NC datasheet recommends 5–10 minutes for evaporation.

Application, case one

Case one, presented in equation 7.7, applies for one or many layers (n_l), when $t_{dry} \leq A_s t_{handle}$. This means the mould release agent is already touch dry for one mould half before the operator has completed the application of the layer on the other side. The application of the layers without any break is possible, as shown in Figure 21.

$$t_{app} = t_{prep,MRA} + n_l A_s t_{handle} + t_{dry} \quad (7.7)$$

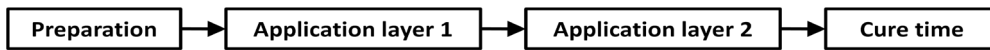


Figure 21: Mould release agent application process, case 1

Application, case two

Case two, presented in equation 7.8, applies for many layers, where $t_{dry} > A_s t_{handle}$. This means that application without interruption is not possible. Intermediate phases with a reduced drying time of $t_{dry} - (A_s t_{handle})$ are necessary for the mould release agent application, as shown in Figure 22.

$$t_{app} = t_{prep,MRA} + n_l A_s t_{handle} + (n_l - 1)(t_{dry} - A_s t_{handle}) + t_{dry} \quad (7.8)$$

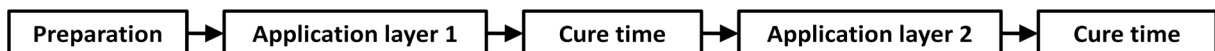


Figure 22: Mould release agent application process, case 2

To determine the predictors with the strongest influence on the total application process time (Chapter 5), the dataset of both shapes was combined (see the box plot in Figure 23) and either application case one or case two was used to generate the total process time. Here the preparation time was neglected in order to provide a better illustration. The Pareto diagram in Figure 24 demonstrates the magnitude of the effect of each variable on the application time.

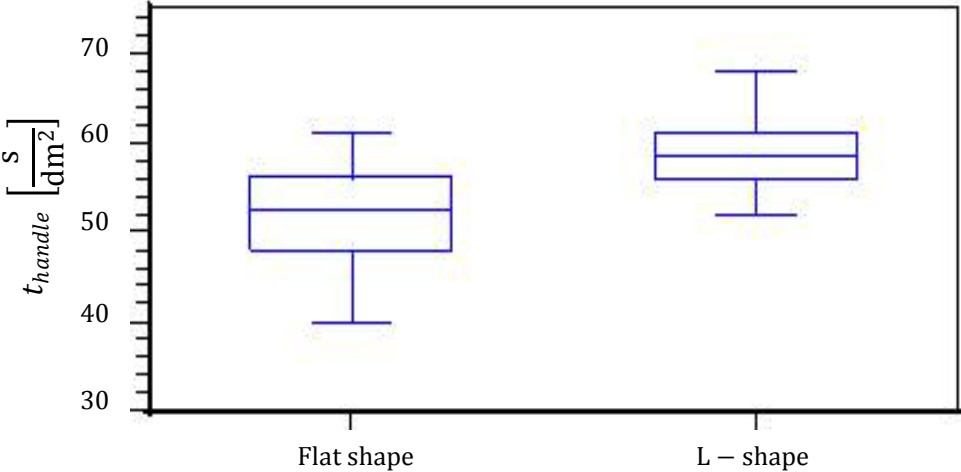


Figure 23: Box-plot of handling time for flat- and L-shape

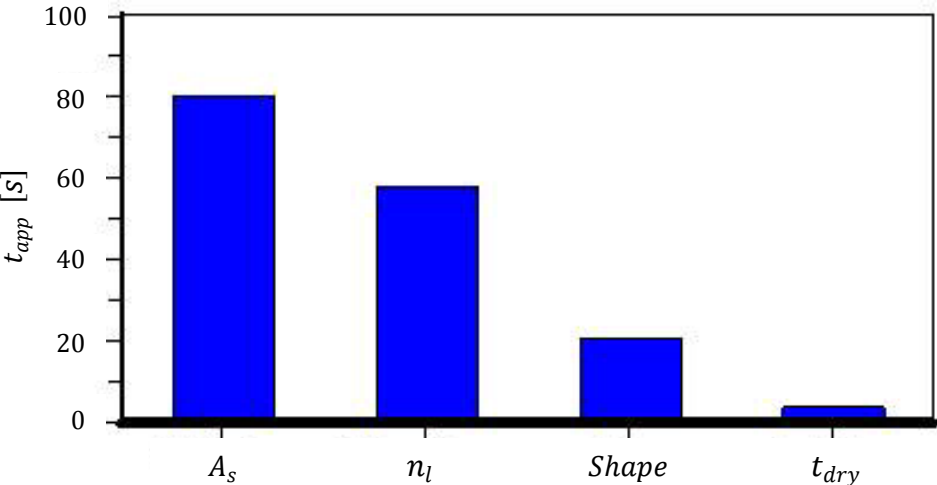


Figure 24: Pareto diagram of predictors on the total mould release agent application time

The handling time for the flat (equation 7.4) and the non-flat (equation 7.5) shaped mould cavities was introduced based on manual paintbrush operation. A handling factor allows the calculation of handling time of a non-flat shaped cavity based on a flat shaped cavity. In the case of an automated process, an equivalent automation factor can be used instead of the handling time. The total application time can be calculated by either case one (equation 7.8) or case two (equation 7.6), and using the appropriate handling time.

7.1.3.Laminate lay-up

The laminate lay-up is the process during which the dry reinforcing fibres are placed in the mould cavity. The procedure follows a defined working plan, which must be strictly followed. The process preparation includes carrying of the reinforcing material to the table where the lay-up takes place. This is followed by inspection for defects and then fibre-oriented placement in the cavity, which includes smoothing and gluing of each ply with an adhesive spray (Section 3.2) if warping of fibre plies occurs. Care has to be taken that no unwanted gaps occur to avoid part defects later. The lay-up process is usually performed manually, although automated processes do exist. The reason for the little degree of automation of the lay-up process might be the high price of the lay-up machines and the limitation on non-complex parts. Figure 25 illustrates a collection of possible predictors of the lay-up process. The radius and angle are explained in more detail in Section 4.2. The following sub-sections describe the procedure of generating a universal equation for the total lay-up time: the measurement method and then the results are described.

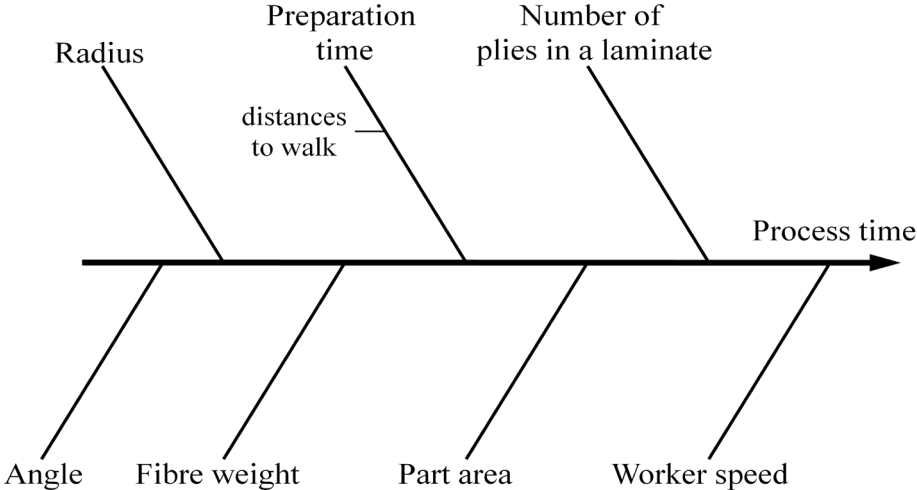


Figure 25: Variables that possibly influence the laminate lay-up process

7.1.3.1. Measurement methods

The data presented here are based on experimentally measured times (measures using a stopwatch). The lay-up time in the mould cavity with different numbers of plies was measured for the flat shaped and L-shaped parts. The part area on both moulds is equivalent. For the statistical prediction, it was decided to test larger areas using a simplified test. This test is a simple practical simulation, which aims to determine a relative difference between the flat shape and the L-shape on larger areas using wrapping paper. To reflect the lay-up difficulty of the mould, certain features (see Figure 26a and Figure 26b) such as holes were implemented, which allows placement in only one position, and a taped frame, which represents the outer dimensions of the mould cavity.



Figure 26a: Simplified test flat shape



Figure 26b: Simplified test L-shape

7.1.3.2. Results

The total laminate lay-up time comprises the preparation time ($t_{prep,lay}$ [s]), the number of plies in a laminate (n_p) and the working time ($t_{work,lay}$ [s]). For the lay-up working time a distinction was made between flat shaped parts and non-flat shaped parts, such as parts with an angle and radius. The non-flat shaped parts fall into the category of the tested L-shaped. The data generated by the simplified test, based on the same part area (A_p [cm²]), compared well with the data obtained from the mould tests. Therefore, results of both tests for each shape were combined, and handled in the same way.

Working time for flat shaped lay-up

A linear regression for the working time ($t_{work,lay,f}$ [s]) was generated using the number of lay-ups and the time for each area respectively. The plot in Figure 27 shows the residual working time based on one ply lay-up for all 18 conducted tests. The regression function for each number of plies is presented in the equations 7.9.1 – 7.9.10.

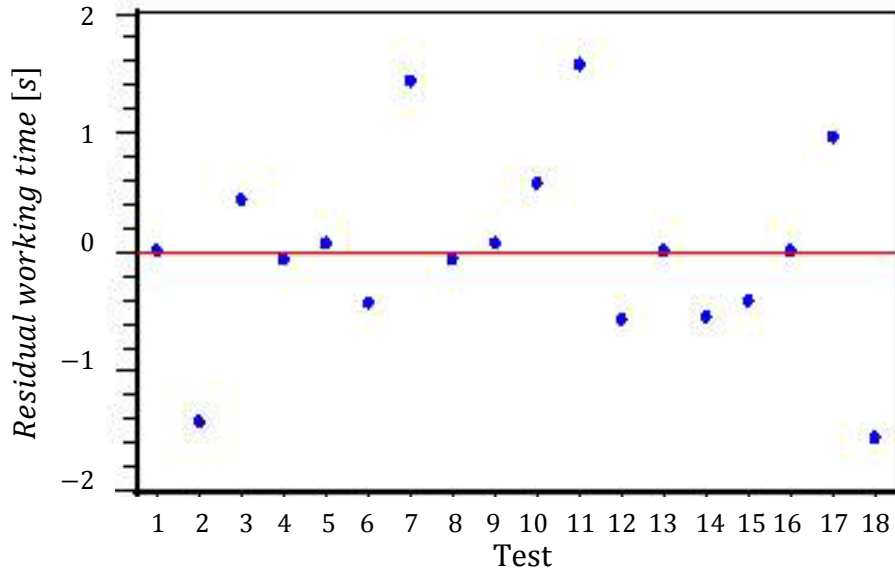


Figure 27: Residual working time for one fibre ply lay-up by flat shaped cavity
 $(\epsilon_{RMS} = 1.28, R^2 = 0.993)$

$$n_p = 1: t_{work,lay,f1} = 4.36 \pm 0.43 + (8.64E-3 \pm 2.9E-4)A_p - (2.095 \pm 1.208)n_p \quad (7.9.1)$$

$$n_p = 2: t_{work,lay,f2} = 4.36 \pm 0.43 + (8.64E-3 \pm 2.9E-4)A_p - (0.027 \pm 0.877)n_p \quad (7.9.2)$$

$$n_p = 3: t_{work,lay,f3} = 4.36 \pm 0.43 + (8.64E-3 \pm 2.9E-4)A_p + (0.473 \pm 0.877)n_p \quad (7.9.3)$$

$$n_p = 4: t_{work,lay,f4} = 4.36 \pm 0.43 + (8.64E-3 \pm 2.9E-4)A_p + (0.95 \pm 0.734)n_p \quad (7.9.4)$$

$$n_p = 5: t_{work,lay,f5} = 4.36 \pm 0.43 + (8.64E-3 \pm 2.9E-4)A_p - (1.527 \pm 0.877)n_p \quad (7.9.5)$$

$$n_p = 6: t_{work,lay,f6} = 4.36 \pm 0.43 + (8.64E-3 \pm 2.9E-4)A_p - (0.027 \pm 0.877)n_p \quad (7.9.6)$$

$$n_p = 7: t_{work,lay,f7} = 4.36 \pm 0.43 + (8.64E-3 \pm 2.9E-4)A_p - (0.095 \pm 1.208)n_p \quad (7.9.7)$$

$$n_p = 8: t_{work,lay,f8} = 4.36 \pm 0.43 + (8.64E-3 \pm 2.9E-4)A_p + (0.473 \pm 0.877)n_p \quad (7.9.8)$$

$$n_p = 9: t_{work,lay,f9} = 4.36 \pm 0.43 + (8.64E-3 \pm 2.9E-4)A_p + (0.973 \pm 0.877)n_p \quad (7.9.9)$$

$$n_p = 10: t_{work,lay,f10} = 4.36 \pm 0.43 + (8.64 \pm 2.9E-4)A_p + (0.905 \pm 1.208)n_p \quad (7.9.10)$$

An analysis of the working time showed that the regression seemed to be unnecessarily complicated. The Pareto graph (see Chapter 5) in Figure 28 shows the magnitude of influence for each variable (neglecting the preparation time). Based on the little deviation caused by the number of plies in a batch, it was decided to simplify the equation by neglecting the plies in the working time. The newly generated linear regression presented in equation 7.10 and in Figure 29 now has a constant increase in time with the number of layers.

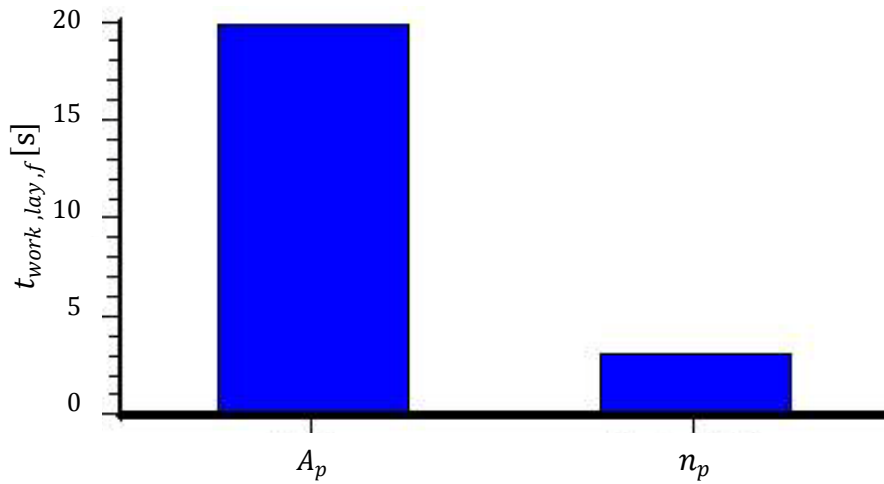


Figure 28: Pareto diagram for the variables of the flat shape lay-up time

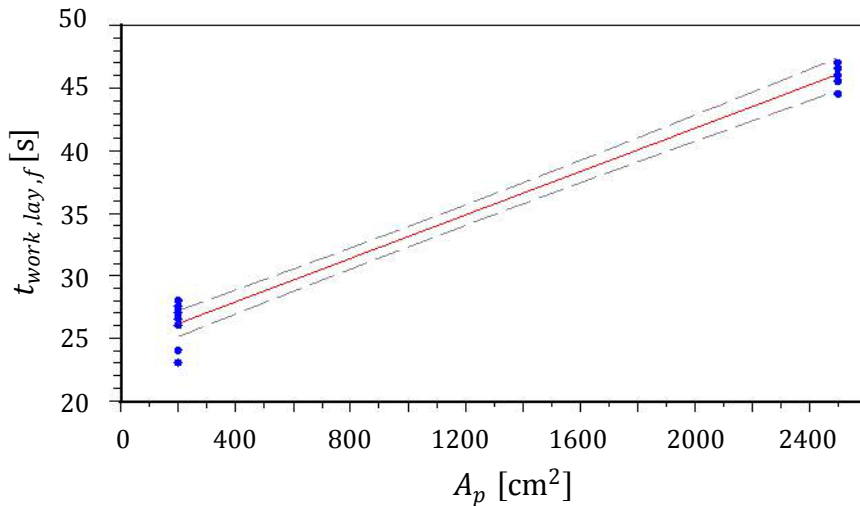


Figure 29: Working time for laminate lay-up for flat shaped parts
(neglecting plies, $\varepsilon_{RMS} = 1.287, R^2 = 0.9847$)

$$t_{work,lay,f} = (24.44 \pm 0.42) + A_p (8.68E - 3 \pm 2.7E - 4) \quad (7.10)$$

Working time for non-flat shaped lay-up

The data for the non-flat shapes parts ($t_{work,lay,angle}$) are generated in the same way as was done for the working time for the flat shaped lay-up. Figure 30 presents the residuals of the working time for lay-up of the 18 specimen tested on an L-shaped part. The Pareto graph in Figure 31 shows a similar magnitude of influence as for the previous analysis. However, the influence of the number of plies is now double that of the flat shape. The number of plies in the working time were also neglected. The new linear regression of the working time, which represents all non-flat shaped parts, is shown in Figure 30 and in equation 7.11.

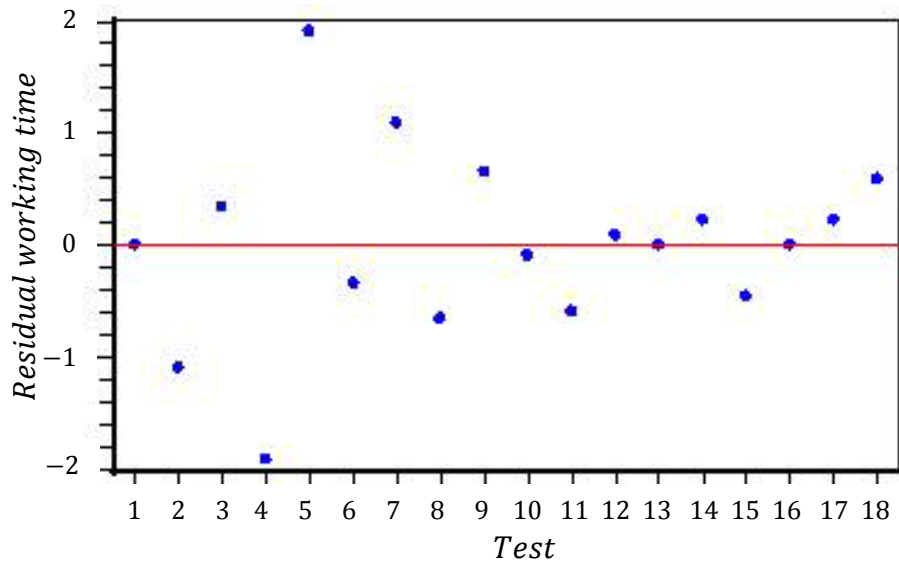


Figure 30: Residuals working time for one fibre ply lay-up for L-shaped cavity ($\epsilon_{RMS} = 1.30, R^2 = 0.997$)

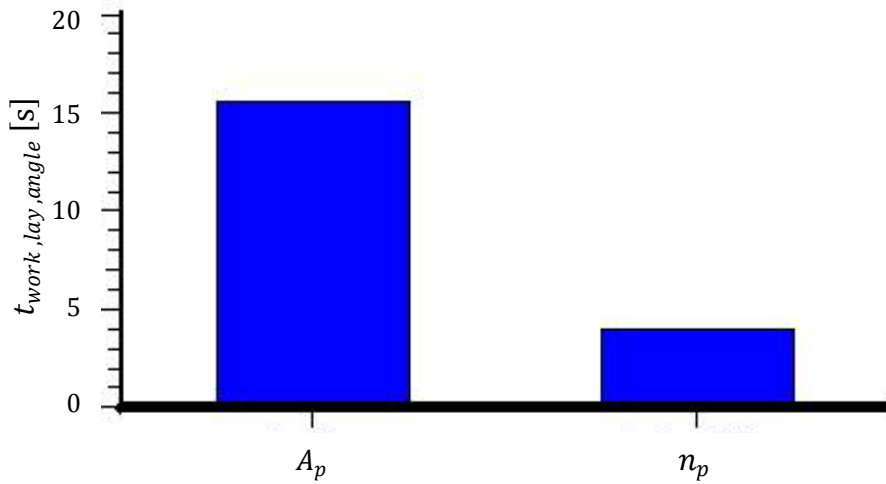


Figure 31: Pareto diagram for the variables of the L-shape lay-up time

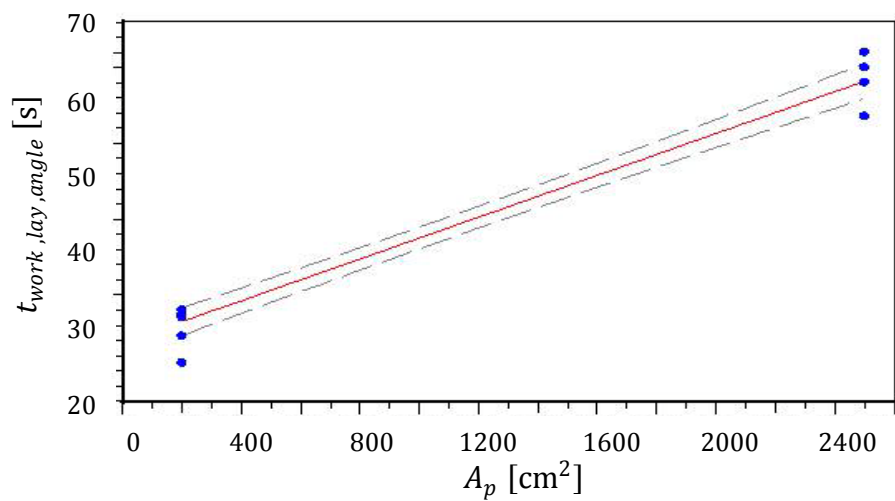


Figure 32: Working time for laminate lay-up for non-flat shaped parts (neglecting plies, $\epsilon_{RMS} = 2.26, R^2 = 0.981$)

$$t_{work,lay,angle} = (27.72 \pm 0.74) + A_p (1.379E-2 \pm 4.7E-4) \quad (7.11)$$

Total lay-up time

The total lay-up time (t_{layup}), shown in equation 7.12, comprises the preparation time and the number of plies multiplied by the working time for one ply lay-up. The preparation time is dependent on the workshop conditions. The good average value is here 2 minutes, during which the operator checks the type and number of laminate plies.

$$t_{layup} = t_{prep,lay} + n_p t_{work,lay} \quad (7.12)$$

Based on the two predictions for the working times, a complexity factor is introduced. The factor demonstrates the deviation between the flat and the non-flat shaped parts (Figure 33, $R^2 = 0.981$). Equation 7.13 gives the corresponding linear regression, which can be used to calculate an equivalent total lay-up time for non-flat shaped parts on basis of a flat shape with the same area, or vice versa.

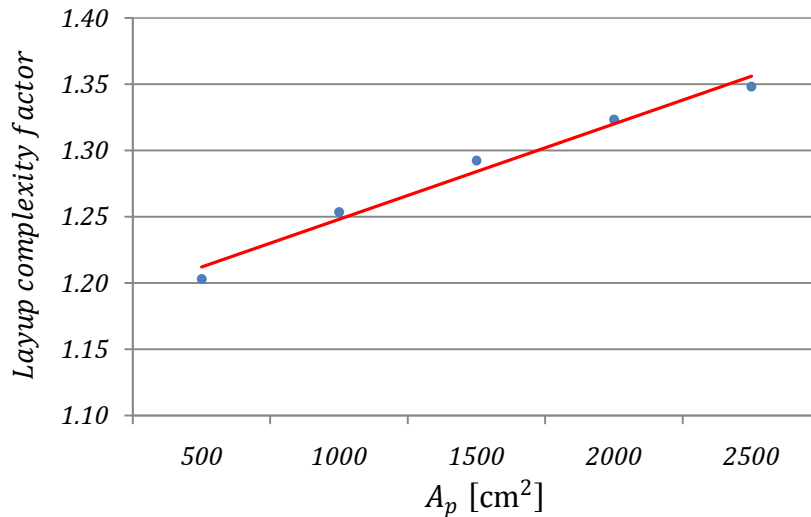


Figure 33: Lay-up complexity factor on base of flat shaped lay-up

$$Layup\ complexity\ factor = 1.176 + 0.036 A_p \quad (7.13)$$

The universal lay-up time in equation 7.12 and can be used for flat and non-flat shaped parts. It was observed that the lay-up time of the first ply to the last ply could be interpreted as constant. Nevertheless, the influence of the plies for non-flat shaped parts is stronger. The constant lay-up time can be explained by the operator, which initially is new to the process but later becomes more familiar with it, but the lay-up complexity increases caused by the warping of the increasing amount of fibre plies. This also explains why non-flat shaped parts are more dependent on the number of plies – because the bending will start earlier.

All experimental measurements in this section were conducted between $201 \leq A_p \leq 2500$ [cm²] and $1 \leq n_p \leq 10$.

7.1.4. Mould clamping, positioning, pipe mounting and resin mixing

This section describes each of the following process steps: mould clamping, mould positioning, pipe mounting and resin mixing (CPFM). The resin degassing and leakage tests are also discussed (see Figure 34). Mould clamping refers to the closing of the mould without pinching the laminate or changing its position. The mould is closed with bolts or a clamp to achieve a vacuum-tight cavity. Mould positioning is desired to allow complete removal of air during infiltration. The mould is placed according to the recommendations of Veldsman (1995). The pipe connects the resin bucket, the mould and the vacuum pump. A flexible hose (Polyethylene 12/10 mm Transparent), tacky tape and hose clamps are used to seal the connections in the vacuum system. The resin is mixed according to the specifications of the resin system manufacturer (SP Gurrit, UK). Here it is important to mix the resin and the hardener in a gentle motion.

Additional steps are the leakage test and the resin degassing. The leakage test is performed to check that the mould is tightly closed, in order to avoid failure parts. The test is carried out after the application of piping. It includes the observation of the system under pressure and the checking of the pressure level. This step is time consuming and costly, and the benefit should be reviewed for each case. Resin degassing (Section 2.3.2) involves boiling the mixed resin under vacuum. The volatile matter escapes from the resin mixture under close to high vacuum conditions. This process step eliminates voids caused by the dissolved volatile matter. In this study, the resin was degassed using a resin trap. Although this step is optional, it is strongly recommended for the fabrication of high quality parts. Figure 34 shows a collection of variables that can influence the total process time of the four main processes. The sequence of all steps is given in Figure 35. All steps require high geometrical flexibility; therefore, they were performed manually in this study.

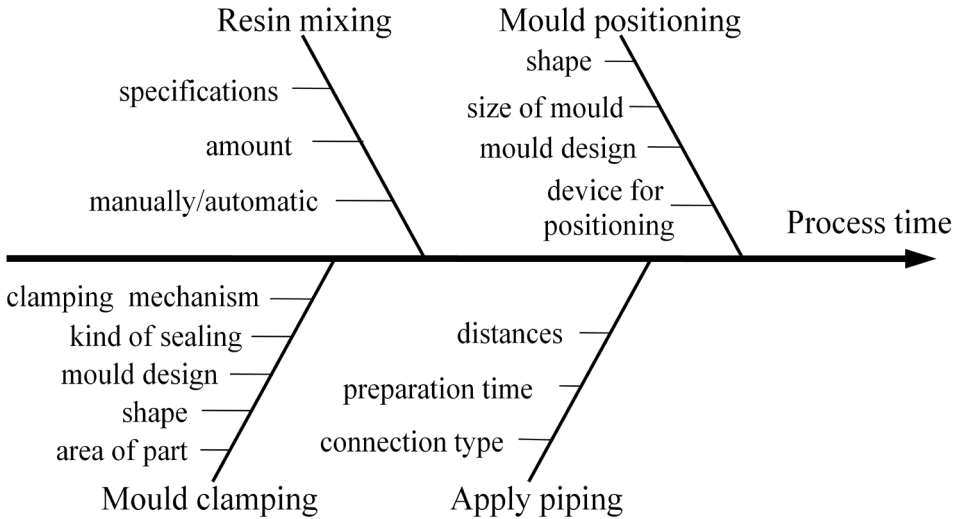


Figure 34: Variables that possibly influence the CPFM process

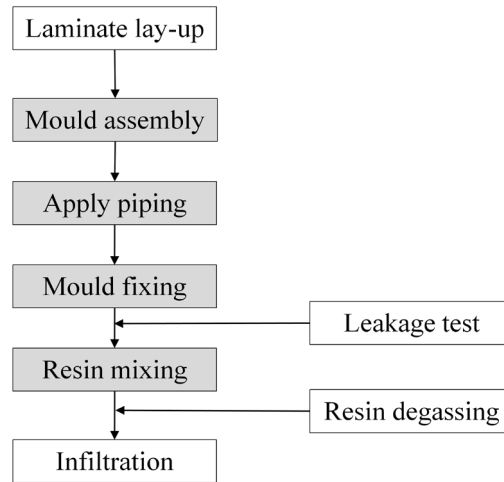


Figure 35: Sequence of mould and resin preparation

7.1.4.1. Measurement method

Measurements were carried out for flat and L-shaped parts, for each process step, using a stopwatch. The working time refers to the time that the operator is occupied with the task.

7.1.4.2. Results

The leakage test takes about 5 minutes, for the observation of the mould and the checking of the pressure level. The leakage test was analysed but not considered further for cost calculation, because this test is optional.

The resin degassing step takes about 30 minutes. This step is complete once all the volatiles in the pressure chamber have evaporated. The step is not time consuming in terms of working time because the operator is not occupied while the process is running, and can carry out other work simultaneously. This process was therefore also neglected for the cost calculation.

The median of the working time measurements for each obligatory step is listed in Table 6. The total working time for the flat shape and for the L-shape was found to be 1325 s and 1338 s, respectively.

Table 6: Median of the mould and resin preparation process times

	Flat shape [s]	L-shape [s]
Mould clamping	355	558
Mould fixing	172	100
Apply piping	356	331
Resin mixing	442	349
Total working time	1325	1338

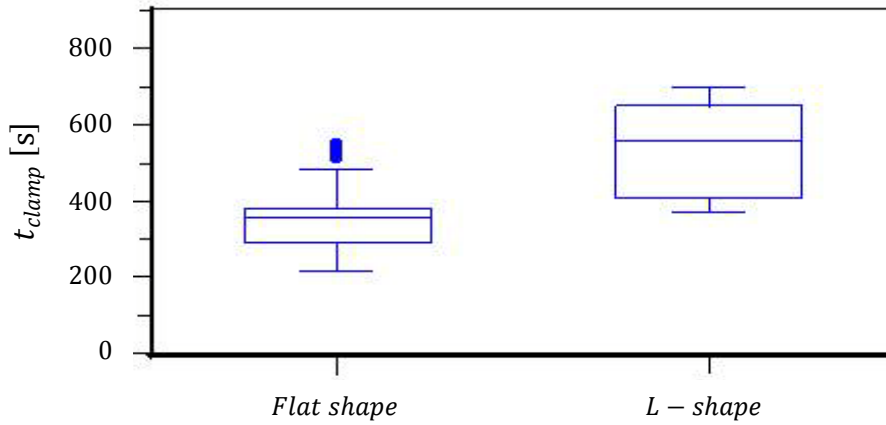


Figure 36: Clamping time comparison for both shapes

The L-shaped part had a 57% higher clamping time (t_{clamp}) (see Figure 36). Other working steps gave relatively small deviations between the two different shape types. Therefore, the dataset of both shapes is combined using the median to reduce the influence of outliers. The mould clamping was left separate because of the large deviation (Table 7).

Table 7: Median of mould and resin preparation process times combined

	Flat shape [s]	L-shape [s]
Mould clamping	355	558
Mould fixing	154	
Apply piping	352	
Resin mixing	418	
Total working time	1279	1482

The results show that the total working time for the mould clamping, piping, fixing, leakage test and the resin mixing for flat shaped parts with the defined dimensions in Table 3 will be 1279 s and for the L-shaped parts with the same size e about 1482 s. This is an increase of 15.8%. In relation to the defined composite part dimensions for this study, the total working time for both measured parts are considered minimal. Larger part dimensions might increase the working time; the times for mould clamping and mould fixing especially will increase the most. However, the defined dimensions of this study limit this, so the mould fixing and mould clamping times are expected to remain acceptable. All non-flat shaped parts ($t_{CPFM,angle}$) are rather more complex and fall into the category of the L-shape measurements. The following assumptions in equation 7.14 for flat shaped parts ($t_{CPFM,flat}$) and equation 7.15 for all non-flat shaped parts of the mould clamping, application of piping, mould fixing and the resin mixing process can be used.

$$t_{CPFM,flat} = 1279 \text{ s} \quad (7.14)$$

$$t_{CPFM,angle} = 1482 \text{ s} \quad (7.15)$$

7.2. Infusion

Infusion is the step during which the laminate and the matrix material are combined to form the composite part. Here the pot-life is an important parameter – it is the period during which the resin system must be processed. The aim of this analysis is to identify the cost drivers as well as the limitations of the composite design, not to determine the minimal infusion time. A further aim is to study the interactions between the different variables to be able to explain the obtained behaviour. The process starts when the vacuum draws the resin (Prime 20 ULV) through the cavity where the woven fibreglass (195 PW Tight) stack is infiltrated. On completion of the infiltration the subsequent curing phase follows.

Pressure is a very important parameter for this process and must be adapted to the characteristic conditions, such as the mould size, the resin system and the fibre volume fraction. Other important considerations include the placing of the inlet port and the air vents (Section 2.2.1.1). A practical consideration is to place more fibres close to the vent to reduce the resin flow front velocity, to allow complete removal of air before the resin closes up the vent pipe.

This process step requires much expertise to manufacture high quality structures that are free of voids and thermal stresses, even if the latter is sometimes intended for special applications. Figure 37 shows the factors that have an influence on the infusion process. These factors were obtained from literature and from experience.

This section will describe a detailed analysis of the predicted infusion time; measurement methods and results are described.

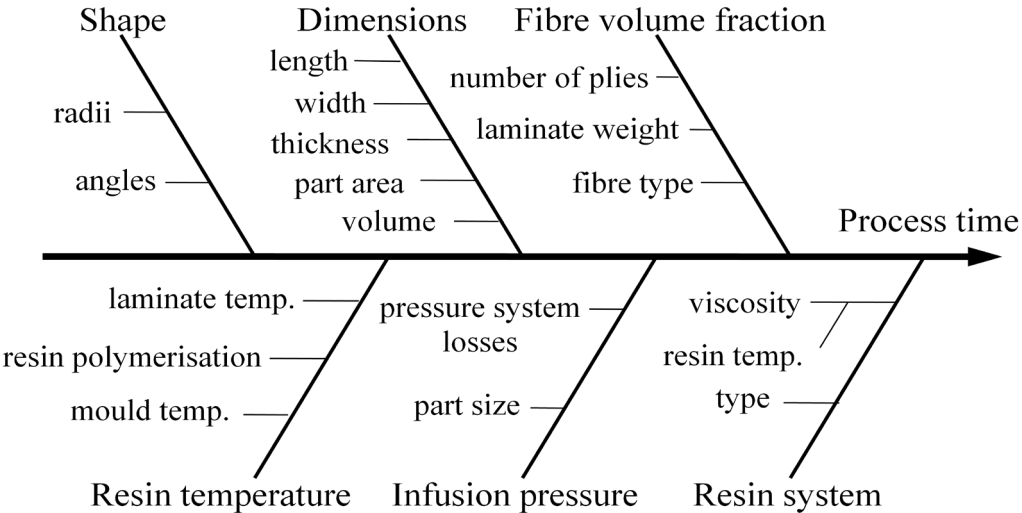


Figure 37: Variables that possibly influence the infusion process

7.2.1. Measurement method

The infusion time during the experimental tests was determined using a stopwatch. The flat and L-shaped moulds were designed to allow the manufacture of moulds each with three different part thicknesses. Timing of the infusion process commenced when the resin entered the mould fitting and ended when it reached the vent fitting on top (Section 4.1).

About half the data were determined using this method. The other half was obtained using verified infusion software (Chapter 6). Various geometries were modelled and different parameters simulated. Especially parts with the defined minimum and maximum dimensions, as well as shapes with different angles and various sized radii, were required for the DOE.

Gravity has a relatively minor effect on parts in the studied size range. It was decided to position the mould inlet at the lowest point and the vent at the highest point, as illustrated in the experimental set-up (Section 4.1).

7.2.2. Results

Analysis of the infusion process time (t_{inf} [s]) was carried out according to the procedure described in Section 5.1.1. After careful screening of variables, the following were used: part surface area A_p [cm²], thickness of part D [mm], angle Ψ [°], outer radius R [mm], fibre volume fraction V_f , differential pressure p [kPa], resin temperature T [K]. As mentioned earlier the mould temperature is assumed to be equal to the resin temperature. These selected variables do not only have an influence on the infusion time, they also interact. This creates complications for conducting the DOE. The DOE used is suited to inspect correlations (Section 5.2.1), however, many tests are necessary.

A useful approximation of the predictors to the response, the infusion time, is limited with a linear approach. Used for the infusion time is therefore a quadratic model which gives a more detailed description. The multiple quadratic regression with all seven predictors resulted in a large equation. Some expressions of the equation have an insignificant contribution to the result. In order to reduce the number of expressions it was decided to set the significance level to 2.5% (Nisbet et al., 2009). The advantage is a simplified equation while still maintaining accuracy at an adequate level. The final result for the infusion time is presented in equation 7.16 ($R^2 = 0.95$). A residual plot is shown Figure B.3 in Appendix B.2. The range of tests for this equation is listed in Table 8. An interpretation is not possible at this stage; it will be presented in the next section. These graphs should be viewed for the trends. The regression models should be used with care, as negative times are possible for unrealistic input values.

$$\begin{aligned} t_{inf} = & 3839.666 + 4.381 A_p - 1.406 p - 9.928 T - 2804.923 V_f - 38.482 D - 1.044 \Psi \\ & - 10.272 R + 9.76E-5 A_p^2 - 5.193E-3 A_p p - 0.012 A_p T - 0.829 A_p V_f + 0.018 A_p D \\ & + 2.314E-3 A_p \Psi - 4.246E-3 A_p R + 0.401 D p + 2787.577 V_f^2 + 0.535 DR \\ & + 0.146 \Psi R \end{aligned} \quad (7.16)$$

Table 8: Range of resin infusion variables tested

Variable	Unit	Range (min/max)	
A_p	[cm ²]	100	2500
D	[mm]	1	10
ψ	[°]	0	90
R	[mm]	0	50
V_f		0.3	0.8
p	[kPa]	30	95
T	[K]	285	310

7.2.3. Application graphs

The following graphs (Figure 38–45) are based on common values shown in Table 9 to illustrate the results of equation 7.16. All graphs show the effect of the variable with increasing part area on the infusion time (t_{inf}).

Table 9: Common values used for the VARTM infusion

Variable	Unit	Average assumption
A_p	[cm ²]	1500
D	[mm]	2.5
ψ	[°]	60
R	[mm]	10
V_f		0.5
p	[kPa]	60
T	[K]	293.15

Figure 38 shows that the infusion time increases rapidly with increasing angle and area. This indicates an increase in complexity and might be caused by the transversal permeability from the fibres. Clearly, to reduce infusion time the part area should be reduced and sharp angles must be avoided.

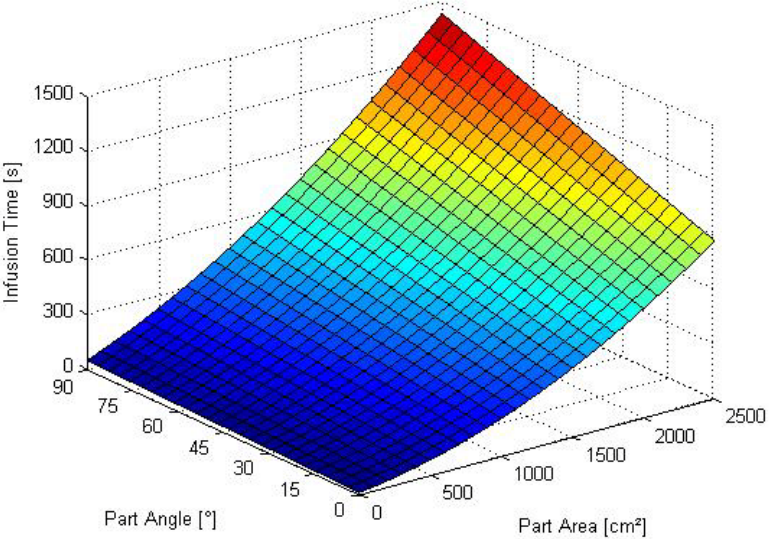


Figure 38: Influence of angle and part area on infusion time

Figure 39 is related to Figure 38, because there must be an angle to have a radius. Figure 39 is based on an angle of 60°. It can be seen that the smaller the radius becomes and as the area increases, the higher is the infusion time. The reason for this might be similar to that proposed for the part angle: sharp radii moderate the resin flow because the transversal permeability is higher.

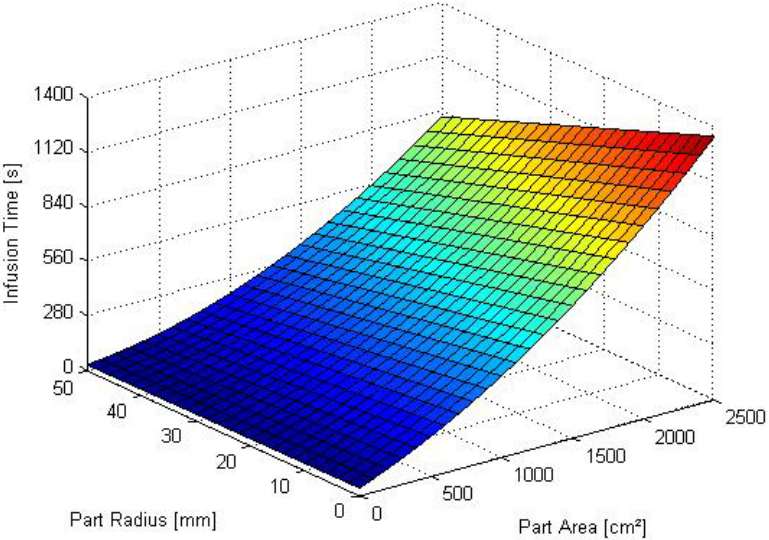


Figure 39: Influence of radius and part area on infusion time

Figure 40 shows the influence of the part thickness and part area on the infusion time for a constant fibre volume fraction of 50%. It is evident that the lowest infusion time is achieved with a large thickness (10 mm) and a minimum part area. With increasing part area, the largest defined thickness (10 mm) increases the infusion time to its maximum.

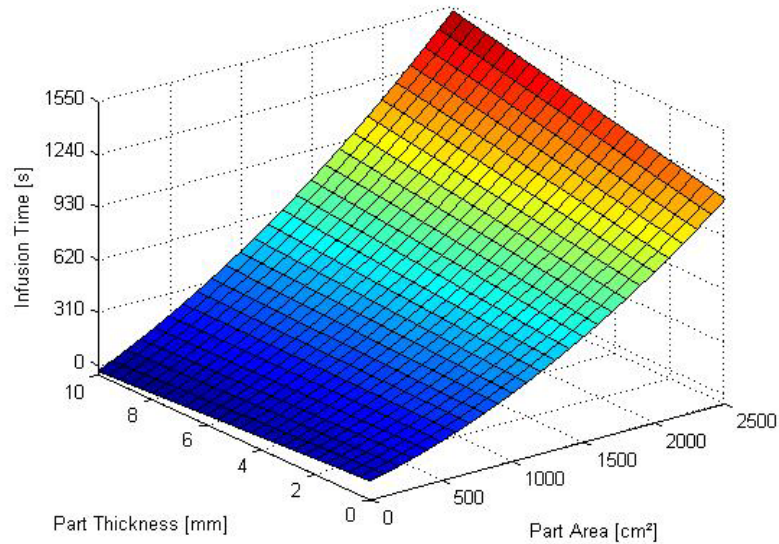


Figure 40: Influence of part thickness and part area on infusion time

Figure 41 shows that the infusion time is lowest for fibre volume fraction of 0.54 and minimum part area. Increasing the area changes the behaviour, and then the lowest fibre volume fraction has the highest infusion time. This behaviour seems logical; if the fibre volume fraction is high then the resistance of the fibre is higher and if the fibre volume fraction is low then the cavity is larger and more resin is required to fill the cavity.

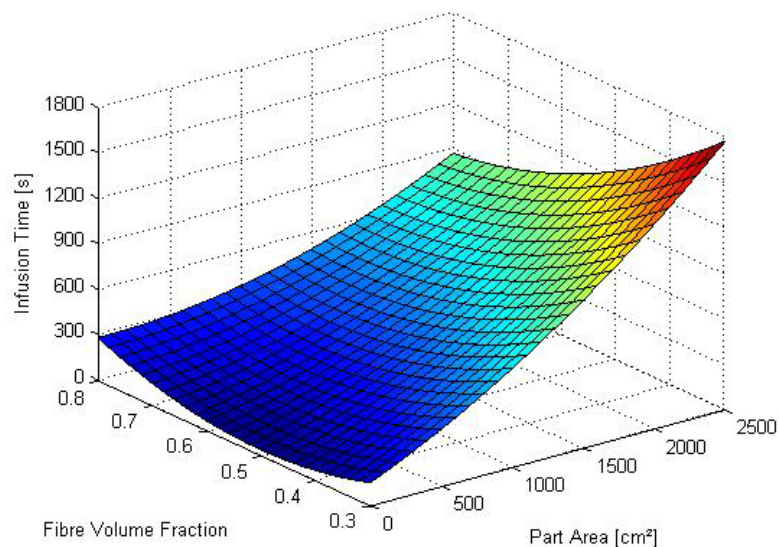


Figure 41: Influence of fibre volume fraction and part area on infusion time

Figure 42 shows that the infusion time increases quadratically with increasing area, and is relatively linear with decreasing pressure difference. The highest infusion time is achieved at the lowest pressure and for the largest area. A second resin inlet port would reduce the area and lead to time saving.

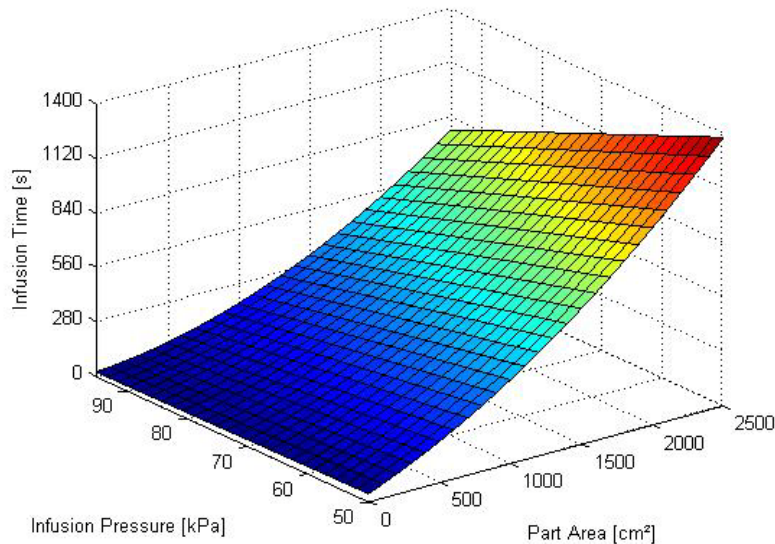


Figure 42: Influence of infusion pressure and part area on infusion time

Figure 43 shows the increasing infusion time with colder temperatures and larger area. The higher viscosity of the resin system at colder temperatures causes this. This graph clearly shows that use of resins with lower viscosity is far more advantageous for the infiltration time than medium viscosity resins.

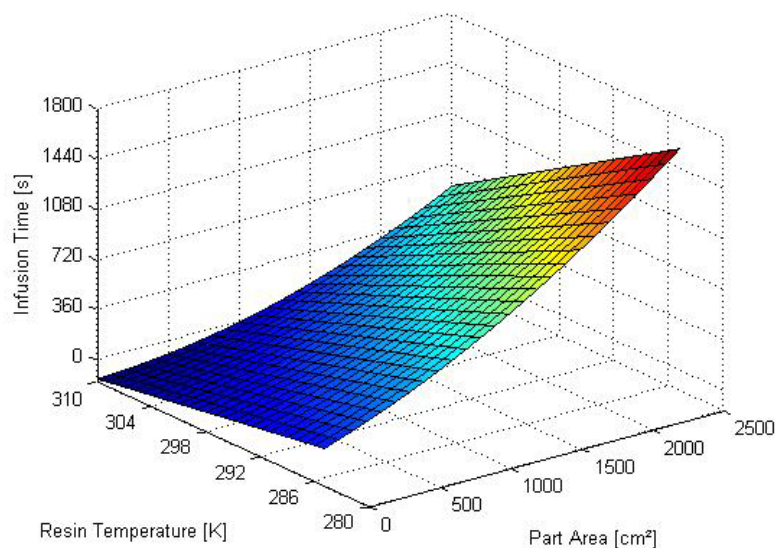


Figure 43: Influence of resin temperature and part area on infusion time

7.3. Curing

Curing is the crystallisation of the matrix material. On completion of infusion the mould remains closed until the composite has reached dimensional stability for demoulding. The demoulded part cures further until the chemical conversion is complete. This is also the point in time when the composite has its maximum mechanical properties. It is optionally possible to speed the process up by preheating the mould; however, the mechanical properties will be affected. The curing time depends on the resin system, added fillers, pigments, accelerators and (of course) on the factors given in Figure 44. Highly reactive resin systems are preferred in order to reach shorter cycle times.

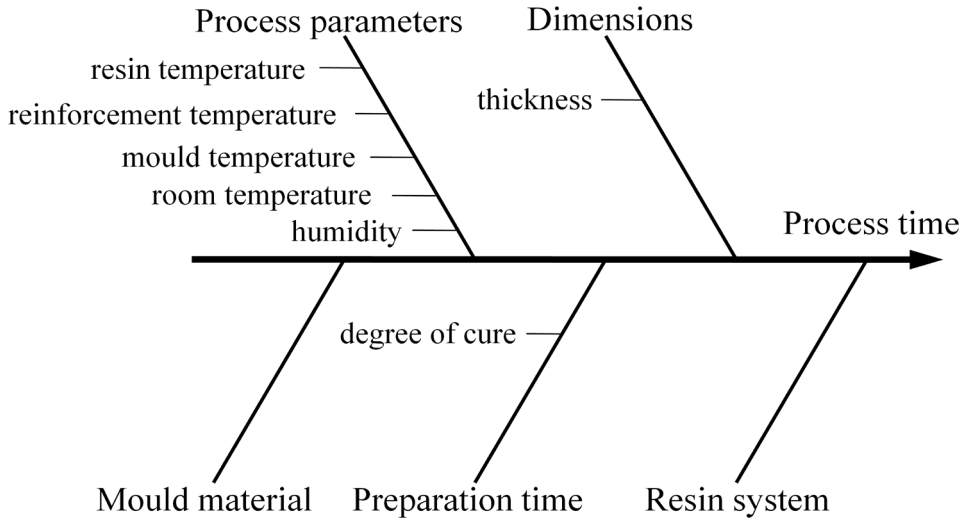


Figure 44: Possible predictors of the curing time

An overview of various resin systems and handling precautions was given in Section 2.2.2.2. The resin system is chosen according to the application and the required mechanical properties. The manufacturer’s specifications for pot-life time are 95 minutes and for demoulding time are 23 hours. These values were used in all calculations for curing.

The temperature of the resin mixture was measured to illustrate the exothermic reaction. The temperature profile is shown in Figure 45. A demoulding point in relation to the exothermic temperature profile would be beneficial for faster demoulding times.

A long curing time is not costly in terms of labour but it reduces the output per mould, and thus the total production capacity.

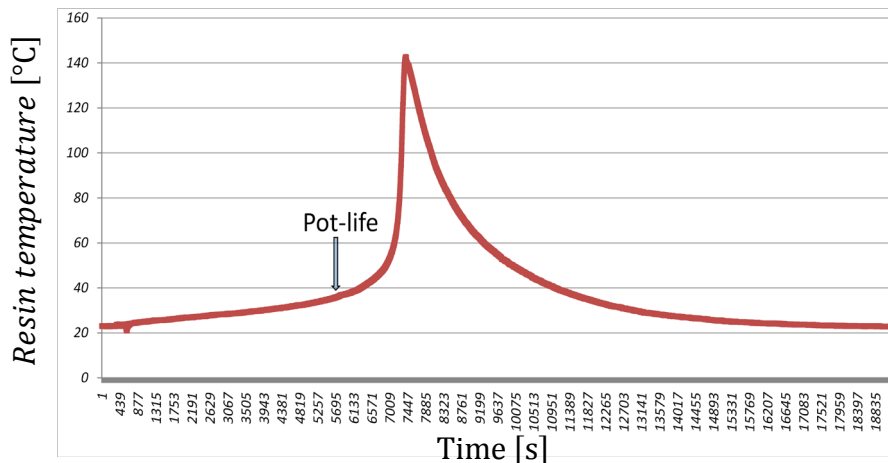


Figure 45: Temperature measurement of Prime 20 ULV

7.4. Demoulding

Demoulding is the removal of the finished composite part. This process step commences with disconnecting the pipes and opening the two mould halves, and then the composite part can be removed from the mould. Ideally, not much force should be necessary. Any force applied might have an impact on the quality of part in terms of surface defects and distortions. The aim of this part of the study is to obtain a demoulding time and to determine whether different shapes might have an influence on it.

7.4.1. Measurement method

The demoulding times for flat- and L-shaped parts were determined separately, using a stopwatch. The experimental moulds and the test equipment were used for this investigation. For better clarity, the process was split in two working sequences. The first sequence is the mould opening and the second part is the removal. The timing commenced with the loosening of the bolts and stopped when the mould was opened. Afterwards the part removal time was started and stopped after the part was released. With the experimental moulds used, it was necessary to drill the hardened resin out of the inlet and outlet ports before the part could be released.

7.4.2. Results

The part removal time presented in Figure 46 showed a great difference in the working time between the flat- and L-shape parts. In contrast, there was no significant difference in the mould opening time.

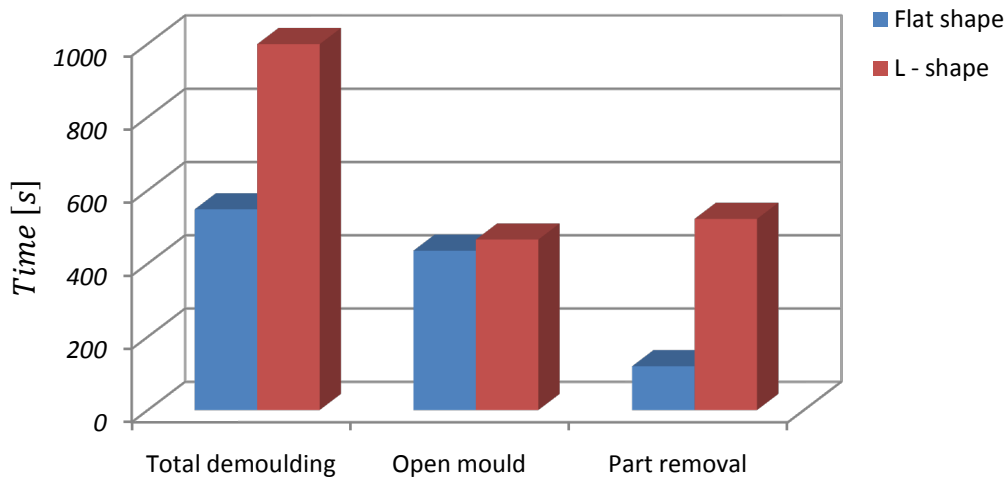


Figure 46: Demoulding times for flat and L-shaped parts

Open mould

The open mould measurements did not show a large deviation. Based on this, it was decided to use the arithmetic mean as a representation of the flat part and angled part opening times (t_{open} [s]), as shown in equation 7.17. The second part of equation 7.17 represents the standard deviation.

$$t_{open} = 423.6 \pm 79.2 \quad (7.17)$$

Part removal

The part removal dataset was sorted in chronological order. The graph in Figure 47 represents the sorted tests for both investigated shapes. A slight improvement in the working time for the release of flat shaped parts is observed. Tests for the L-shaped parts show a strong decrease in the working time, despite the fact that the tests for the L-shaped parts were performed after the tests for the flat shaped parts.

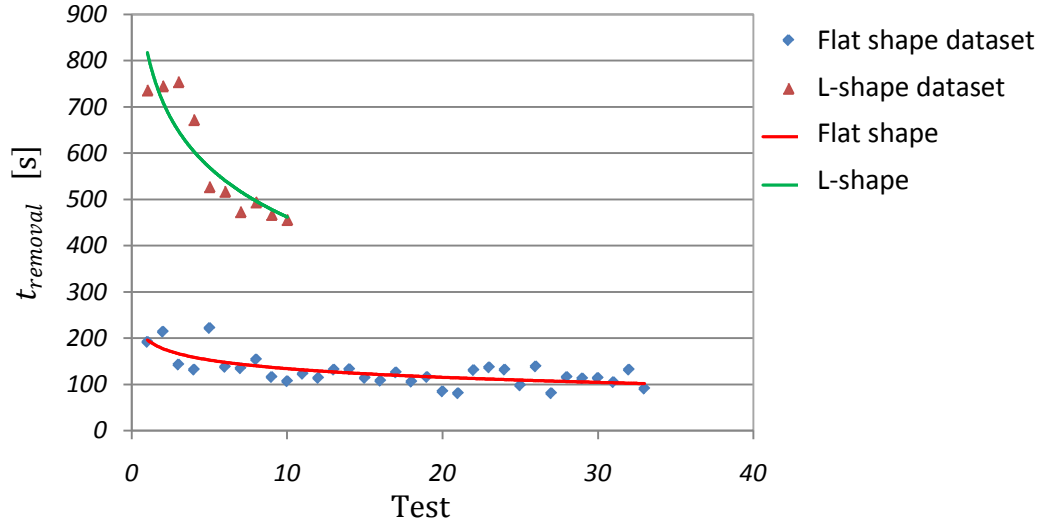


Figure 47: Chronological measurements for the part removal sequence

Analyses revealed that there is a difference in the demoulding time between the flat- and L-shaped parts. To determine the part removal time ($t_{removal}$ [s]), which includes the learning effect, a logarithmic regression for each shape was generated. The logarithmic regression was suitable to represent a time-wise evolution. The results are shown in equation 7.18 ($R^2 = 0.512$) and equation 7.19. ($R^2 = 0.804$). Here n_{test} stands for the test.

It was further decided that the measurements for the L-shape are representative of all non-flat shaped parts. A non-flat shape factor was introduced to describe the complexity, shown in equation 7.20. An example is presented in Appendix B.3.

$$t_{removal, flat} = -26.89 \ln(n_{test}) + 195.97 \quad (7.18)$$

$$t_{removal, non-flat} = -154.7 \ln(n_{test}) + 817.7 \quad (7.19)$$

$$\text{non-flat shape factor} = \frac{t_{removal, non-flat}}{t_{removal, flat}} \quad (7.20)$$

Total demoulding time

The total demoulding time ($t_{demould, flat}$ [s]) is calculated with equation 7.21, using the removal time for flat shaped parts. In the case of non-flat shaped parts, the second term in the equation must be multiplied by the non-flat shape factor; alternatively, the removal time for non-flat shaped parts can be directly used. An example is given in Appendix B.3.

$$t_{demould} = 423.6 (\pm 79.2) + t_{removal} \quad (7.21)$$

7.5. Mould cleaning

Mould cleaning is the step where excess resin is removed from the tools. The aim is to bring the tools to their initial condition and then to inspect the mould for damages. A scraper was used to remove cured excess resin of the mould, occasionally additional wiping with acetone is required. The seal is the most important focus of the inspection; it needs to be carefully inspected for any damage caused during the demoulding.

Analyses were carried out to determine a total working time for cleaning, as well as the dependence thereof on the part size or type of shape.

7.5.1. Measurement method

Time measurements for the cleaning process were conducted on both the manufactured mould shape types. The stopwatch was started when the demoulding was complete and stopped after the mould was ready to begin with the next mould release agent application.

7.5.2. Results

In the first step of the analysis, the same procedure was followed as for the removal of the part. The measurements based on a mould surface area of 4 dm² were chronologically sorted after the time of testing. The graph in Figure 48 shows the mixed dataset from the tests (n_{th}) for both mould types. The first 33 test are conducted on the flat shaped mould and the remaining on the L-shaped one. The Figure 48 demonstrates a considerably large distribution of measurements and a decreasing trend. No significant deviation between the flat and L-shape measurements can be observed. The estimation can be seen as the red line in Figure 48 ($R^2 = 0.33$) and is represented by equation 7.22.

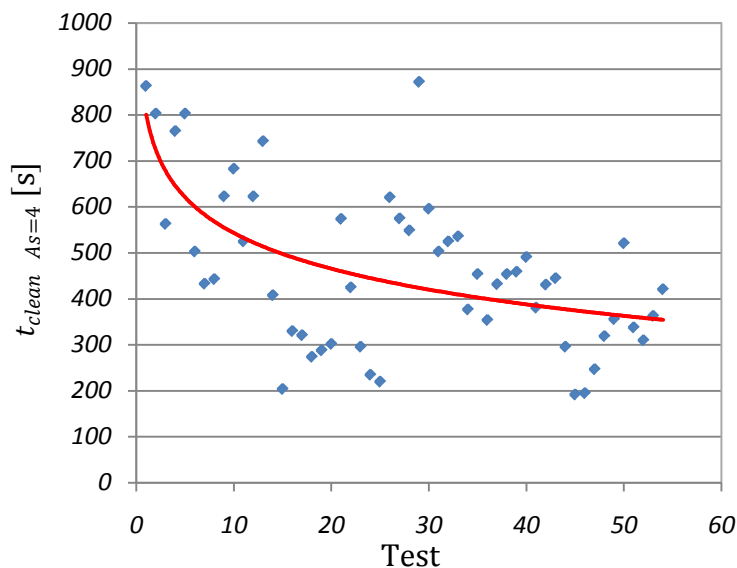


Figure 48: Measurements for the working time spend for cleaning the tools

$$t_{clean \ As=4} = -111.8 \ln(n_{th}) + 800.62 \quad (7.22)$$

The cleaning time ($t_{clean \ As=4}$ [s]) was halved after 36 tests, from the initial value of 801 s to 400 s. Cleaning of the seal was particularly time expensive. It was decided to base the working time for cleaning on the length of the seal in order to relate the size of the mould to the working time. The distance from the seal to the cavity depends on the mould design; therefore, it was decided to base the length of the seal on the circumference of the part surface area, which already takes into consideration that there are two mould halves to be cleaned. The measurements for cleaning were conducted on the mould with a surface area of 4 dm²; each mould half has an approximate seal length of 12 dm. The generated linear relationship between the circumference of the part (C_{As} [dm]) and the total cleaning time (t_{clean}) is shown in equation 7.23.

$$t_{clean} = \frac{t_{clean \ As=4}}{12} C_{As} \quad (7.23)$$

A logarithmic function describes the learning effect, that is for this application suitable. The function should be handled with care for higher production volumes than defined for this study, because of possible unrealistic cleaning times. An example for the use of the total cleaning time is given in Appendix B.4.

8. Transformation to complex shaped parts

This chapter describes the transformation to complex shaped parts. It will be shown, how to split complex parts into the basic shaped parts and how the total manufacturing time for complex part is calculated. The laminate cutting, the mould clamping and positioning, the pipe mounting, resin mixing, the curing and the mould cleaning do not need transformation in the defined range of this study. Therefore, one partitioning procedure is presented for the mould release agent application, the laminate lay-up and demoulding, and a second procedure for the infiltration.

8.1. Mould release agent application, laminate lay-up and demoulding

A complex shaped part can be split into some basic individual shapes and ultimately the manufacturing time can be estimated using existing laws for basic shapes as described in Chapter 7.

For the mould release agent application, the laminate lay-up process and the demoulding of the part, it was decided to base the shape on the main area. The main area is in most cases the centre of the mould design which is often the largest flat area parallel to the mould parting line. All sections parallel to this main area are considered as flat. All the other segments that are positioned with an angle to this main area are considered as angled shapes. In the case of a flat main part area, the manufacturing time is calculated using the equations for flat shapes, and if there is an angle attached then this part area from the edge of the angle is calculated using the equations for angled shaped. The total time for the process step is finally the sum of the working times of each individual part. An application on an industrially manufactured part is presented in Appendix E.

The splitting of complex shaped parts causes an error in process time, which was for reliability reasons investigated for the mould release agent application and the laminate lay-up shown in Appendix B.5. It was found that complex part transformation underestimates the release agent application from 4.4% for the minimum and 10% for the maximum dimensions. It was further shown that the laminate lay-up transformation over predicts the process times of about 78.5% for the minimum dimensions and 29% for the maximum dimensions. The lay-up over prediction of 21 s on average might be caused by the additional pick-up and positioning process which is necessary for the second ply with the complex equivalent part. The demoulding transformation error was not investigated.

8.2. Infusion

The resin infusion follows a flow path from the resin inlet to the vent and needs another approach of transformation, other than above-mentioned process steps. The consideration of

the part areas in the flow path is relevant, because every area, angle or radius in the flow path affects the infusion time for all further individual areas.

Analogous to hydraulic systems the resistance is locally concentrated and is thus related to a fixed location. The coefficient for the flow resistance in hydraulic systems is in most cases experimentally determined, and a functional relationship between the pressure loss (Δp) and the flow rate (v) exists in the form of a constant resistance coefficient (c_R), shown in equation 8.1.

$$\Delta p = c_R v^2 \quad (8.1)$$

For the analysis of complex parts, the covered area has to be split into individual part areas (A_p), as presented in Figure 49. Then the total part area is calculated according to equation 8.2 calculated.

$$A_{p,total} = \sum_i^1 (A_{p_i}) \quad (8.2)$$

Thereafter, flow path for the infusion is investigated. A better understanding develops if the flow path is seen as the travelling path of one particle from the inlet to the outlet. In the case of a runner, one has to decide for the possibly most difficult flow path. This decision can be arbitrary in the case of one vent, because every flow path should reach the outlet at the same time so that the resin does not to close up the vent and trap air.

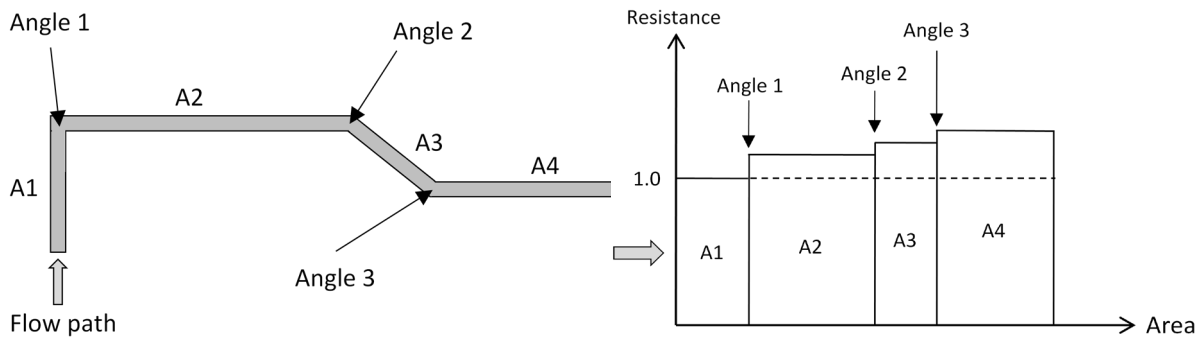


Figure 49: Schematic of flow path and resistance

When the flow path is known, the increasing resistance for each angle and the individual parts can be calculated with the known angle and chamfer design, together with the total part area, as shown in equation 8.3.

$$resistance\ coefficient\ (c_R) = \frac{t_{inf,non-flat, A_{p,total}}}{t_{inf,flat, A_{p,total}}} \quad (8.3)$$

The resistance in the flow path is multiplied with every further resistance in the flow path. Equation 8.4 presents the calculation of the total infusion time ($t_{inf,complex}$) according to the flow path shown in Figure 49.

$$\begin{aligned}
t_{inf,complex} = & \frac{t_{inf,flat\ of\ A_{p,total}}}{A_{p,total}} \left[A_{p_1} (1) + A_{p_2} \left(\frac{t_{Angle\ 1,A_{p,total}}}{t_{flat,A_{p,total}}} \right) \right. \\
& + A_{p_3} \left(\frac{t_{Angle\ 1,A_{p,total}}}{t_{flat,A_{p,total}}} \right) \left(\frac{t_{Angle\ 2,A_{p,total}}}{t_{flat,A_{p,total}}} \right) \\
& \left. + A_{p_4} \left(\frac{t_{Angle\ 1,A_{p,total}}}{t_{flat,A_{p,total}}} \right) \left(\frac{t_{Angle\ 2,A_{p,total}}}{t_{flat,A_{p,total}}} \right) \left(\frac{t_{Angle\ 3,A_{p,total}}}{t_{flat,A_{p,total}}} \right) \right] \quad (8.4)
\end{aligned}$$

An example of the infusion time transformation is presented in the case study in Appendix E.

9. Cost method and model

This chapter introduces the cost method and model. The model enables the preliminary cost calculation of a composite part manufactured with the VARTM technique, using two rigid mould halves. The cost method describes the necessary background information, making it possible for the user to adapt the model to other composite manufacturing techniques, as well as extending it for use in industry. The cost model should provide an indication if it is economic viable to manufacture a product using the VARTM technique or if another technique should be used. First, the chosen cost method will be presented, followed by a summary of results and then the cost model.

9.1. Cost method

This section explains the cost method used for this study. The intention is to show the clear categorisation of each cost item for an exact calculation. The discussion includes the modification of the full costing method on all three-cost categories: direct material costs, manufacturing costs and special once-off expenses.

9.1.1. Modification of the full costing method

One of the requirements for this cost model is the possibility to compare manufacturing costs of different manufacturing methods and materials. To allow a simple and fast comparison of two parts (in industry) it is necessary to use a known base. The full cost accounting method (Kinney & Raiborn, 2008; Young, 2003) is commonly used in industry, because it covers all occurring costs. All of the three cost categories, the material costs, the manufacturing costs and the special once-off expenses usually have overhead costs. Overhead costs cannot be directly added to a specific product. At this point, the calculation differs from the full cost calculation.

A clear picture of the cost develops based on the direct production costs without overhead costs. This leads to the categorisation of direct material costs without indirect material costs, manufacturing costs (direct machining costs & direct labour costs) without overhead costs, and special once-off expenses, which are directly contributing costs of a specific product. The sum of the material, machine and labour costs is the production cost.

Further, there are costs for research and development. Costs for administration and sales can be optionally included. The final sale price can be calculated from the resulting modified primary costs plus the profit margin. The overhead costs and other company specific costs are neglected, but can be integrated into the calculation if necessary (for industry use). Table D.1 in Appendix D.1 shows the calculation scheme of the modified full costing method.

9.1.2. Direct material costs

The direct material costs refer to the expendable materials that are used for each production cycle. These include the resin system, the reinforcement, the mould release agent, the piping and the tacky tape. The sum of all expendables of one manufactured part adds to the direct material costs. It should be noted that excess material could be significant in relation to the part weight. Excess material is no longer usable and must be disposed as waste material, which increases the production cost. Table 10 shows the proposed components of the direct material costs. The prices of all the material are given in Appendix D.2.

Table 10: Proposed components of direct material costs

Material	Price per unit	Dimension considered for cost calculation
Resin mixture	$\frac{R}{\text{kg}}$	matrix weight [kg] + weight for lost material [kg]
Laminate	$\frac{R}{\text{m}^2}$	area [m ²] + area for cutting scrap [m ²]
Mould release agent	$\frac{R}{\text{g}}$	surface area of part [m ²]
PE hose	$\frac{R}{\text{m}}$	length of hose [m]
Tacky tape	$\frac{R}{\text{cm}}$	length of tape [cm]

9.1.3. Manufacturing cost

It is necessary to investigate the entire production process. A systematic analysis requires a breakdown of the manufacturing process into sub-processes and working sequences if necessary. Table 11 presents the breakdown of the sub-process and working sequences. The manufacturing cost comprises the direct machine costs and the direct labour costs of the composite part. This can be further split into the workspace cost rate, the maintenance cost rate, the tooling cost, the energy cost, the space cost and the labour cost – as shown in Table 12. The calculation of the hourly cost rate for this study is presented in Table D.3 (Appendix D.2).

Standard machine cost

The standard machine cost is included in the cost per hour calculation scheme with its repurchase value (RV). This scheme already considers the amortisation and the replacement price of a new machine. Note that the standard machine cost does not have to be fully amortised after one product.

Table 11: General production process plan

Sub-processes	Working sequences
7.1 Set-up	7.1.1 Laminate cutting 7.1.2 Release agent application 7.1.3 Laminate lay-up 7.1.4 Mould clamping, pipe mounting and positioning, resin mixing
7.2 Infiltration	Filling
7.3 Curing	Curing
7.4 Demoulding	Open mould Part removal
7.5 Cleaning	Mould cleaning

Table 12: Determination of hourly cost rate

Repurchase value (RV)	R	
Duration of use	Years	
Interest rate	%	
Operating time	hr/a	
Financial cost hourly rate		R/hr
Maintenance cost from RV	%	
Maintenance cost	R	
Maintenance interval	hr/a	
Maintenance cost rate		R/hr
Tool Costs*	R	
Tool life	working hour	
Total tooling cost		R/hr
Rated power machinery (x%)	kWh	
Rated power vacuum pump (x%)	kWh	
Air ventilation (x%)	kWh	
Pressurised air (x%)	kWh	
Coolants and lubricants (x%)	kWh	
Heating equipment	kWh	
Others x (x%)	kWh	
Σ Power consumption	kWh	
Energy rate	R/kWh	
Energy cost		R/hr
Covered space	m ²	
Space rate/month	R / m ²	
Operating time	hour / month	
Space cost		R/hr
Operator salary	R / hour	
Operator share **	%	
Operator cost		R/hr
Σ Manufacturing expenses		R / hour

Tool costs*

Tool costs comprise the cost of tools in the classical meaning, such as knives and scissors, as well as wear and tear elements, where the specific material is known but the amount is not measureable; example include adhesive spray, acetone and gloves.

Operator share**

The operator share is the percentage of time an operator spends on a product per hour.

9.1.4. Special once-off expenses

Special once-off expenses refers to all machines and tools that are needed exclusively for the manufacturing of a special product, such as the mould. No further usage of the materials in this category is planned. Important factors for the calculation of special once-off expenses are the production volume and the expected product lifetime. These two factors play a large role in the capacity planning, the working plan and the equipment, for production and quality assurance. The distinction between standard machine cost and special once-off expenses is summarised in Table 13. Table D.4 presents the total special once-off expenses cost calculation scheme.

Table 13: Distinction between standard machine cost and special once-off expenses

	Standard machine cost	Special once-off expense
Distinction	Equipment can be used for “all” product variations	Equipment used for manufacturing one specific product
Amortisation	The price of the machine will be depreciated by the expected tool life, number of parts, or years	The price of the machine will be depreciated to the number of parts in one order

9.2. Summary and cost model

This section summarises the results of analysis of Chapter 7 and presents the cost model. The first part summarises the calculation of the total working time for each process step and the second part tabulates the cost calculation.

9.2.1. Summary of working time equations

The working times are calculated according to the equations for each sub-process, as given in Chapter 7. A summary of the total working time for each process step is given below.

Laminate cutting

$$t_{cut} = t_{prep,cut} + n_p \left(\frac{C}{v_{cut}} \right) \quad (7.3)$$

$$v_{cut,m} = 0.253 \ln(n_p) + 0.188 \quad (7.1)$$

$$v_{cut,a} = 50 \left[\frac{\text{cm}}{\text{s}} \right] \quad (7.2)$$

Application of mould release agent

$$t_{handle,flat} = 53.86 \pm 1.84 - (0.16 \mp 0.13) A_s \quad (7.4)$$

$$t_{handle,angle} = 58.29 \pm 2.71 + (0.05 \pm 0.20) A_s \quad (7.5)$$

for $t_{dry} \leq A_s t_{handle}$:

$$t_{app} = t_{prep,MRA} + n_l A_s t_{handle} + t_{dry} \quad (7.7)$$

for $t_{dry} > A_s t_{handle}$:

$$t_{app} = t_{prep,MRA} + n_l A_s t_{handle} + (n_l - 1)(t_{dry} - A_s t_{handle}) + t_{dry} \quad (7.8)$$

Laminate lay-up

$$t_{work,lay,f} = (24.44 \pm 0.42) + A_p (8.68E-3 \pm 2.7E-4) \quad (7.10)$$

$$t_{work,lay,angle} = (27.72 \pm 0.74) + A_p (1.379E-2 \pm 4.7E-4) \quad (7.11)$$

$$t_{layup} = t_{prep,lay} + n_p t_{work,lay} \quad (7.12)$$

Mould clamping, positioning, pipe mounting and resin mixing

$$t_{CPFM,flat} = 1279 \text{ s} \quad (7.14)$$

$$t_{CPFM,angle} = 1482 \text{ s} \quad (7.15)$$

Infusion

$$\begin{aligned} t_{inf} = & 3839.666 + 4.381 A_p - 1.406 p - 9.928 T - 2804.923 V_f - 38.482 D - 1.044 \Psi \\ & - 10.272 R + 9.76E-5 A_p^2 - 5.193E-3 A_p p - 0.012 A_p T - 0.829 A_p V_f + 0.018 A_p D \\ & + 2.314E-3 A_p \Psi - 4.246E-3 A_p R + 0.401 D p + 2787.577 V_f^2 + 0.535 DR \\ & + 0.146 \Psi R \end{aligned} \quad (7.16)$$

Curing

The curing time is resin system dependent and should be adapted to the current mix. The given time represents the manufacturer instructions of Prime 20 ULV.

$$t_{curing} = 23 \text{ h}$$

Demoulding

$$t_{removal, flat} = -26.89 \ln(n_{test}) + 195.97 \quad (7.18)$$

$$t_{removal, non-flat} = -154.7 \ln(n_{test}) + 817.7 \quad (7.19)$$

$$t_{demould} = 423.6 (\pm 79.2) + t_{removal} \quad (7.21)$$

Mould cleaning

$$t_{clean, As=4} = -111.8 \ln(n_{th}) + 800.62 \quad (7.22)$$

$$t_{clean} = \frac{t_{clean, As=4}}{12} C_{As} \quad (7.23)$$

Lead time

The lead time in equation 9.1 shows the total manufacturing time for a certain composite part.

$$t_{lead\ time} = t_{cut} + t_{app} + t_{layup} + t_{CPFM} + t_{inf} + t_{curing} + t_{clean} \quad (9.1)$$

9.2.2. Cost model

This section presents the cost model for the VARTM process. The method of the model was discussed earlier in Section 9.1. It is based on the direct material cost (Appendix D.2), the hourly cost rate (Appendix D.3), and subsequently the total manufacturing cost according to Appendix D.6.

Direct material cost

The direct material cost (C_D) in equation 9.2 comprises the cost per unit of material (R_M) and the consumption of each material (c_M), for all materials (i).

$$C_D = \sum_i^1 R_{M_i} c_{M_i} \quad (9.2)$$

The labour cost rate (R_L) for each process step is assumed to be constant for one workshop, and is calculated according to the scheme in Appendix D.3.

Manufacturing cost

Based on average conditions, the labour cost rates for the Composite Lab were calculated (Table D.3 in Appendix D.3) and gave:

- Set-up process cost rate $135.3 \frac{\text{R}}{\text{h}}$
- Infusion process cost rate $136.7 \frac{\text{R}}{\text{h}}$
- Curing cost rate $4.96 \frac{\text{R}}{\text{h}}$
- Demoulding and cleaning cost rate $135.1 \frac{\text{R}}{\text{h}}$

The manufacturing cost (C_M) consists of the labour cost rate (R_L) and the total working time (t) for each process step (i).

$$C_M = \sum_i^1 R_{H_i} t_i \quad (9.3)$$

Special once-off expenses

The special once-off expenses (C_S) cover mainly the moulding cost; therefore for the mould costs is referred to as a cost model for mould manufacturing. There is also a need for infusion mould cost models. An alternative would be the plastic injection mould cost model. Chin & Wong (1996) have presented a cost estimation model for injection moulding. They claim that their model estimated their case study's cost within 8%.

Total manufacturing cost

The total manufacturing cost consists of the direct, manufacturing and special once-off expense costs.

$$C_{Total} = C_D + C_M + C_S$$

An example calculation shown in Table D.6 illustrates the full procedure involved in calculating the total manufacturing cost. This cost model is very simple; any standard cost calculation in industry can be used to compare the manufacturing cost by simply removing the overhead costs of the calculation, as shown in Table D.1. This gives the freedom to compare costs of composites to, for example, parts manufactured from aluminium.

10. Case study: Refrigerator panel

The complex shaped refrigerator fridge panel shown in the Appendix E is currently manufactured at a collaborating industrial partner. The partner company produces the part in a medium series production volume using the light resin transfer moulding (LRTM) technique. This technique is characterised by a rigid and a semi-rigid mould half and is therefore acceptable for a comparison of manufacturing process times with the generated cost estimation model. The purpose of analysing the fridge panel is to demonstrate the application of the model and to develop a sense of its precision. To accomplish this, the time for each manufacturing step was measured at the industrial partner and the mean of the times compared to the estimated times of the generated cost model. The calculations are presented in Appendix E.

The laminate lay-up times compared best with 27.1% deviation to the industrial part and the largest deviation was found for the filling process with 258%. The mould release agent application and the curing time were not compared, because of a different release agent (wax) and the different application tool (sponge). The curing time depends very much on the used resin system and optional components; therefore, the large range of available products does not allow a general estimation. The laminate cutting time, gelcoat application time and the part demoulding time deviation were in the range 43–59% to the measured times. The deviation for the mould clamping, fixing, piping, resin mixing times and the mould cleaning time were 85% and 161%, respectively.

The general deviation was found to be relatively high, but it has to be taken into consideration that the values from a medium production volume series are being compared to those from a prototyping and low production volume environment. The large deviation of the infusion can be explained by the runner, two vents and different fibre and resin systems. The runner is generally known to drastically reduce the manufacturing time. The mould cleaning times were not in agreement, which could be due to the different moulding concept. The deviation in the demoulding is mainly due to a different sealing and the resin drilling of the experimental mould fitting that was necessary for the removal of the part.

In conclusion, it can be said that the laminate lay-up compares well. All other manufacturing process steps are very specific and the influence of parameters such as runners, different fibre mats and different resin systems have to be investigated in detail.

11. Summary and conclusion

A cost model for composite parts manufactured with the VARTM technique and the configuration of two rigid mould halves was developed. For the experimental testing two different shaped moulds with three different part thicknesses respectively were designed and manufactured. The manufacturing process was split into sub-processes and working sequences, where each process step was separately investigated. The process step times for flat and L-shaped parts were measured, and subsequently analysed with the D-optimal Design of Experiments (DOE) method and other statistical tools. Here special attention was given to the infusion process. Infusion simulation software was used to complement the experimental DOE for parts with different angles as well as larger dimensions. The result for the infusion was an estimation equation based on area, pressure, temperature, fibre volume fraction, thickness, angle and radius. Further, a method to split the complex geometry into the two basic shapes was proposed.

Finally, a modular designed cost model, open for adaptation to other infusion techniques as well as flexible for industry use was developed. This cost model is based on the full costing method which is modified to provide a standardised interface for comparison with other manufacturing processes. Ultimately, the cost model times of each process step were verified to a complex shaped composite part that is currently manufactured at a collaborating industrial partner. The comparison showed good agreement for the laminate lay-up process. Other process step results showed reasonable to large deviations, considering that a medium production series is compared to a prototype and low production volume.

The developed cost model can be used as a DFM tool to reduce the product costs with relatively little effort in the design phase and to determine the most cost efficient manufacturing technique. The model was shown to be relatively process specific. It is recommended to confirm the accuracy for each case of utilising different materials. In the case of an unacceptable process step time deviation, the cost model can be customised according to the presented procedure. Despite the fact that the model is material specific, it can be generally used as a relative comparison to select the most cost effective design variant.

The model is limited to prototypes and low production volumes and the maximum dimensions of $L_i = L_o = 500$ mm, $W = 500$ mm and $D = 10$ mm. Parts with higher dimensions could also be considered, however this has to be tested for every case. Further, the model precision should be proven in a case study with the same material properties and character. It also should be investigated in detail how the splitting of the complex part affects the accuracy of the estimation.

References

- 3M, 2010. *3M Corporation*. [Online] Available at: <http://www.3m.com> [Accessed 22 July 2010].
- Aerontec, 2010. *Aerontec, 14C Warrington Road, Claremont, 7780, Cape Town, South Africa*. [Online] Available at: <http://www.aerontec.co.za> [Accessed 22 July 2010].
- AMT_Composites, 2010. *AMT Composites, Units 3 & 4, M5 Freeway Park, CNR Upper Camp and Berkley Roads, Maitland, 7405, Cape Town, South Africa*. [Online] Available at: <http://www.amtcomposites.co.za> [Accessed 22 July 2010].
- Antony, J. & Antony, F.J., 2001. Teaching the Taguchi method to industrial engineers. *Work study*, 50(4), pp.141-49.
- Bauer, K., 2005. KPI identification with fishbone enlightenment. *DM review*, 15(3), p.12.
- Beckwith, S.W., 2007. Resin infusion technology: part 2 - process definitions and industry variations. *SAMPE journal*, 43(3).
- Bickerton, S., Sozer, E.M., Simacek, P. & Advani, S.G., 2000. Fabric structure and mould curvature effects on preform permeability and mould filling in the RTM process. part 2. predictions and comparisons with experiments. *Composites, Part A 31: Applied science and manufacturing*, pp.439-58.
- Black, S., 2008. Simulating VARTM for better infusion. *High-performance composites*, 16(1), pp.38-41.
- Chase, R.B. & Aquilano, N.J., 1992. Production and operations management: A life cycle approach. *Richard D. Irwin*, (6), pp.511-14.
- Chin, K.S. & Wong, T.N., 1996. Developing a knowledge-based injection mould cost estimation system by decision tables. *International journal of advanced manufacturing technology*, pp.353-64.
- Cooper, C., 2010. Controlling the flow front in vacuum infusion composite part moulding. *Final year project report, Department of Mechanical & Mechatronic Engineering, Stellenbosch University*.
- Ezey, M.D., 2000. Human Learning: From Learning Curves to Learning Organizations. *Springer*, (1), pp.161-77.
- FiberSim, 2010. *Vistagy*. [Online] Available at: <http://www.vistagy.com> [Accessed 26 Augustus 2010].
- FXStreet, 2010. *Interest rate*. [Online] Available at: www.fxstreet.com/fundamental/ [Accessed 2 November 2010].
- García, J.A. et al., 2010. An efficient solver of the saturation equation in liquid composite molding processes. *International journal of material forming*.
- García, J.A. et al., 2009. Meshless methods with application to liquid composite moulding simulation. *Computer methods in applied mechanical engineering*, 189, pp.2700-09.

- Gokce, A., Chohra, M., Advani, S.G. & Walsh, S.M., 2005. Permeability estimation algorithm to simultaneously characterize the distribution media and the fabric preform in vacuum assisted resin transfer molding process. *Composite science and technology*, 65, pp.2129-39.
- Golestanian, H., 2008. Preform permeability variation with porosity of fiberglass. *Journal of material science*, 43, pp.6676-81.
- Gripper_and_Co, 2010. *Gripper & Co (PTY) LTD, 158 Lower Main Road, Observatory, 7925, Cape Town, South Africa*. [Online] Available at: <http://www.gripper.co.za> [Accessed 22 July 2010].
- Grujicica, M., Chittajallua, K.M. & Walsh, S., 2005. Non-isothermal preform infiltration during the vacuum-assisted resin transfer moulding (VARTM) process. *Applied surface science*, 245, pp.51-64.
- Gutowski, T.G. et al., 1987. Consolidation experiments for laminate composites. *Journal of composite material*, 21(7), pp.650-69.
- Gutowski, T. et al., 1994. Development of a theoretical cost model for advanced composite fabrication. *Composites manufacturing*, 5(4).
- Harrison, M.W., 1998. *Handbook of statistical methods for engineers and scientists*. 2nd ed. USA: McGraw-Hill Professional.
- Henkel, 2010. *Henkel AG & Co. KGaA*. [Online] Available at: <http://www.henkel.co.za> [Accessed 22 July 2010].
- Hsiao, K.T., Gillespie, J.W., Advani, S.G. & Fink, B.K., 2001. Role of vacuum pressure and port locations on flow front control for liquid composite moulding processes. *Polymer composites*, 22(5), pp.660-67.
- IMEch, E., 2002. International conference on statistics and analytical methods in automotive engineering. UK, 2002. John Wiley and Sons.
- Inventor, 2010. *Autodesk*. [Online] Available at: <http://www.autodesk.co.za> [Accessed 26 Augustus 2010].
- Joubaud, L. & Trochu, F., 2002. Simulation of the manufacturing of an ambulance roof by vacuum assisted resin infusion (VARI). *Composites 2002 convention and trade show, Composites fabricators association*.
- Kaynak, C., Akgul, E. & Isitman, N.A., 2008. Effects of RTM mould temperature and vacuum on the mechanical properties of epoxy/glass fiber composite plates. *Journal of composite materials*, 42(15), pp.1505-21.
- Kim, S.K. & Daniel, I.M., 2003. Determination of three-dimensional permeability of fiber preforms by the inverse parameter estimation technique. *Composites, Part A-34: Applied science and manufacturing*, pp.421-29.
- Kinney, M.R. & Raiborn, C.A., 2008. Cost accounting: Foundations and evolutions. *South Western Educ Pub*, (7), pp.60-78.

- Lam, Y.C. & Seow, L.W., 2000. Cavity balance for plastic injection moulding. *Polymer engineering and science*, 40(6), pp.1273-80.
- Lawrence, J.M. et al., 2002. An approach to couple mould design and on-line control to manufacture complex composite parts by resin transfer molding. *Composites*, Part A 33: Applied science and manufacturing, pp.981-90.
- Lebrun, G., Gauvin, R. & Kendall, K.N., 1996. Experimental investigation of resin temperature and pressure during filling and curing in a flat steel RTM mould. *Composites*, Part 27 A: Applied Science and Manufacturing(5), pp.347-56.
- Lee, L.J., Young, W.B. & Lin, R.J., 1994. Mould filling and cure modeling of RTM and SRIM processes. *Composite structures*, 27, pp.109-20.
- Lekakou, C., Johari, M.A.K., Norman, D. & Bader, M.G., 1996. Measurement techniques and effects on in-plane permeability of woven cloths in the resin transfer moulding. *Composites*, Part A 27, pp.401-08.
- Liu, B., Bickerton, S. & Advani, S.G., 1996. Modelling and simulation of resin transfer moulding (RTM) - gate control, venting and dryspot prediction. *Composites*, Part A 27(2), pp.135-41.
- Luo, Y., 2001. Resin Transfer Molding of Knitted Fabric Reinforced Composites. *PhD Thesis, Katholieke Univeriteit Leuven Belgium*.
- Manson, R.L., Gunst, R.F. & Hess, J.L., 2003. *Statistical design and analysis of experiments: With applications to engineering and science*. 2nd ed. USA: John Wiley & Sons.
- Mathur, R., Fink, B.K. & Advani, S.G., 1999. Use of generic algorithms to optimize gate and vent locations for the resin transfer moulding process. *Polymer composites*, 20(2), p.167.
- McGill, R., John, W.T. & Larsen, W.A., 1978. Variations of box plots. *The american statistician*, 32(1), pp.12-16.
- Moldflow, 2010. Autodesk. [Online] Available at: <http://www.moldflow.com/stp/> [Accessed 24 Augustus 2010].
- Moore, M.F. & Bland, R.J., 1999. RTM equipment and process automation. *SAMPE journal*, 2(35), pp.39-46.
- myRTM, 2010. *University of Rapperswil in Switzerland*. [Online] Available at: <http://iwk.hsr.ch/myRTM.3575.0.html?&L=4> [Accessed 14 July 2010].
- Nedeß, C. & Holst, G., 1992. Hilfen für die statistische Versuchsplanung, Qualität und Zuverlässigkeit. *Carl Hanser Verlag*, (4), pp.202-04.
- Nisbet, R., Elder, J.F. & Miner, G., 2009. *Handbook of statistical analysis and data mining applications*. USA: Academic Press.

Owen, M.G., Middleton, V. & Jones, I.A., 2000. *Integrated design and manufacture using fibre-reinforced polymeric composites*. UK: Owen, M. G.

PAM-FORM, 2010. *ESI*. [Online] Available at: <http://www.esi-group.com/products/composites-plastics/pam-form> [Accessed 27 Augustus 2010].

PAM-RTM, 2010. *ESI*. [Online] Available at: <http://www.esi-group.com/products/composites-plastics/pam-rtm> [Accessed 14 July 2010].

Patran, 2010. *MSC*. [Online] Available at: <http://www.mscsoftware.com/Products/CAE-Tools/Patran.aspx> [Accessed 26 Augustus 2010].

Peters, S.T., 1997. *Handbook of composites*. 2nd ed. Springer.

RTM-Worx, 2010. *Polyworx*. [Online] Available at: <http://www.polyworx.com> [Accessed 11 July 2010].

Rudd, C.D., Long, A.C., Kendall, K.N. & Mangin, C.G.E., 2007. *Liquid moulding technologies: Resin transfer moulding, structural reaction injection moulding and related processing techniques: A guide to RTM, SRIM and related composites processing techniques*. UK.

Scholz, S., Gillespie, J.W. & Heider, D., 2007. Measurement of transverse permeability using gaseous and liquid flow. *Composites, Part A 38: Applied science and manufacturing*, pp.2034-40.

SimXpert, 2010. *MSC*. [Online] Available at: <http://www.mscsoftware.com/Products/CAE-Tools/SIMXpert.aspx> [Accessed 26 Augustus 2010].

Song, X. et al., 2004. Modeling the VARTM composite manufacturing process. *SAMPE 2004 symposium and exhibition*, pp.1-13.

SP_Gurrit, 2010. *Gurit (UK) Ltd, St Cross Business Park, Newport, Isle of Wight, PO30 5WU, United Kingdom*. [Online] Available at: <http://www.gurit.com> [Accessed 22 July 2010].

Van de Ven, E.C., Loendersloot, R. & Akkerman, R., 2006. Experimental investigation of the compressibility and permeability of fabric reinforcements. *The 8th international conference on flow process in composite material*.

Veldsman, G., 1995. *Aspects of design for manufacturability in RTM*. MSc thesis, University of Stellenbosch ed. Stellenbosch.

Visconti, C., Langella, A. & Durante, M., 2003. Analysis of transversal permeability for different types of glass fiber reinforcement. *Applied composite materials*, 10, pp.119-27.

Wember, T., 2008. *Technische Statistik und statistische Versuchsplanung*. 8th ed. Germany: Wember, T.

Williams, C., Simmerscalest, J. & Grove, S., 1996. Resin infusion under flexible tooling (RIFT): A review. *Composites, Part 27 A: Applied science and manufacturing*(7), pp.517-24.

Young, D., 2003. Techniques of Management Accounting : An Essential Guide for Managers and Financial Professionals. *McGraw-Hill*, (1), pp.9-37.

Zaloom, V. & Miller, C., 1982. A review of cost estimating for advanced composite materials applications. *Engineering cost and production economics*, 7, pp.81-86.

Zhou, F., Alms, J. & Advani, S.G., 2008. A closed form solution for flow in dual scale fibrous porous media under constant injection pressure conditions. *Composites science and technology*, 68, pp.699-708.

Appendices

Appendix A: Analytical procedure and analysis

A.1 Examples of data types

There are two types of measuring types, as shown in Table A.1.

Table A.1: Measuring types

Type	Description	Data type	Examples
continuous	measuring	floating point	volume, area, length, weight, time, pressure, temperature, velocity
discrete	counting results	integer	number of plies, number of layers, number of batches

Appendix B: Process analysis of basic shapes

B.1 Application graphs for mould releasing agent

The graphs in this section are based on assumed values in order to obtain an illustration of relationships and a fast estimation of process times. Figure B.1 and Figure B.2 present the process application times for flat shaped moulds and non-flat shaped moulds, respectively. Both graphs are based on paintbrush application, with the recommended 5 minutes preparation time and a drying phase of 5 minutes.

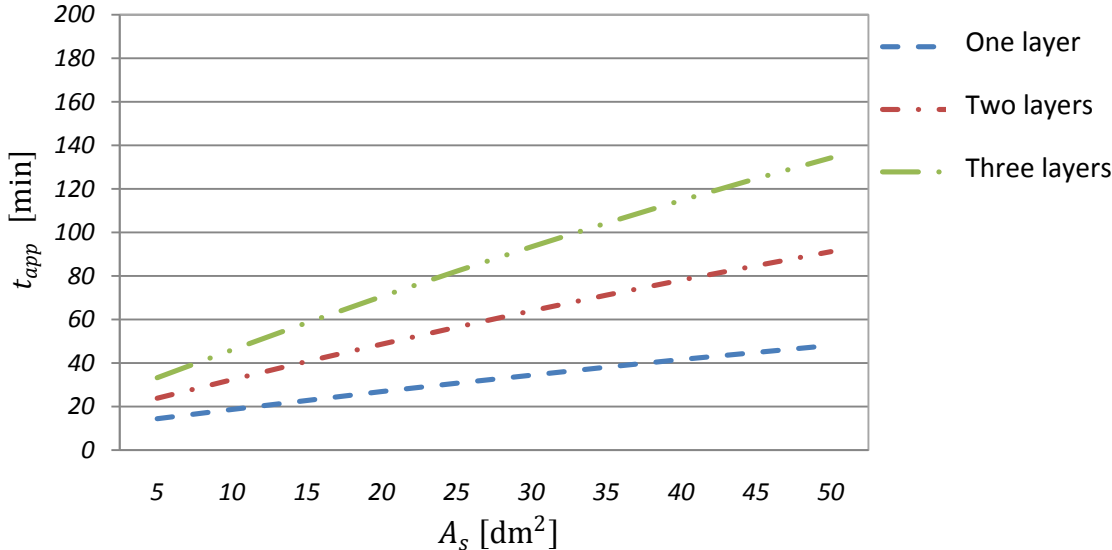


Figure B.1: Application time for one, two and three layers of mould release agent on flat shaped moulds

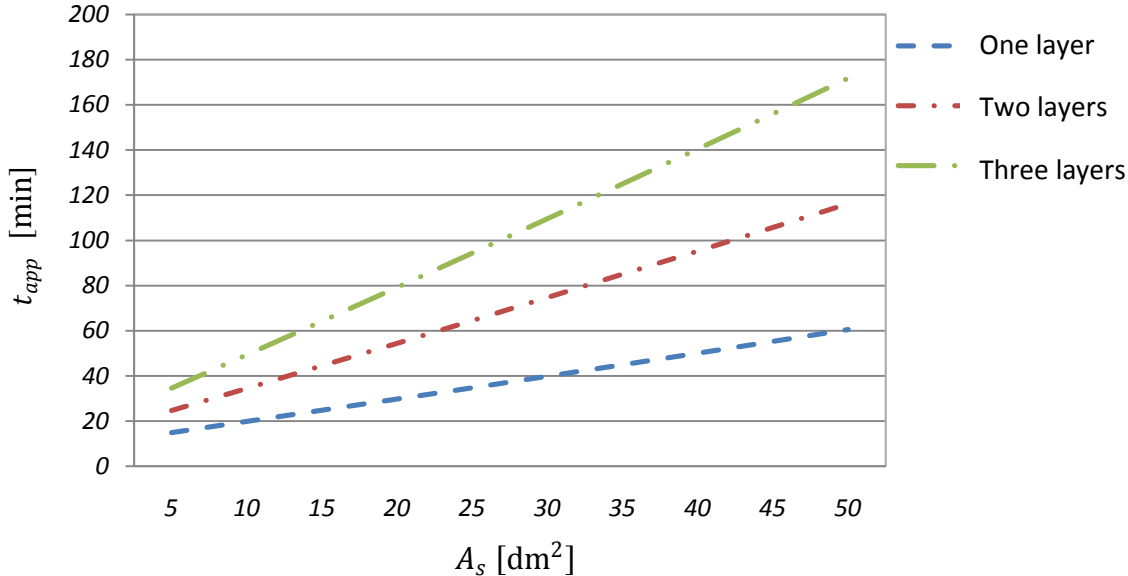


Figure B.2: Application time for one, two and three layers of mould release agent on non-flat shaped moulds

B.2 Infusion

The Figure B.3 shows the standardised residual plot of the infusion process. The standardised residual means that an independent estimate was divided by its standard error and thus is useful to show outliers. From test number 54 to the end are the experimentally determined data points.

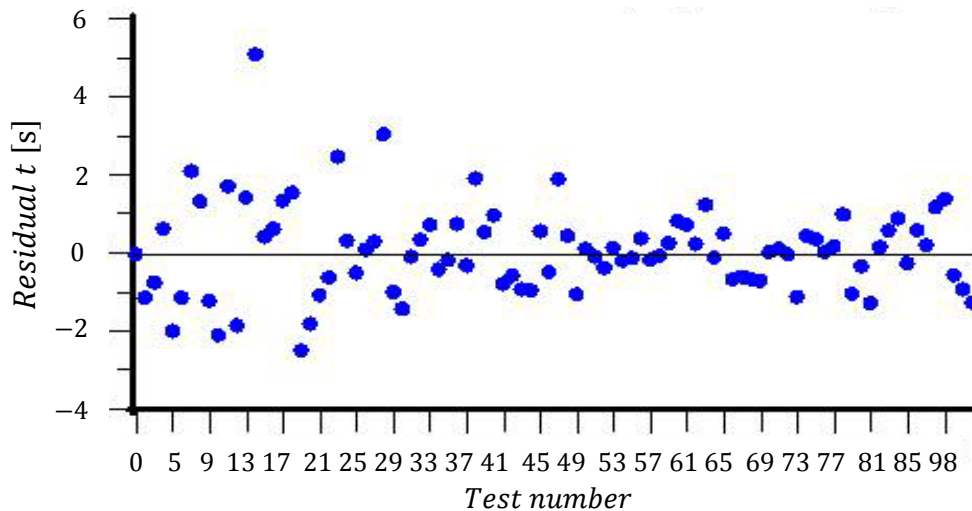


Figure B.3: Residual plot of infusion estimation on test number

B.3 Demoulding

Example calculation for the demoulding process time according to equations 7.18 – 7.21. In the case of 30th test, for flat and non-flat shaped parts.

$$t_{release, flat} = -26.89 \ln(30) + 195.97 = 104.51 \text{ s}$$

$$t_{release, non-flat} = -154.7 \ln(30) + 817.7 = 291.53 \text{ s}$$

$$non - flat \text{ shape factor} = \frac{291.53}{104.51} = 2.79$$

$$t_{demould, flat} = 423.6 (\pm 79.2) + 104.51 = 528.11 \text{ s}$$

$$t_{demould, non-flat} = 423.6 (\pm 79.2) + 104 \cdot (2.79) = 715.2 \text{ s}$$

B.4 Mould cleaning

Example calculation for the mould cleaning process time. The basis for this calculation of cleaning time is the 36th test (399.98 s). The seal circumference is 15 dm². Equations 7.16 and 7.17 are used.

$$t_{clean \ A_s=4} = -111.8 \ln(36) + 800.62 = 399.98 \text{ s}$$

$$t_{clean} = \frac{399.98 \text{ s}}{12 \text{ dm}} 15 \text{ dm} = 499.96 \text{ s}$$

B.5 Transformation error

Mould release agent application

To represent the defined part dimensions, it was decided to use a part surface area of 4 dm² as minimum and 50 dm² as the maximum area (see Table B.1). The calculation neglects preparation and drying time and is based on one applied layer.

Table B.1: Mould release agent application error calculation

	$A_s = 4 \text{ dm}^2$	$A_s = 50 \text{ dm}^2$
L-shape estimation acc. to equation 7.7	234 s	3039.5 s
Basic flat shape	(2 dm ² ⇒ 106.9 s)	(25 dm ² ⇒ 1246.5 s)
Basic L-shape	(2 dm ² ⇒ 116.8 s)	(25 dm ² ⇒ 1488.5 s)
Complex equivalent part (basic flat shape + L-shape)	223.7 s	2735 s
Deviation	10.3 s / - 4.4%	304.5 s / - 10%

Laminate lay-up

The minimum part area dimension is defined as 200 cm² and the maximum area is specified as 2500 cm². The calculation shown in Table B.2 assumes on laminate layer and neglects the preparation time.

Table B.2: Laminate lay-up error calculation

	$A_p = 200 \text{ cm}^2$	$A_p = 2500 \text{ cm}^2$
L-shape estimation according to equation 7.11 & equation 7.12	30.5 s	62.2 s
Flat shape $A_p = 100 \text{ cm}^2$	(100 cm ² ⇒ 25.3 s)	(1250 cm ² ⇒ 35.3 s)
L-shape	(100 cm ² ⇒ 29.1 s)	(1250 cm ² ⇒ 45 s)
Complex equivalent part	54.4 s	80.3 s
Deviation	23.9 s / +78.5%	28.1 s / +29%

Appendix C: Simulation

C.1 Equivalent permeability for "runners", and inlet and outlet zones

Equation C.1 gives the equivalent permeability for "runners", and inlet and outlet zones in all three directions. The runners and zones do not contain any fibres, therefore the law of Poiseuille flow applies. Equation C.2 shows the calculation for the example of the verification model.

$$K = \frac{D^2}{12} \quad (C.1)$$

$$K = \frac{(0.006 \text{ m})^2}{12} = 3 \cdot 10^{-6} \text{ m}^2 \quad (C.2)$$

C.2 Runners, and inlet and outlet zones: properties

The inlet and outlet zones were kept constant, with the properties tabulated in Table C.1.

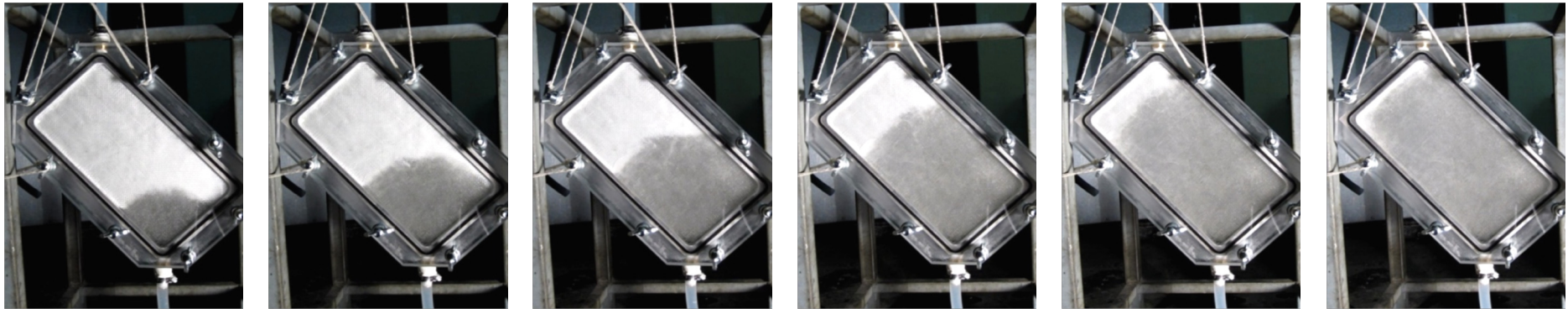
Table C.1: Zone properties for inlet and outlet for simulation software

Description	Symbol	Value	Unit
Permeability	K_1, K_2, K_3	$3 \cdot 10^{-6}$	m^2
Density	ρ_f	1.293	$\frac{\text{Kg}}{\text{m}^3}$
Thermal conductivity (isotropic, const.)	k_{th}	0.0261	$\frac{\text{W}}{\text{m K}}$
Effective conductivity (isotropic, const.)	k_{eff}	0.0261	$\frac{\text{W}}{\text{m K}}$
Specific heat	c	1005	$\frac{\text{J}}{\text{Kg}} \text{K}$

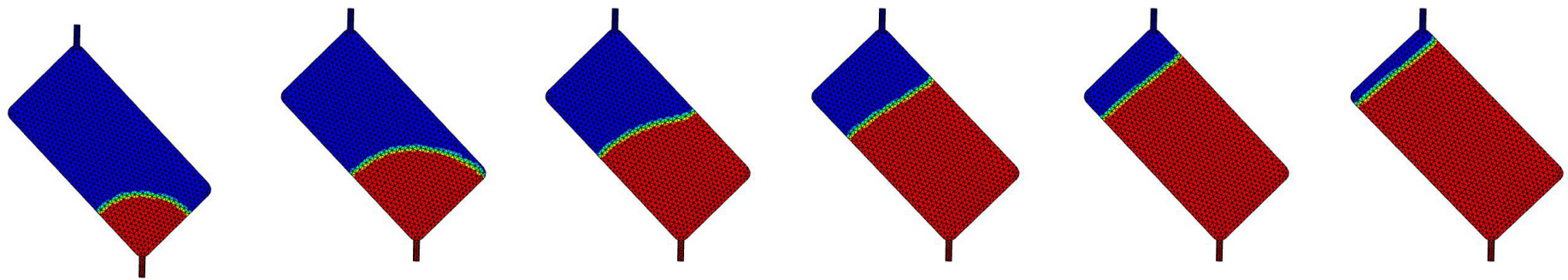
C.3 Further simulation verification figures

Figure C.1 and Figure C.2 show the validation and verification for 90 kPa and 35 kPa respectively.

a. *b.* *c.* *d.* *e.* *f.*



g. *h.* *i.* *k.* *l.*



$t = 5 \text{ s}$

$t = 11 \text{ s}$

$t = 18 \text{ s}$

$t = 25 \text{ s}$

$t = 32 \text{ s}$

$t = 37 \text{ s}$

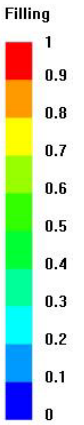
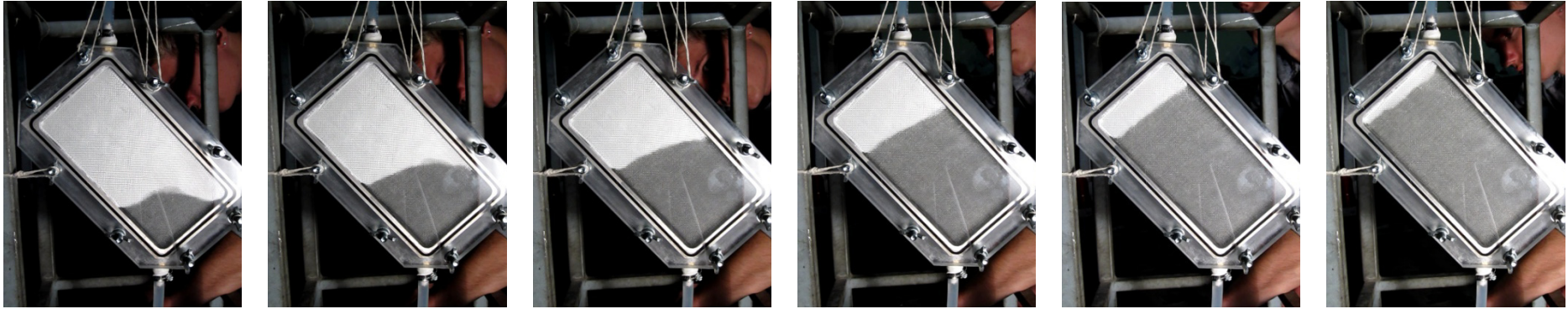
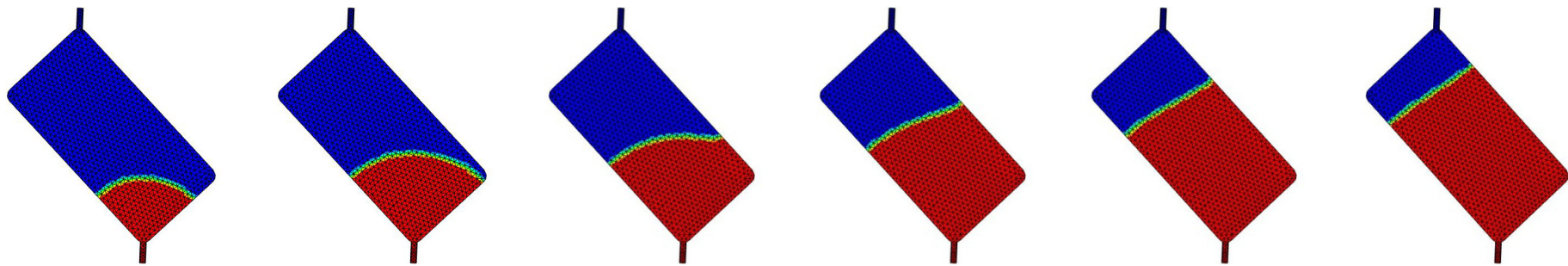


Figure C.1: Comparison of experimental to simulation results at 90 kPa

a. *b.* *c.* *d.* *e.* *f.*



g. *h.* *i.* *j.* *k.* *l.*



$t = 11 \text{ s}$

$t = 23 \text{ s}$

$t = 33 \text{ s}$

$t = 45 \text{ s}$

$t = 57 \text{ s}$

$t = 66 \text{ s}$

Figure C.2: Comparison of experimental to simulation results at 35 kPa

Appendix D: Cost model

This section contains reports of the costs calculation and assumptions for the cost model.

D.1 Full costing method modifications

Table D.1: Full costing method with modifications

Direct material costs		R ...	
Indirect material costs	%	R ...	
Overall material costs			R ...
Machine cost		R ...	
Machine overhead costs	%	R ...	
Overall machine cost			R ...
Labour costs		R ...	
Labour overhead costs	%	R ...	
Overall labour costs			R ...
Manufacturing cost			R ...
Special once-off expenses			R ...
∑ Production costs			R ...
R&D costs	%		R ...
Administration costs	%		R ...
Sales costs	%		R ...
Prime costs			R ...
Profit	%		R ...
Target sales price			R ...

D.2 Direct material costs

Table D.2 lists the material costs applicable in this study.

Table D.2: Details of materials used

Amount	Material description	Cost [R]	Manufacturer/Reseller
1 kg	Prime 20 Ultra Low Viscosity (ULV) resin system mixed	120.3	(SP_Gurrit, 2010) / (AMT_Composites, 2010)
1 m ²	Plain woven Fibreglass FAW 195 $\frac{\text{g}}{\text{m}^2}$	33.4	(Aerontec, 2010)
1 m	PE hose 12/10 mm white	19.36	(Gripper_and_Co, 2010)
5 l	Loctite Frekote 770-NC release agent	1293	(Henkel, 2010) / (AMT_Composites, 2010)
400 ml	Airtec 2 adhesive spray	181.26	(3M, 2010) / (Aerontec, 2010)
1	Aceton solvent	15.39	(Aerontec, 2010)
100 pieces	Latex gloves	76.67	(Aerontec, 2010)
22.5 m	AT 140 white tacky tape	72.39	(Aerontec, 2010)

D.3 Hourly cost rate

Table D.3 presents the calculation of the labour costs for each process step. The assumptions made here were also used for the case study calculation in Chapter 10.

Table D.3: Calculation of hourly cost rate

Work process		Set-up	Infusion	Curing	Demolding	Cleaning
Repurchase value (RV)	R	20000	30000	20000	20000	20000
Duration of use	Years	5	5	5	5	5
Interest rate	%	6.5	6.5	6.5	6.5	6.5
Operating time	hr/annum	2000	2000	2000	2000	2000
Financial cost hourly rate	R/hr	2.33	3.49	2.33	2.33	2.33
Maintainance cost from RV	%	5	5	0	5	5
Maintainance cost	R	1000	1500	0	1000	1000
Maintainance interval	hr/annum	2000	2000	0	2000	2000
Machine maintainance cost rate	R hr	0.50	0.75	0	0.50	0.50
Cost	R	300	300	0	0	0
Tooling interval	working hours	2000	2000	0	0	0
Tooling cost	R/h	0.15	0.15	0	0	0
Rated power machinery	kWh	2 (50%)	2 (50%)	0	2 (50%)	2 (50%)
Air ventilation (x%)	kWh	0.4 (100%)	0.4 (100%)	0.4 (100%)	0.4 (100%)	0.4 (100%)
Pressurised air (x%)	kWh	0	0	0	0	0
Heating equipment	kWh	0	0	0	0	0
Energy rate	R/kWh	1.0	1.0	1.0	1.0	1.0
Energy cost	R/hr	1.4	1.4	0.40	1.4	1.4
Covered space	m ²	10	10	10	10	10
Space rate/month	R/m ²	15	15	15	15	15
Operating time	hr/month	160	160	160	160	160
Space cost	R/hr	0.93	0.93	0.93	0.93	0.93
Operator salary	R/hr	130	130	130	130	130
Operator share	%	100	100	1,0	100	100
Operator cost	R/hr	130	130	1,3	130	130
Houly cost rate	R/hr	135.3	136.7	4.96	135.1	135.1

D.4 Special once-off expenses

Table D.4 shows the calculation procedure of the special once-off expenses, such as the mould.

Table D.4: Special once-off expenses cost calculation procedure

Mould			
Cost of mould	R	
Output	Number of parts	
<hr/>			
Mould cost per part		
Fixture (control equipment, specific tools)			
Cost of fixtures	R	
Fixture intervals	working hours	
<hr/>			
Cost of fixtures per part		
<hr/>			
Σ Specific tool cost per part	R	
Σ Specific tool cost in total	R	

D.5 Company related assumptions

Table D.5 presents the company related assumptions for the cost calculation.

Table D.5: Company related assumptions used for cost calculation

Specific company assumptions	Unit	Value	Based on
Operator's salary	R/hr	130	Average trained labour, without tax
Working time	hr/day	8	Average trained labour
	hr/week	40	
	hr/annum	2000	
Space costs	R/m ²	15	Per month
Specific environmental assumptions		Value	Based on
Energy rate	R/kWh	1.0	Average for RSA
Interest rate	%	6.5	Average for RSA (FXStreet, 2010)

D.6 Calculation of total manufacturing cost

Table D.6: Calculation of total manufacturing cost (without the special once-off expenses)

Direct material costs	R/unit	Consumption	Costs [R]
Resin + hardener	120.3 R/kg	0.1 kg	12.03
Laminate	33.4 R/m ²	0.60 m ²	20.04
Mould release agent	258.6 R/l	0.05 l	12.93
PE hose	19.36 R/m	2 m	38.72
Direct material costs (total)			83.72

Manufacturing costs	R/hr	R/min	Working time [min]	Costs [R]	
Set-up	135.3	2.25	Laminate cutting	30	67.5
			Application of mould release agent	25	56.25
			Laminate lay-up	10	22.5
			Mould clamping and resin mixing	20	45.0
Infusion	136.7	2.27	5	11.35	
Curing	4.96	0.082	1380	113.1	
Demoulding	135.1	2.25	Open mould, part release	10	22.5
			Cleaning	8	18.0
Manufacturing cost (total)				356.2	
Sum of direct material costs + Manufacturing costs				439.92	

Appendix E: Case study: Refrigerator panel

The refrigerator panel shown on the left of Figure E.1 is shaped like a tub. It was geometrically simplified using the assumption that the front area (A1) is flat. The sides have an almost 90° angle to the front area and the thickness is assumed to be constant at 2 mm. The applied pressure on the two vents (V1 and V2) is 50 kPa. Other manufacturing parameters are defined as $T = 294.15$ K, $V_f = 0.45$. Further dimensions are illustrated in Figure E.1.

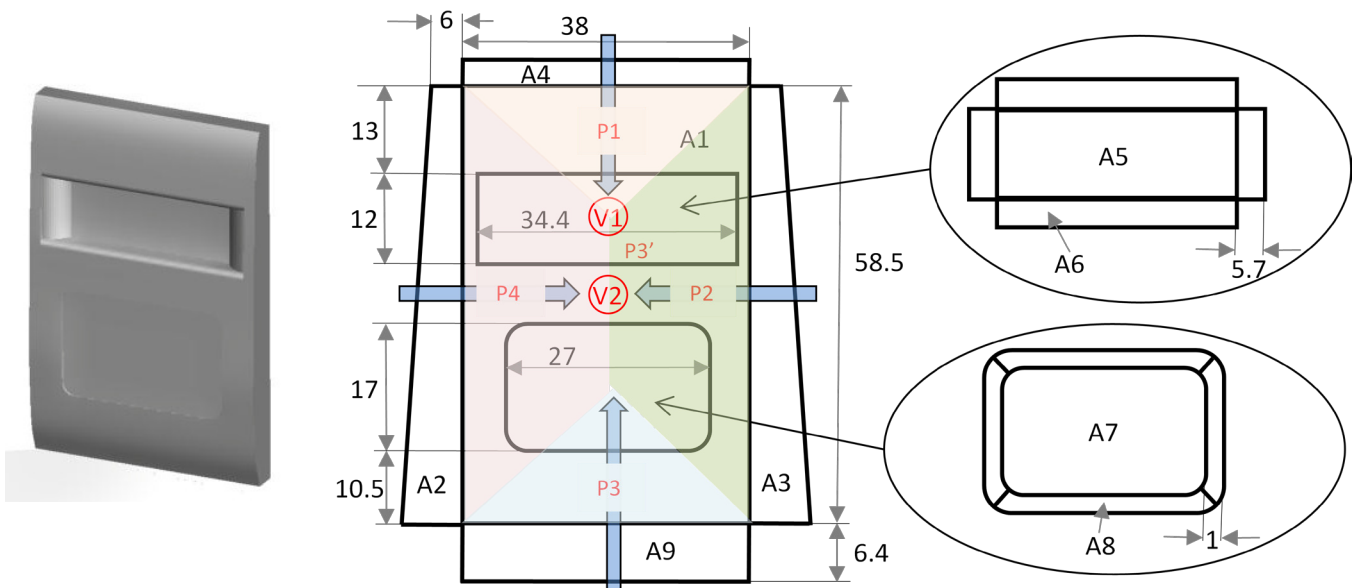


Figure E.1: Refrigerator panel with dimensions [cm]

The results of the case study are tabulated in Table E.1: Results of case study. The results of calculations and comments are discussed in the sections that follow.

Table E.1: Results of case study

Process step	Mean of measured	Estimated time [s]	Deviation [%]
Laminate cutting	234 ($\sigma=\pm 22$)	373	59.4
Gelcoat application	733 ($\sigma=\pm 62$)	1119.7	52.8
Laminate lay-up	179 ($\sigma=\pm 7$)	227.5	27.1
CPFM	803 ($\sigma=\pm 47$)	1482	84.6
Infusion	187 ($\sigma=\pm 11$)	668.76	257.6
Part demoulding	337 ($\sigma=\pm 13$)	533	42.9
Mould cleaning	527 ($\sigma=\pm 47$)	1417.9	169.1

E.1 Laminate cutting

Most of the laminates are pre-cut, therefore only the cutting of the main laminate is compared to the estimated times. The main laminate is one layer (Rowy Core Saertex; 300 x 300 $\frac{\text{g}}{\text{m}^2}$ top/bottom), which covers all part areas, except the areas A5 and A6. The laminate cutting time is calculated according to equations 7.1 and 7.3 and assuming that the 25th layer in a batch is cut.

$$C_{Ap} = 373.8 \text{ cm}$$

$$v_{cut,m} = 0.253 \ln(25) + 0.188 = 1.002 \frac{\text{cm}}{\text{s}}$$

$$t_{cut} = 1 \left(\frac{373.8}{1.002} \right) = 373 \text{ s}$$

E.2 Application of gelcoat

Although there is no model for the gelcoat application time, the process is estimated with the mould release agent application model. One gelcoat layer (LS 88PA Black AC 2) is applied with a paintbrush on specific areas with the assumed size of quarter of the part surface area. For a clearer evaluation of the cost model equations, drying time for the measurements and the estimation of the process time were neglected. Results of calculations are tabulated in Figure E.2.

Table E.2: Determination of gelcoat application time on refrigerator panel

Area	$A_s/4$ [dm ²]	Shape	t_h [s/dm ²]	t_{app} [s]
A1	6.76	flat	52.78	356.8
A2	1.81	angled	58.38	105.7
A3	1.81	angled	58.38	105.7
A4	1.14	angled	58.35	66.5
A5	2.06	flat	53.53	110.3
A6	2.65	angled	58.42	154.8
A7	2.3	flat	53.49	123
A8	0.44	angled	58.31	25.7
A9	1.22	angled	58.35	71.2
Total application time				1119.7

The estimated gelcoat handling time for A2 according to equation 7.4 is:

$$t_{handle,angle A2} = 58.29 + 0.05 \cdot 1.81 = 58.38 \frac{\text{s}}{\text{dm}^2}$$

The application time according to equation 7.8

$$t_{app\ A2} = 1 \cdot 1.81 \cdot 58.38 + (1 - 1)(120 - 1.81 \cdot 58.38) + 0 = 105.7\text{ s}$$

E.3 Laminate lay-up

In this step the lay-up time of the one main laminate layer for the refrigerator panel is estimated. Separately prepared woven fibreglass plies on surrounding sides and at the vents are neglected. The laminate layer is split into the areas covered and the total process step time is finally the sum as shown in Table E.3.

Table E.3: Estimation of laminate lay-up time of refrigerator panel

Area	A_p [cm ²]	Shape Character	$t_{work,lay}$ [s]	t_{layup} [s]
A1	1351.2	flat	36.17	36.17
A2	362.7	angled	32.7	32.7
A3	362.7	angled	32.7	32.7
A4	228	angled	30.86	30.86
A6	529	angled	35.02	35.02
A8	88	angled	28.93	28.93
A9	243	angled	31.07	31.07
Total application time				227.5

Example of calculation for area three (A3) is according equation 7.11 and equation 7.12 calculated.

$$t_{work,lay,angle\ A3} = 27.72 + 1.379E-2 \cdot 362.7 = 32.7s$$

$$t_{layup\ A3} = 0 + 1 \cdot 32.7\text{ s} = 32.7\text{ s}$$

E.4 Infusion

The refrigerator panel is manufactured with a runner around the mould cavity. In this study the influence of runners was not investigated. However, an approach used to estimate the infusion time will be described here. The first step is to determine the ideal flow paths (P1 to P4) and flow path areas, as shown as the background colour in Figure E.1. The refrigerator panel is symmetric, thus the flow paths P2 and P4 are assumed to take the same time. P3 does not have large obstacles in the flow path and P3 is assumed to never reach the vent, as shown in Figure E.1. The analysis will concentrate on P1 and P2, and the longest time will determine the infusion time of the whole part. Figure E.2 shows the ideal flow areas of P1 and P2. The resin inlet port feeds a runner that surrounds the whole mould cavity.

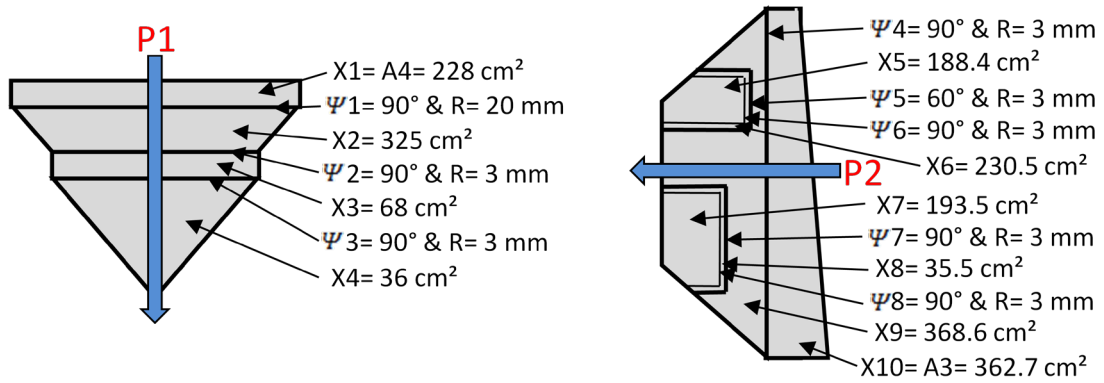


Figure E.2: Infused areas of flow paths one and two

Analysis, flow path one (P1)

Flow path one will end at V1. The areas infiltrated, the angles and radii are shown in Figure E.2. Here the third area is simplified as a rectangular form. The total part area ($A_{p,total P1}$) of path one is 657 cm². The total infusion time is calculated according to equation E1.

$$\begin{aligned}
 t_{inf,complex P1} &= \frac{t_{inf,flat} \text{ of } A_{p,total P1}}{A_{p,total P1}} \left[A_{pX1} (1) + A_{pX2} \left(\frac{t_{\psi=90, A_{p,total P1}}}{t_{flat, A_{p,total P1}}} \right) \right. \\
 &\quad + A_{pX3} \left(\frac{t_{\psi=90, A_{p,total P1}}}{t_{flat, A_{p,total P1}}} \right) \left(\frac{t_{\psi=90, A_{p,total P1}}}{t_{flat, A_{p,total P1}}} \right) \\
 &\quad \left. + A_{pX4} \left(\frac{t_{\psi=90, A_{p,total P1}}}{t_{flat, A_{p,total P1}}} \right) \left(\frac{t_{\psi=90, A_{p,total P1}}}{t_{flat, A_{p,total P1}}} \right) \left(\frac{t_{\psi=90, A_{p,total P1}}}{t_{flat, A_{p,total P1}}} \right) \right] \\
 &= \frac{296.15}{657} \left[228(1) + 325 \left(\frac{361.41}{296.15} \right) + 68 \left(\frac{361.41}{296.15} \right) \left(\frac{342.41}{296.15} \right) \right. \\
 &\quad \left. + 36 \left(\frac{361.41}{296.15} \right) \left(\frac{342.41}{296.15} \right) \left(\frac{342.41}{296.15} \right) \right] = 351.28 \text{ s} \tag{E1}
 \end{aligned}$$

Analysis, flow path two (P2)

The right side of Figure E.2 illustrates the areas of flow path two. The total part area ($A_{p,total P2}$) of path two is 1379.2 cm². The longest time is the determining infusion time for the cost calculation, thus the path over the upper pocket to V1 is seen as the most critical path and is defined using equation E2 for the calculation.

$$\begin{aligned}
t_{inf,complex P2} &= \frac{t_{inf,flat of A_{p,total P2}}}{A_{p,total P2}} \left[A_{pX10} (1) + A_{pX9} \left(\frac{t_{\psi=90,A_{p,total P2}}}{t_{flat,A_{p,total P2}}} \right) \right. \\
&\quad + A_{pX6} \left(\frac{t_{\psi=90,A_{p,total P2}}}{t_{flat,A_{p,total P2}}} \right) \left(\frac{t_{\psi=60,A_{p,total P2}}}{t_{flat,A_{p,total P2}}} \right) \\
&\quad \left. + A_{pX5} \left(\frac{t_{\psi=90,A_{p,total P2}}}{t_{flat,A_{p,total P2}}} \right) \left(\frac{t_{\psi=60,A_{p,total P2}}}{t_{flat,A_{p,total P2}}} \right) \left(\frac{t_{\psi=30,A_{p,total P2}}}{t_{flat,A_{p,total P2}}} \right) \right] \\
&= \frac{593.14}{1379.2} \left[362.7(1) + 368.6 \left(\frac{780.61}{593.14} \right) + 230.5 \left(\frac{780.61}{593.14} \right) \left(\frac{703.07}{593.14} \right) \right. \\
&\quad \left. + 188.4 \left(\frac{780.61}{593.14} \right) \left(\frac{703.07}{593.14} \right) \left(\frac{703.07}{593.14} \right) \right] = 668.76 \text{ s} \tag{E2}
\end{aligned}$$

Path two represents the total infusion time for the whole complex shaped fridge panel. All other infusion paths can be manipulated by closing one vent or by moderating the infusion velocity, by placing additional fibre plies close to the vent.

E.5 Mould clamping, positioning, pipe mounting and resin mixing

The mould clamping, positioning, pipe mounting and resin mixing are handled according to equation 7.14, because the panel clearly has a higher percentage of flat shaped area.

$$t_{CPFM,angle} = 1482 \text{ s}$$

E.6 Demoulding

The demoulding is orientated on the shape of the largest area. Therefore, the part is mainly flat shaped and the demoulding process time can be calculated according to equation 7.18. The estimation equations are generated for low production volumes, therefore for this estimation the manufacturing time of the 25th part is used.

$$t_{removal,flat} = -26.89 \ln(25) + 195.97 = 109.4 \text{ s}$$

$$t_{demould} = 423.6 + 109.4 = 533 \text{ s}$$

E.7 Mould cleaning

For the mould cleaning, the manufacturing time of the 25th part is used to account for the medium production volume. Equation 7.22 and equation 7.23 are applied, as shown.

$$C_{As} = 19.3 \cdot 2 = 38.6 \text{ dm}$$

$$t_{clean \text{ } As=4} = -111.8 \ln(25) + 800.62 = 440.8 \text{ s}$$

$$t_{clean} = \frac{440.8}{12} 38.6 = 1417.9 \text{ s}$$

Appendix F: Mould dimensions

F.1 Flat shaped mould drawings

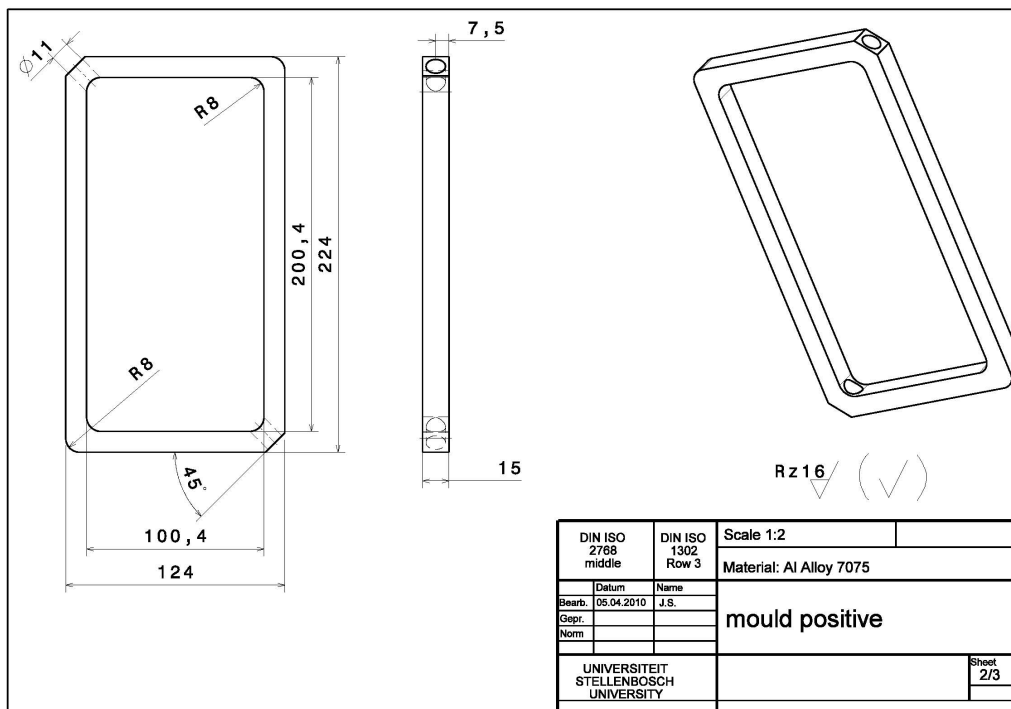
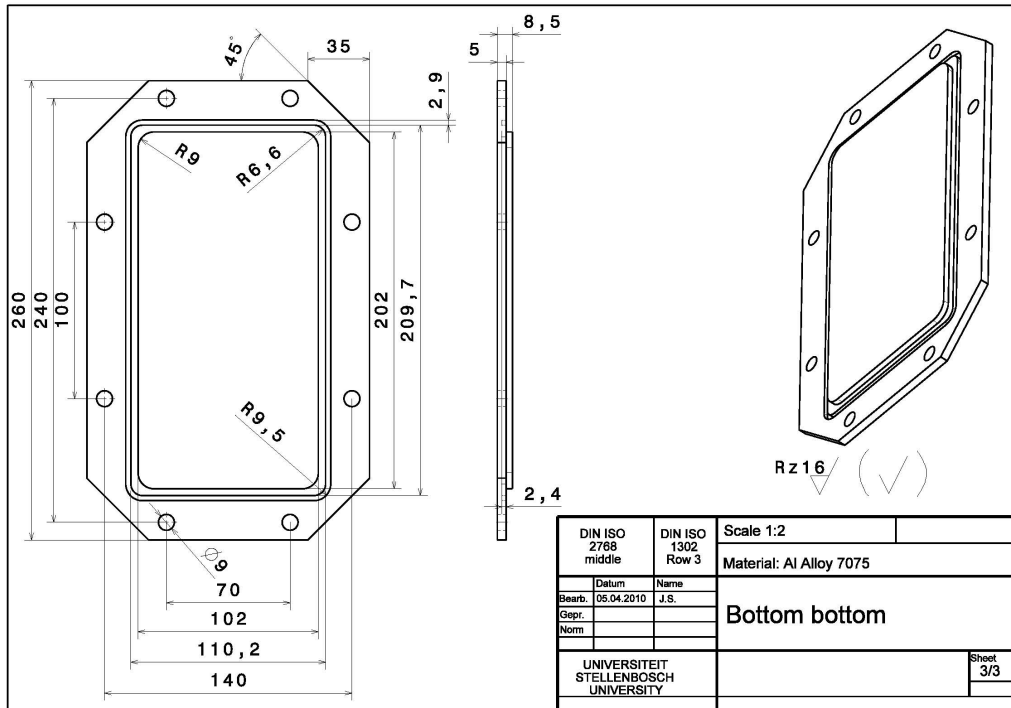


Figure F.1: Mould dimensions flat shaped mould (1)

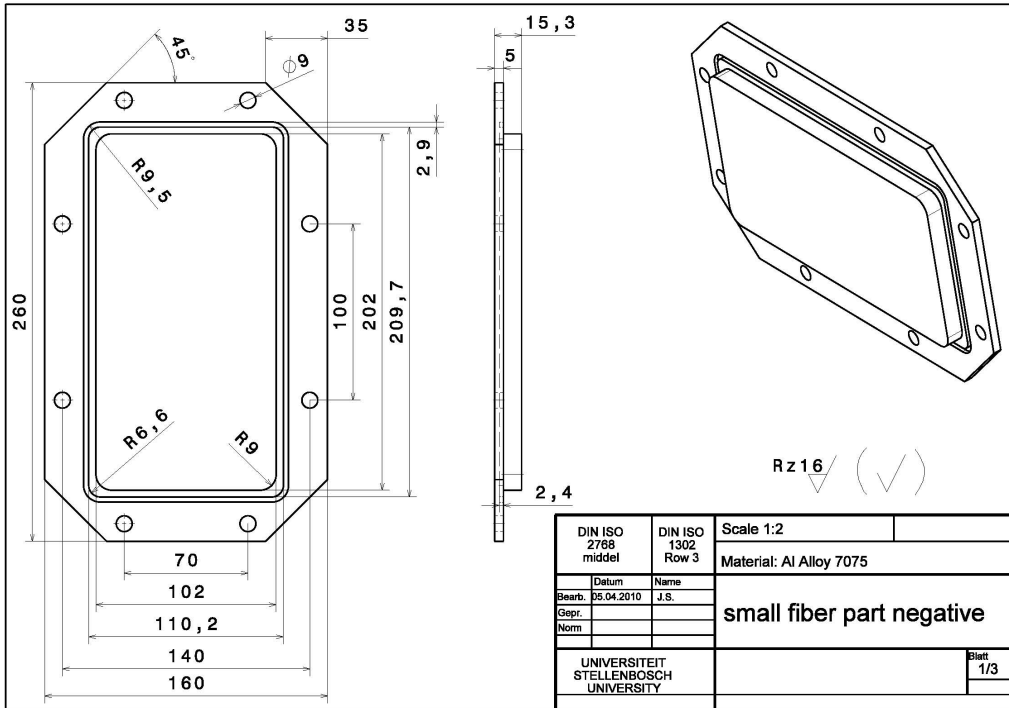


Figure F.2: Mould dimensions flat shaped mould (2)

F.2 L-shaped mould drawings

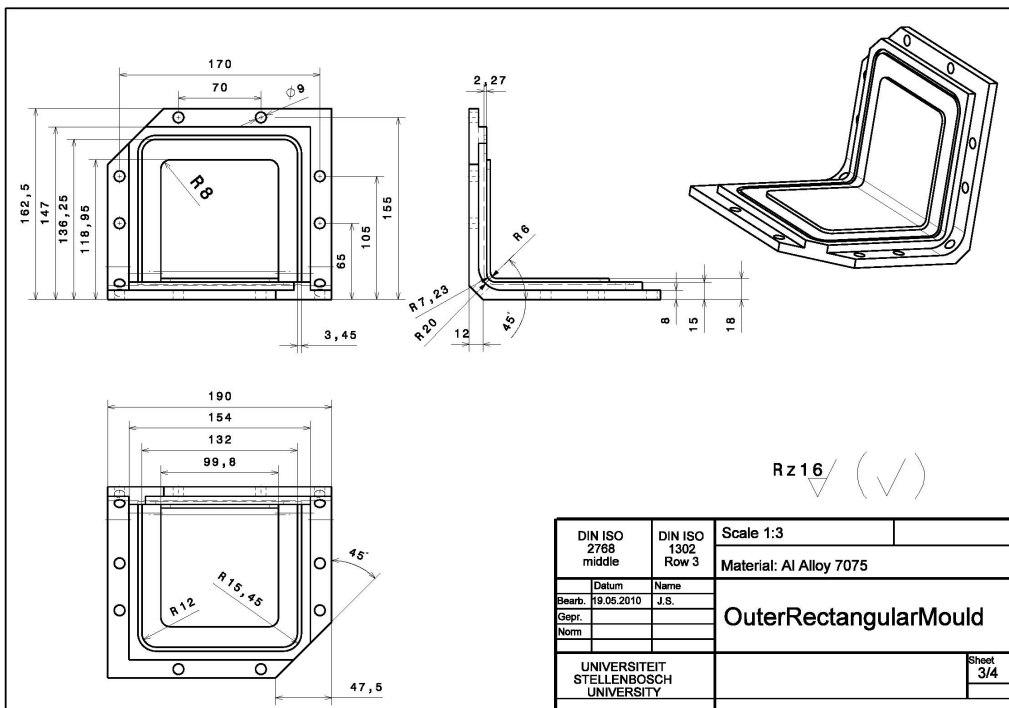


Figure F.3: Mould dimensions L-shaped mould (1)

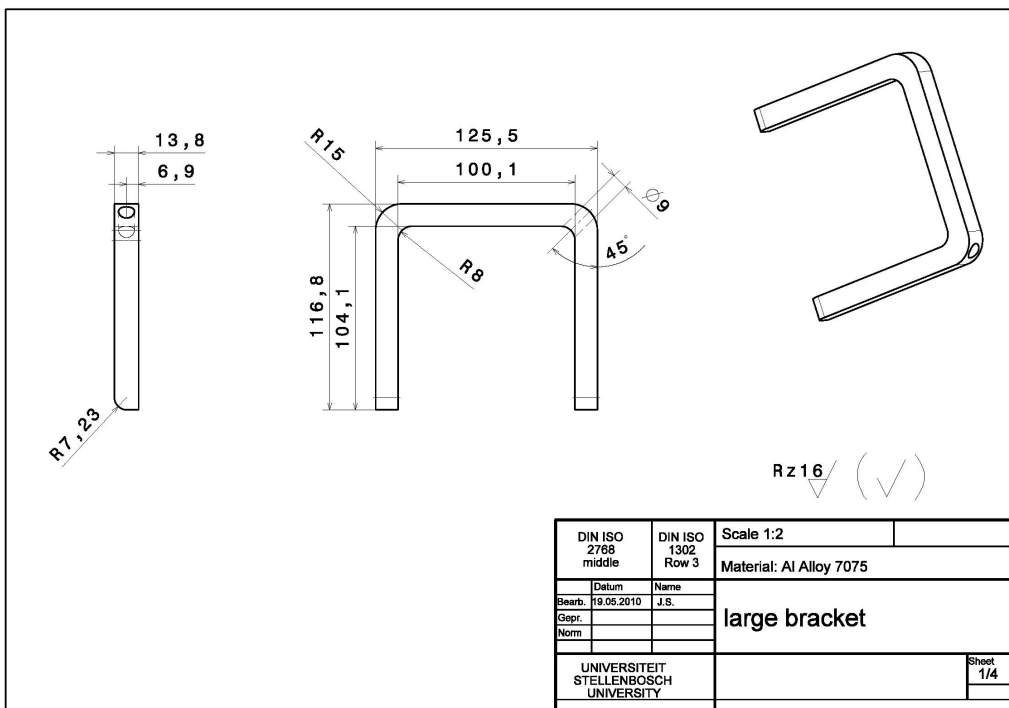
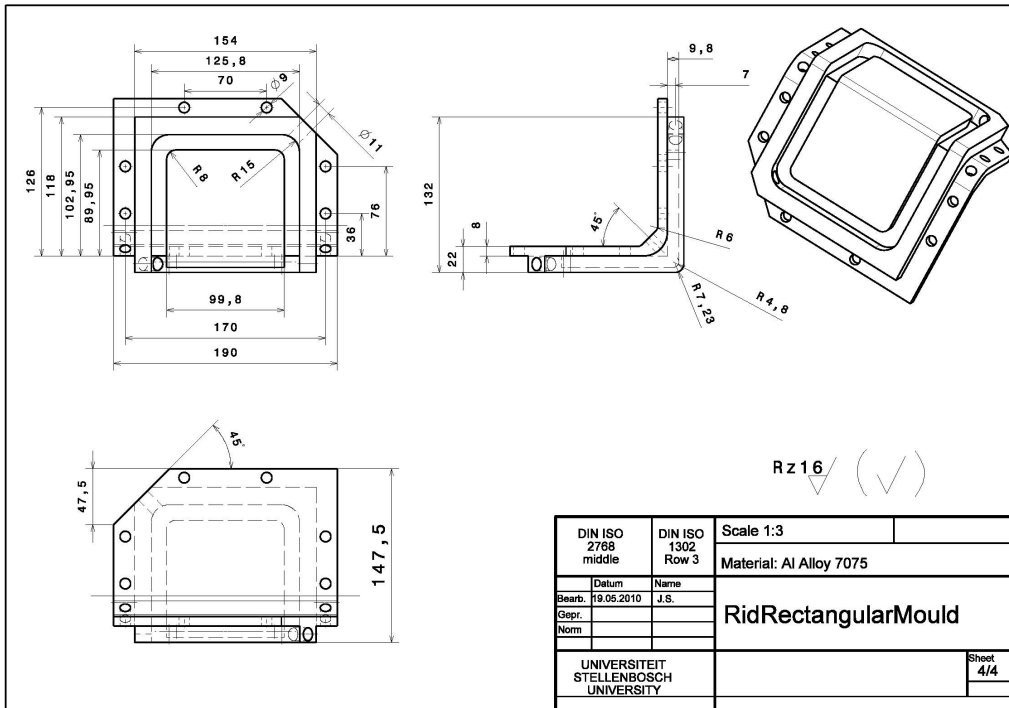


Figure F.4: Mould dimensions L-shaped mould (2)

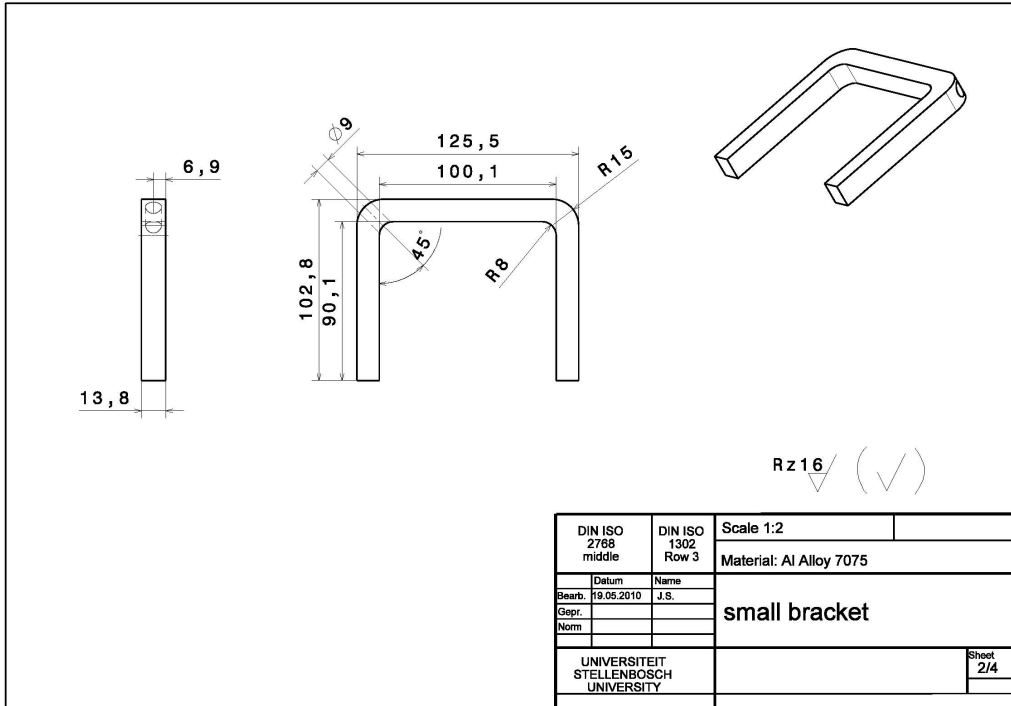


Figure F.5: Mould dimensions L-shaped mould (3)